On the pricing of Bermudan swaptions in the multi-curve LIBOR Market Model

Alice Gianolio

Delft University of Technology

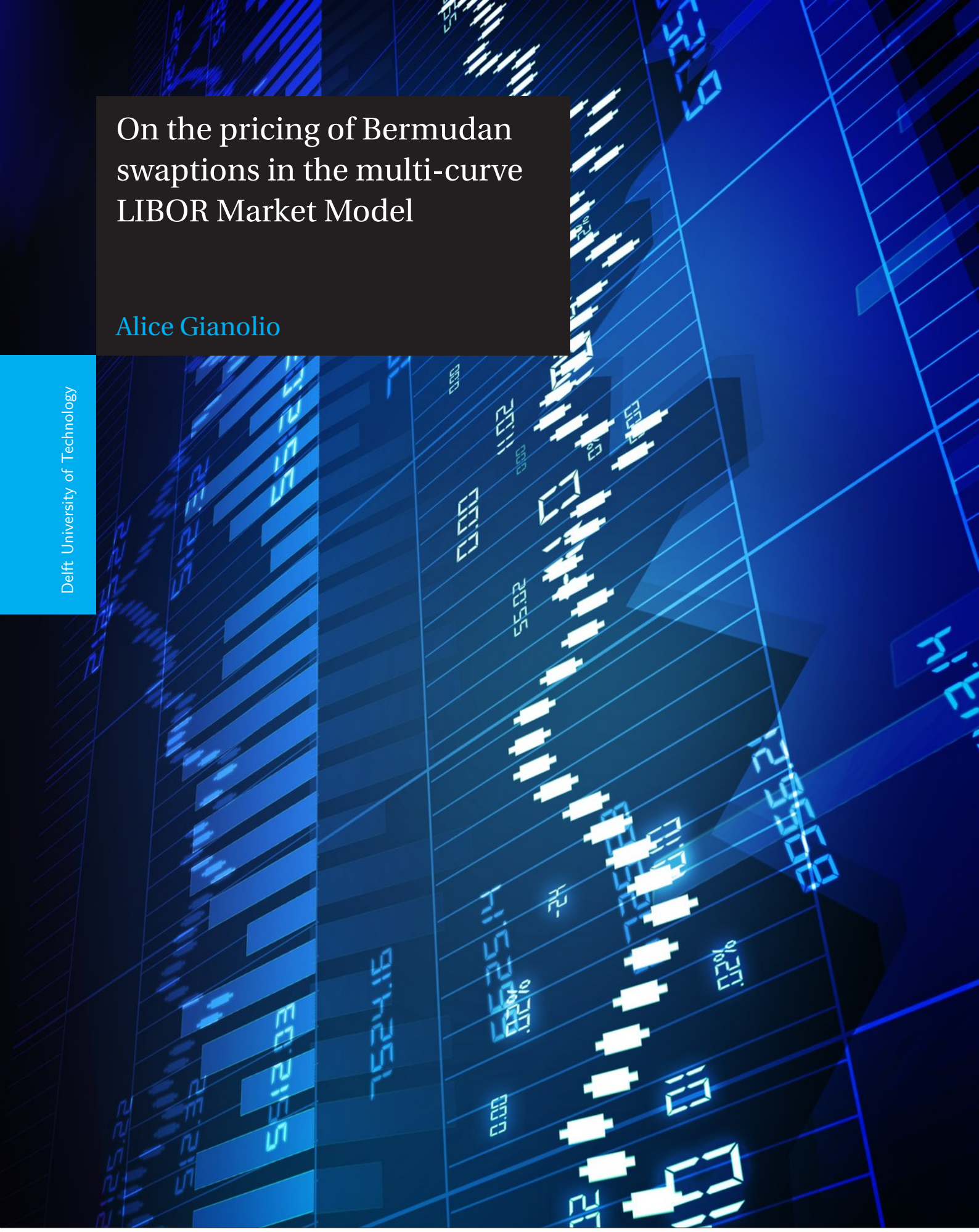

TU Delft Delft University of Technology

Challenge the future

DELFT UNIVERSITY OF TECHNOLOGY

MASTER OF SCIENCE THESIS

On the pricing of Bermudan swaptions in the multi-curve LIBOR Market Model

in partial fulfillment of the requirements for the degree of

Master of Science
in Applied Mathematics

at Delft University of Technology
November, 2016

Author
Alice GIANOLIO

Daily supervisors
Dr. Ir. J.H.M. ANDERLUH[1]
Ir. B. HOORENS[2]
Dr. V. MALAFAIA[2]

Responsible professor
Prof. Dr. F.H.J. REDIG[1]

Other thesis committee member
M.B. VAN GIJZEN[3]

[1] Delft University of Technology, Faculty of Electrical Engineering, Mathematics and Computer Science, Department of Applied Probability
[2] ING, Credit and Trading Risk FI/FM, Interest Rate and Inflation Quantitative Analytics
[3] Delft University of Technology, Faculty of Electrical Engineering, Mathematics and Computer Science, Department of Numerical Analysis

ACKNOWLEDGEMENTS

This thesis is submitted in partial fulfillment of the requirements for the Master's degree in Applied Mathematics at Delft University of Technology. The research of this thesis was carried out for the Interest Rate and Inflation Quantitative Analytics team of the Credit and Trading Risk FI/FM department at ING Bank Amsterdam.

I would like to express my gratitude to those who have contributed in the process of writing this thesis. First of all, I thank Veronica Malafaia and Bart Hoorens, who hired me as an intern and provided me with an interesting topic for my master thesis. Their advice and guidance during the graduation period were an essential component in making this project a success. A special thanks goes to Jasper Anderluh for his supervision on behalf of the university. Furthermore, I would like to acknowledge Frank Redig and Martin van Gijzen for being part of the thesis committee.

Alice Gianolio
Delft, November 2016

ABSTRACT

The aim of this research is to extend the classical LMM to a multi-curve framework and to analyze the impact of this extended model on the most liquid exotic interest rate derivatives. A possible parametrization for the instantaneous volatility and correlation structure is presented and the (log-)normal dynamics of the OIS rates under different measures are obtained. The forward LIBOR rates are modeled at a constant additive spread over the OIS curve. An analytical closed-form approximation of the European swaption volatility in the multi-curve framework is derived and its accuracy is verified by comparing the Monte Carlo prices of a set of European swaptions with the corresponding prices obtained using the approximation. It is demonstrated that the approximation reaches the highest accuracy for swaptions characterized by short underlying tenors and strikes close to the swap rate. The multi-curve LIBOR Market Model is calibrated to the swaption market applying this approximation. Using the calibrated model distinct Bermudan swaptions are priced by means of Monte Carlo. These prices are compared to the corresponding prices obtained using the one-factor Hull-White model and the impact of the model selection is analyzed.

GLOSSARY

Below a list of frequently used abbreviations and symbols is presented.

Abbreviations

1FHW	One-factor Hull White	Chapter 1
ATM	At-the-money	Section 2.5
bp	Basis point: 0.01%	Section 3.7
CPU	Central processing unit	Section 3.6
GBP	Great Britain Pound	Section 2.2
ITM	In-the-money	Section 2.5
LIBOR	London Interbank Offer Rank	Section 2.2
LMM	LIBOR Market Model	Chapter 1
LS	Longstaff & Schwartz	Section 5.1
M	Months	Section 2.4
MC	Multi-curve	Chapter 1
OIS	Overnight indexed swap	Chapter 1
OTM	Out-of-the-money	Section 2.5
PCA	Principal component analysis	Section 3.4
SC	Single-curve	Chapter 1
SDE	Stochastic differential equation	Section 3.6
Std	Standard deviation	Section 3.6
USD	United States Dollar	Section 2.2
Y	Years	Section 3.2

Greek letters

$\alpha(t)$	First upcoming reset moment with respect to time t	Section 3.1
β	Constant correlation parameter	Section 3.2
μ_i	Drift term of $F_i(t)$ (in SC) or $F_i^d(t)$ (in MC)	Section 3.1
$\rho_{i,j}$	Correlation between $F_i(t)$ and $F_j(t)$ (in SC) or between $F_i^d(t)$ and $F_j^d(t)$ (in MC)	Section 3.2
ρ	Correlation matrix whose entries are given by $\rho_{i,j}$	Section 3.2
$\sigma_i(t)$	Instantaneous volatility at time t of $F_i(t)$ (in SC) or $F_i^d(t)$ (in MC)	Section 3.1
$\widetilde{\sigma}_i$	Implied Bachelier/Black volatility of a caplet/floorlet defined on $[T_i, T_{i+1}]$	Section 2.5
$\widetilde{\sigma}_{[r,N]}$	Implied Bachelier/Black volatility of a swaption defined on $[T_r, T_N]$	Section 2.5
$\widetilde{\sigma}^{MKT}_{[r,N]}$	Market provided implied Bachelier/Black volatility of a swaption defined on $[T_r, T_N]$	Section 4.1
τ_i	Year fraction between time T_i and time T_{i+1}	Section 2.5
$\phi(x)$	Time-homogeneous local volatility function where $\phi(x) = 1$ and $\phi(x) = x$ specify normal and log-normal dynamics, respectively	Section 3.1

Roman letters

a	Constant instantaneous volatility parameter	Section 3.2
$A_{[r,N]}\left(t, \mathbf{P}^d(t)\right)$	Annuity factor at time t corresponding to an interest rate swap over $[T_r, T_N]$ and depending on $\mathbf{P}^d(t)$	Section 2.5
b	Constant instantaneous volatility parameter	Section 3.2
$B(t)$	Money-market account at time t	Section 2.2

$B^*\left(\mathbf{F}^d(t)\right)$	Rolling over bank account at time t depending on $\mathbf{F}^d(t)$	Section 3.3
c	Constant instantaneous volatility parameter	Section 3.2
$\mathcal{C}^d$	OIS discount curve	Section 2.4
$\mathcal{C}^x$	Forward LIBOR curve corresponding to a specific tenor x	Section 2.4
$C_{[r,N]}\left(t,\mathbf{P}^d(t),\mathbf{F}^x(t)\right)$	Value at time t of a cap/floor over $[T_r,T_N]$ depending on $\mathbf{P}^d(t)$ and $\mathbf{F}^x(t)$ (in MC)	Section 2.5
d	Constant instantaneous volatility parameter	Section 3.2
dt	Constant simulation grid step size	Section 3.6
E_i	Bermudan call date	Section 5.1
$\mathscr{E}$	Set of Bermudan call dates	Section 5.1
$F_i(t)$	Simply compounded forward LIBOR rate at time t for the expiry T_i and the maturity T_{i+1} (in SC)	Section 3.1
$F_i^d(t)$	Simply compounded forward OIS rate at time t for the expiry T_i and the maturity T_{i+1} (in MC)	Section 3.5
$F_i^x(t)$	Simply compounded forward LIBOR rate at time t for the expiry T_i and the maturity T_{i+1} (in MC)	Section 3.5
$\mathbf{F}^d(t)$	Vector of forward OIS rates $F_i^d(t)$	Section 3.5
$\mathbf{F}^x(t)$	Vector of forward LIBOR rates $F_i^x(t)$	Section 3.5
$G_i(t)$	Spread between $F_i^x(t)$ and $F_i^d(t)$	Section 3.5
h	Number of driving Brownian motions	Section 3.1
H	Number of Monte Carlo simulations	Section 3.6
k_i	Instantaneous volatility parameter depending on maturity T_i	Section 3.2
K	Fixed payment rate	Section 2.3
$L(t,T)$	Simply compounded spot LIBOR rate at time t for the maturity T (in SC)	Section 2.4
$L^d(t,T)$	Simply compounded spot OIS rate at time t for the maturity T (in MC)	Section 2.4
$L^x(t,T)$	simply compounded spot LIBOR rate at time t for the maturity T (in MC)	Section 2.4
M	Notional	Section 2.3
$n(x)$	Standard normal probability density function evaluated in x	Section 2.3
$\mathcal{N}(x)$	Standard normal cumulative distribution function evaluated in x	Section 2.3
$P_i(t)$	Value at time t of zero coupon bond paying one unit of currency at maturity T_i associated with the LIBOR curve (in SC)	Section 3.1
$P_i^d(t)$	Value at time t of zero coupon bond paying one unit of currency at maturity T_i associated with the OIS curve (in MC)	Section 3.5
$\mathbf{P}^d(t)$	Vector of zero coupon bonds $P_i^d(t)$	Section 3.5
$\mathbb{Q}_d^{B^*}$	Spot measure induced by numéraire $B^*\left(\mathbf{F}^d(t)\right)$	Section 3.5
$\mathbb{Q}_d^{T_i}$	T_i-forward measure induced by the numéraire $P_i^d(t)$	Section 2.5
$\mathbb{Q}_d^{r,N}$	Annuity measure induced by the numéraire $A_{[r,N]}\left(t,\mathbf{P}^d(t)\right)$	Section 2.5
$R_{[r,N]}\left(t,\mathbf{P}^d(t),\mathbf{F}^x(t)\right)$	Fixed payment rate that gives a fair price at time t of an interest rate swap over $[T_r,T_N]$, depending on $\mathbf{P}^d(t)$ and $\mathbf{F}^x(t)$ (in MC), referred to as the swap rate	Section 2.5
$\mathbf{s}_i(t)$	Diffusion coefficient of $F_i(t)$ (in SC) or $F_i^d(t)$ (in MC)	Section 3.1
$S_{[r,N]}\left(t,\mathbf{P}^d(t),\mathbf{F}^x(t)\right)$	Value at time t of an interest rate swap over $[T_r,T_N]$ depending on $\mathbf{P}^d(t)$ and $\mathbf{F}^x(t)$ (in MC)	Section 2.5
$\widetilde{S}_{[r,N]}\left(t,\mathbf{P}^d(t),\mathbf{F}^x(t)\right)$	Value at time t of a European swaption over $[T_r,T_N]$ depending on $\mathbf{P}^d(t)$ and $\mathbf{F}^x(t)$ (in MC)	Section 2.5
T_i	Tenor date with $i\in\{0,\ldots,N\}$	Section 2.5
$V(t)$	Value at time t of a Bermudan swaption	Section 5.1

w	Indicator function with $w = 1$ referring to a payer swap/swaption and $w = -1$ to a receiver swap/swaption	Section 2.5
$\mathbf{W}^{\mathbb{Q}}(t)$	h-dimensional, element-wise independent Brownian motion under a measure $\mathbb{Q}$	Section 3.1

LIST OF FIGURES

LIST OF TABLES

CONTENTS

1

INTRODUCTION

This thesis focusses on the multi-curve (MC) LIBOR Market Model (LMM) that belongs to the class of market models. While plain vanilla swaps are priced by simple cash flow discounting and the value of caps/floors and swaptions is determined by means of Bachelier's or Black's model, more exotic instruments require the use of term structure models. Short rate models and market models are the two most frequently used classes of models for this purpose. The popularity of the latter derives from the modeling of market observable interest rates in contrast to the former, which instead specifies the dynamics of the unobservable short rate.

The classical LMM, proposed by Brace et al. (1997) and Miltersen et al. (1997), describes the evolution of a non-overlapping set of simply compounded LIBOR rates. These rates are assumed to follow a log-normal distribution. The model admits a wide use of volatility functions and correlation structures between the forward rates. It is derived in the so-called single-curve (SC) framework, which prevailed before the credit crisis of 2007.

Differences between same-currency rates of distinct index tenors have always been present in the market, also prior to 2007. Before the most recent crisis, for example, the LIBOR rates and the Overnight Indexed Swap (OIS) rate with the same maturity would closely track each other, keeping a distance (spread) of a few basis points. Similarly, swap rates with the same maturity, but based on LIBOR rates with different tenors, would be quoted at a relatively small non-zero (basis) spread. These spreads were in general assumed to be zero when constructing zero-coupon curves or pricing interest rate derivatives. Because of the neglected spreads, the forward rates and discount factors could be represented by the same curve. This consideration characterizes the SC framework, in which LIBOR rates could be seen as risk-free and forward rates were obtained by replication with risk-free discount bonds.

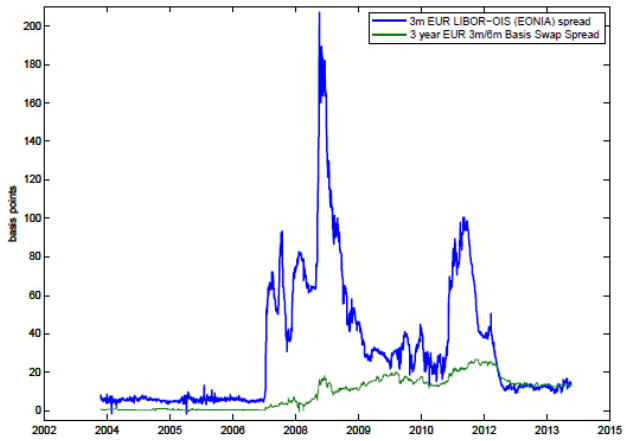

Figure 1.1: Spread development from January 2004 to April 2014 (Grbac et al., 2015).

After August 2007, market rates that had always been consistent with each other suddenly revealed a degree of incompatibility that worsened with time. The spreads started to evolve randomly over time and became too large to be considered negligible. For instance, the spread between the three-month LIBOR rate and the corresponding EONIA rate drastically widened after the credit crunch, as can be observed in Figure 1.1. Likewise, the swap rate based on semiannual payments of the six-month LIBOR rate became different from the same-maturity swap rate based on quarterly payments of the three-month LIBOR rate (see again Figure 1.1). The implicit assumption that the market is free of default risk was not valid anymore and the LIBOR rates stopped being seen as risk-free. Consequently, these rates could no longer be replicated by risk-free discount bonds.

The notion that one curve could be used for both generating and discounting cash flows was challenged, which led to the rise of the so called MC framework. Within this new framework, plain vanilla interest rate derivatives are priced by calculating the forward rates on a curve representing the LIBOR rates, whilst the discount factors are computed using a curve that reflects the funding cost. In order to price exotic interest rate derivatives, the term structure models have to be extended to incorporate the new market conditions. Two main approaches are identified in literature. The first assumes a deterministic spread between the discount and the forward curves, whereas the second models the evolution of the spread as a stochastic process.

The first research objective consists in extending the classical LMM to accommodate the MC framework. In this thesis a constant spread is considered between the forward LIBOR curve and the OIS curve that is used for discounting. Similarly to the SC LMM case, the forward OIS/LIBOR rates and the swap rates cannot be jointly (log-)normal. In order to be able to price a swaption analytically, the dynamics of the corresponding swap rate are approximated by a (log-)normal formulation. The approximated swap rate instantaneous volatility can be used in Bachelier's or Black's model to price the swaption. The accuracy of this volatility approximation is tested by comparing the Monte Carlo prices of a set of European swaptions with the corresponding prices obtained using the approximation.

The second research objective is to investigate the impact of the MC LMM on exotic interest rate derivatives. In this thesis Bermudan swaptions are considered. The Bermudan swaption prices computed with the MC LMM are compared to the ones generated by the one-factor Hull-White (1FHW) model. The most noticeable difference is that the 1FHW assumes perfectly correlated interest rates, while the MC LMM admits more involved correlation structures among the forward rates. The prices of 30 distinct Bermudan swaptions, whose underlying payer or receiver swaptions have different underlying tenors and strikes, are compared.

This resport is structured as follows. Chapter 2 presents the fundamentals of interest rate modeling. Discount bonds are introduced and the definition of the forward LIBOR rate is given under the SC and MC frameworks. The valuation of swaps is addressed and subsequently market pricing formulas for caps/floors and swaptions are presented for both the SC and the MC setups. Chapter 3 is devoted to the description of the LMM. The first half of this chapter describes the LMM in the SC framework, defining the dynamics of the forward LIBOR rates and presenting a possible parametrization for the instantaneous volatility and for the correlation structure. The second half focuses on the MC LMM, explaining potential model extensions and detailing the model formulation. It also illustrates how Monte Carlo can be used to pricederivatives and it shows how to price swaptions under the MC LMM using the swaption volatility approximation. Before being able to price exotic derivatives, the model has to be calibrated to market data. In Chapter 4 the MC LMM is calibrated to the swaption market, in particular to implied swaption volatilities. The use of the analytical closed-form swaption volatility approximation ensures a fast calibration as the swaption volatilities can be determined rapidly without Monte Carlo. Results are shown for 15 different sets of implied swaption volatilities, each characterized by volatilities corresponding to swaptions with different underlying tenors and strikes. In Chapter 5 the price impact of the MC LMM on the Bermudan swaption prices is investigated. Chapter 6 presents the conclusions of this research.

2

FUNDAMENTALS OF INTEREST RATE MODELING

The purpose of this chapter is to give the reader a complete overview of the mathematical framework of interest rates derivative pricing. The first section is devoted to the presentation of a short selection of concepts from stochastic calculus that are required to understand the subsequent parts. A special relevance will be given to the changing of numéraire technique. The sections that follow focus on interest rate modeling. Zero coupon bonds are introduced in Section 2.2. These type of bonds are considered to be the building blocks for the pricing formulas of the interest rate products that are analyzed in this thesis. Furthermore, the interest rates that play a fundamental role throughout this thesis will be addressed. Section 2.3 describes Bachelier's and Black's model, which offer a tool for pricing interest rate options. The classical single-curve interest rate modeling framework is presented in Section 2.4, together with the multi-curve approach used after the credit crisis. The last section of this chapter will introduce the pricing formulas for some basic interest rate instruments including swaptions and swaps. Swaptions will be used in the calibration of the LMM in Chapter 4, whereas swaps are relevant for the definition of Bermudan swaption instruments, as will be seen in Chapter 5. The vanilla interest rate products will be valuated under both the single-curve and the multi-curve frameworks.

2.1. PRELIMINARIES

Consider a financial market on the finite time horizon $[0, T]$ where d financial assets are traded. It is assumed that the market is continuous and frictionless such that a market participant can enter into bids or offers at any time during a trading day with no transaction costs and no taxation. The prices of the traded assets, denoted as the d-dimensional stochastic process $\mathbf{X}(t) = (X_1(t), \ldots, X_d(t))^\top$, are Itô processes:

$$d\mathbf{X}(t) = \mu(t, \mathbf{X}(t))\, dt + \sigma(t, \mathbf{X}(t))\, d\mathbf{W}^{\mathbb{Q}}(t), \tag{2.1}$$

where $\mu(t, \mathbf{X}(t)) \in \mathbb{R}^{d\times 1}$, $\sigma(t, \mathbf{X}(t)) \in \mathbb{R}^{d\times p}$ and with $\mathbf{W}^{\mathbb{Q}}(t) = \left(\mathbf{W}^{\mathbb{Q}}(t)\right)_{t\geq 0}$ representing a p-dimensional Brownian motion under a probability measure $\mathbb{Q}$.

Let $N(t)$ be a strictly positive, non-dividend-paying asset following an Itô process. $N(t)$ is said to be a numéraire if the asset prices $\mathbf{X}(t)$ in the market are denominated in terms of this process. $\mathbf{X}^N(t) = (X_1(t)/N(t), \ldots, X_d(t)/N(t))^\top$ represent these normalized prices. Associated with each numéraire $N(t)$ there exists a probability measure $\mathbb{Q}^N$ such that $\mathbf{X}^N(t)$ is a martingale under this measure. $\mathbb{Q}^N$ is said to be a probability measure induced by N.

Consider a derivative security whose payoff at time T is given by the random variable $V(T)$. According to the fundamental pricing formula the following holds:

$$V(t) = N(t)\, \mathbb{E}_t^{\mathbb{Q}^N}\left[\frac{V(T)}{N(T)}\right]. \tag{2.2}$$

Let $M(t)$ and $N(t)$ be two numéraires with associated equivalent martingale measures $\mathbb{Q}^M$ and $\mathbb{Q}^N$, respectively. From (2.2) follows

$$V(t) = M(t)\,\mathbb{E}_t^{\mathbb{Q}^M}\left[\frac{V(T)}{M(T)}\right] = N(t)\,\mathbb{E}_t^{\mathbb{Q}^N}\left[\frac{V(T)}{N(T)}\right],$$

that can be rewritten as

$$V(t) = \mathbb{E}_t^{\mathbb{Q}^M}\left[\frac{V(T)}{M(T)}\right] = \mathbb{E}_t^{\mathbb{Q}^N}\left[\frac{V(T)}{M(T)}\,\frac{M(T)/M(t)}{N(T)/N(t)}\right]. \tag{2.3}$$

The relation in (2.3) shows how to obtain the price of a derivative security under different equivalent martingale measures by changing numéraires. This changing of numéraire technique is often used in practice when complex expectation functions of derivatives with multiple sources of risk are considered. With a properly chosen numéraire, the technique allows the applicant to reduce the number of sources of risk and therefore it simplifies the computations involved in the pricing of a particular derivative (Benninga et al., 2002). Formula (2.2) will be used in Section 2.5 to price swaps, swaptions and caps/floors. For a more extensive discussion on the change of numéraire technique, see (Andersen and Piterbarg, 2010a), (Brigo and Mercurio, 2007) and (Pelsser, 2000).

2.2. DISCOUNT BONDS AND INTEREST RATES

Interest rates play a prominent role in the economy. They reflect the cost of borrowing or the profit from lending money and can be seen as a measure of the time value of money. The dependence of the rates on time is shown in the *term structure of interest rates*. This concept is represented as a curve where a specific interest rate (or discount bond, see below) is assigned to every future date.

Consider a money-market account $(B(t))_{t\geq 0}$. This account represents a risk-less investment with value 1 at initial time 0, which accrues a continuously compounded risk-free interest rate r. It satisfies the ordinary differential equation

$$dB(t) = r(t)\,B(t)\,dt, \quad B(0) = 1,$$

which implies

$$B(t) = e^{\int_0^t r(s)ds}. \tag{2.4}$$

Let $D(t,T)$ be a quantity at time t that is equivalent to one unit of currency at time T. This quantity is known as the stochastic discount factor and is defined as

$$D(t,T) = \frac{B(t)}{B(T)} = e^{-\int_t^T r(s)ds}. \tag{2.5}$$

A *zero coupon bond* with maturity T, also called a discount bond, is an asset that guarantees the holder a payment of a unit amount at some future date T and without intermediate cash flows occurring. Let $P(t,T)$ denote the value of such a bond at time t, hence $P(T,T) = 1$ by definition. Zero coupon bonds are fictitious financial securities as their prices are not directly observable. They are considered to be the building blocks for pricing formulas of all interest rates products since each fixed income security can be represented in terms of those discount bonds. The forward price at time t of a zero coupon bond spanning $[T,S]$, where $0 < T < S$, is given by the no-arbitrage relation

$$P(t,T,S) = \frac{P(t,S)}{P(t,T)}, \tag{2.6}$$

or equivalently $P(t,S) = P(t,T)\,P(t,T,S)$.

Each payoff has its own convention for measuring the time between two instances, including a different set of days in the calculation. Define $\tau(T,S)$ as the difference between T and S, expressed in year fractions. A typical *day count convention* is for example $\tau_{ACT/365}(T,S) = (S-T)/365$. For more details on different conventions the reader is referred to (Brigo and Mercurio, 2007).

The two quantities $D(t,T)$ and $P(t,T)$ are linked by relation (2.2) where the money market account is chosen as numéraire:

$$P(t,T) = B(t)\,\mathbb{E}_t^{\mathbb{Q}}\left[\frac{1}{B(T)}\right] = \mathbb{E}_t^{\mathbb{Q}}\left[e^{-\int_t^T r(s)ds}\right] = \mathbb{E}_t^{\mathbb{Q}}\left[D(t,T)\right],$$

with $\mathbb{Q}$ standing for the equivalent martingale measure induced by the numéraire $B(t)$, also known as the *risk neutral measure*. In particular, if r is deterministic, $D(t,T) = P(t,T)$ holds. In the case that r is stochastic, $D(t,T)$ represents a random quantity while $P(t,T)$ is deterministic.

The market distinguishes between *fixed* and *floating interest rates*. The former refers to a constant rate fixed at initiation time of a contract and that does not change over the instrument's lifetime. The latter represents a variable rate that is based on a reference rate.

The reference rate that will be considered in this thesis in relation to floating rate derivative products is the London Inter-bank Offered Rate (LIBOR). This rate represents the filtered average of bank estimates of interest rates at which a bank is willing to borrow for a given term in the interbank money market, the market in which banks provide unsecured short-term credits to one another. The LIBOR rate is quoted daily for different maturities ranging from 7 days to 1 year and it is fixed for the currencies EUR, USD, GBP, JPY and CHF.

An Overnight Indexed Swap (OIS) rate is an interest rate that banking institutions charge to other institutions in the overnight market, the market consisting of overnight transactions.[1] As the probability of default of one of the parties involved in the transaction is assumed to be very low due to the short loan period, an overnight rate has equally a low level of risk. It is considered by the market as the best proxy for a risk-free rate. The overnight rates for the currencies EUR, USD and GBP are, respectively, the Euro Overnight Index Average (EONIA), the effective Federal Funds Rate and the Sterling Overnight Index Average (SONIA).

2.3. BACHELIER'S MODEL AND BLACK'S FORMULA

Bachelier's model serves as an industry-standard method for pricing European options on forward contracts, relying on the sole assumption of normality of the underlying at expiry under a relevant measure. Because of this assumption, the model admits negative values of the underlying. Black's model, also known as Black-76, forms an alternative pricing model for European options. Contrary to Bachelier's model, the underlying at expiry is assumed to be originating from a log-normal process. These two models will be used in Subsection 2.5.1 to price swaptions and caps/floors.

Consider a European option with maturity T on a specific underlying with value $X(t)$, where $0 \leq t \leq T$. Let $F_T(t)$ be the forward price of $X(T)$ at t such that $F_T(t) = \mathbb{E}_t^{\mathbb{Q}}[X(T)]$. $\mathbb{Q}$ represents the equivalent measure induced by a numéraire $N(t)$. Let K be the strike price of the option and M the notional of the contract.

The value of a European option can typically be simplified to

$$V(t) = MN(t)\,\mathbb{E}_t^{\mathbb{Q}}[w(X(T)-K)], \tag{2.7}$$

where $w = 1$ refers to a call option and $w = -1$ to a put option.
When assuming that $X(T)$ is normally distributed with mean $F_T(t)$ and standard deviation $\sigma\sqrt{T-t}$, the expectation of (2.7) can be computed by means of Bachelier's model:

$$\begin{aligned} V(t) &= MN(t)\,Bachelier\left(t,T,F_T(t),K,\sigma\sqrt{T-t},w\right), \\ &= MN(t)\left(w(F_T(t)-K)\mathcal{N}(-wd)+\sigma\sqrt{T-t}\,n(d)\right), \end{aligned}$$

where

$$d = \frac{K-F_T(t)}{\sigma\sqrt{T-t}},$$

$$\mathcal{N}(x) = \int_{-\infty}^{x} \frac{1}{\sqrt{2\pi}} e^{-\frac{1}{2}y^2}\,dy,$$

$$n(x) = \frac{1}{\sqrt{2\pi}} e^{-\frac{1}{2}x^2}.$$

[1] Formally, an Overnight Indexed Swap (OIS) is an interest rate swap whose floating leg is indexed to an overnight rate, daily compounded over a specific term. The floating rate of an OIS is referred to as the OIS rate. The concept of a swap will be explained in Subsection 2.5.1.

However, if log-normal dynamics are assumed for $X(T)$, then Black's model can be used:

$$\begin{aligned} V(t) &= MN(t)\,Black\left(t,T,F_T(t),K,\sigma\sqrt{T-t},w\right), \\ &= MN(t)\left(w\left(F_T(t)\,\mathcal{N}(wd_1)-K\mathcal{N}(wd_2)\right)\right), \end{aligned}$$

where

$$\begin{aligned} d_1 &= \frac{\log\left(F_T(t)/K\right)+\sigma\sqrt{T-t}/2}{\sigma\sqrt{T-t}}, \\ d_2 &= d_1-\sigma\sqrt{T-t}(t). \end{aligned}$$

The *implied Bachelier* or *Black volatility* $\widetilde{\sigma}(t)$ is the value of the volatility of the underlying financial security such that, respectively,

$$MN(t)\,Bachelier\left(t,T,F_T(t),K,\widetilde{\sigma}(t)\sqrt{T-t}\right)=V_{market}(t),$$

or

$$MN(t)\,Black\left(t,T,F_T(t),K,\widetilde{\sigma}(t)\sqrt{T-t}\right)=V_{market}(t).$$

2.4. THE SINGLE-CURVE AND MULTI-CURVE FRAMEWORKS

Before the credit crunch of 2007, LIBOR rates were seen as risk-free rates and consequently, forward rates could be replicated by discount bonds. Interest rates of different index tenors would closely track each other, keeping a distance of a few basis points. As an example, the spread between the three-month LIBOR and the corresponding EONIA rate had (almost) always been well below 10 bp (see Figure 1.1). These spreads were considered to be negligible, which justified the use of a single curve to value interest rate instruments. This curve served both in the generation of future cash flows and in the calculation of their present value. This methodology is known as the single-curve (SC) framework.

After August 2007, the spread between market rates that had until then been equivalent widened, which led to a segmentation of the interest rate market along distinct tenors. Consequently, different forward LIBOR curves related to distinct tenors were required in order to project cash flows. The implicit assumption that the market is free of default risk broke and the LIBOR rates could not be considered risk-free anymore. For collateralized derivatives this meant that the LIBOR rate was no longer a suitable proxy for the discount rate.[1] In the current market conditions the OIS rate can be regarded as the best available proxy for risk-neutral rates and is therefore used for discounting. This approach, which uses multiple forward LIBOR curves to generate cash flows and one curve to discount it, is knows as the multi-curve (MC) framework.

As mentioned above, the SC framework considers a single curve $\mathtt{C}$ that is used for both discounting and forwarding cash flows, given by

$$\mathtt{C}=\{T\to P(t,T),\,T\geq t\}.^{2}$$

The *simply-compounded spot LIBOR rate* prevailing at time T for maturity $S>T$ is defined as

$$L(T,S)=\frac{1}{\tau(T,S)}\left(\frac{1-P(T,S)}{P(T,S)}\right). \tag{2.8}$$

Furthermore, the *simply-compounded forward LIBOR rate* prevailing at time t for expiry $T>t$ and maturity $S>T$ is given by

$$F(t;T,S)=\mathbb{E}_t^{\mathbb{Q}^S}\left[L(T,S)\right],$$

where $\mathbb{Q}^S$ denotes the S-forward measure induced by the numéraire $P(t,S)$. Note that $F(T;T,S)=L(T,S)$ is valid and that $F(t;T,S)$ is a martingale under $\mathbb{Q}^S$ since it holds that

$$\mathbb{E}_t^{\mathbb{Q}^S}\left[F(T;T,S)\right]=\mathbb{E}_t^{\mathbb{Q}^S}\left[\mathbb{E}_T^{\mathbb{Q}^S}\left[L(T,S)\right]\right],$$

[1] Only fully collateralized derivatives are considered in this thesis.

[2] Strictly speaking, this curve is in the form of a zero rate representation, which can be translated into discount bonds by applying specific transformations.

$$= \mathbb{E}_t^{\mathbb{Q}^S} [L(T,S)],$$
$$= F(t;T,S).$$

Moreover, because quantity (2.8) is deflated by a zero coupon bond having maturity S, it follows that it is a martingale under the measure $\mathbb{Q}^S$. Hence, the forward LIBOR rate can be replicated by discounts bonds:

$$F(t;T,S) = \frac{1}{\tau(T,S)}\left(\frac{P(t,T)-P(t,S)}{P(t,S)}\right). \tag{2.9}$$

Throughout this thesis, the MC framework consisting of two distinct curves will be considered. Let $\mathtt{C}^d$ be the curve used for discounting future cash flows, expressed as a continuous term structure of discount factors. As pointed out previously, in this research the discount curve with reference date t is represented by the OIS zero-coupon curve

$$\mathtt{C}^d = \left\{T \to P^d(t,T), T \geq t\right\},$$

stripped from OIS swap rates and defined for all maturities T. Let $F^d(t;T,T+x)$ be the forward rate defined on $\mathtt{C}^d$, having tenor x. This rate is referred to as the forward OIS rate and is given by

$$F^d(t;T,T+x) = \mathbb{E}_t^{\mathbb{Q}_d^{T+x}}\left[L^d(T,T+x)\right], \tag{2.10}$$

with $\mathbb{Q}_d^{T+x}$ induced by $P^d(t,T+x)$,[1] and $L^d(T,T+x)$ representing the simply-compounded spot rate with tenor x, computed on $\mathtt{C}^d$ as

$$L^d(T,T+x) = \frac{1}{\tau(T,T+x)}\left(\frac{1-P^d(T,T+x)}{P^d(T,T+x)}\right).$$

Since $L^d(T,T+x)$ is deflated by $P^d(T,T+x)$, it is a martingale under $\mathbb{Q}_d^{T+x}$. From (2.10) follows that the forward OIS rate in the MC framework can be replicated by risk-free discount bounds:

$$F^d(t;T,T+x) = \frac{1}{\tau(T,T+x)}\left(\frac{P^d(t,T)-P^d(t,T+x)}{P^d(t,T+x)}\right). \tag{2.11}$$

Furthermore, denote by $\mathtt{C}^x$ the forward yield curve corresponding to a specific tenor x, where commonly $x \in \{1\text{M}, 3\text{M}, 6\text{M}, 12\text{M}\}$. This curve at time t is composed by

$$\mathtt{C}^x = \left\{x \to F^x(t;T,T+x), T \geq t\right\},$$

where the forward LIBOR rates in the MC framework assume the definition

$$F^x(t;T,T+x) = \mathbb{E}_t^{\mathbb{Q}_d^{T+x}}\left[L^x(T,T+x)\right], \tag{2.12}$$

with $L^x(T,T+x)$ representing the simply-compounded spot LIBOR rate having tenor x. As, in the MC framework, the LIBOR rate is not considered to be a risk-free rate anymore, $L^x(T,T+x)$ cannot be replicated by risk-free bonds. For this reason the forward LIBOR rate cannot be expressed in zero coupon bonds as was done in the SC setup. However, using the same line of reasoning as above, it can be shown that $F^x(t;T,T+x)$ is a martingale under $\mathbb{Q}_d^{T+x}$. Furthermore, from (2.12) follows that $F^x(T;T,T+x) = L^x(T,T+x)$.

It can be observed that the SC framework is a special case of the MC setup as the latter approach collapses to the SC scenario when considering $\mathtt{C}^x = \mathtt{C}$ and $\mathtt{C}^d = \mathtt{C}$.

2.5. INTEREST RATE INSTRUMENTS

This section provides an overview of the fundamental fixed income instruments that define the interest rate market. In practice, these basic derivatives often serve as calibration tools in the parametrization of the LIBOR Market Model, while more complex and exotic derivatives are ultimately priced by the calibrated model.

[1] From now on, the measures in the MC framework will adopt the notation $\mathbb{Q}_y^z$, where the subscript y (mainly d) identifies the underlying yield curve and the subscript z defines the measure in question.

The reader will get acquainted with securities that involve the simply-compounded LIBOR rates introduced earlier. It is first shown how interest rate swaps are priced under the MC framework and later how the valuation expressions of these instruments is simplified in order to accommodate the SC setup. Market formulas for caps/floors and swaptions are given for both frameworks.

Consider a finite set of *tenor dates* $\{T_m\}_{m=0}^N$ such that $0 = T_0 < T_1 < \ldots < T_N$, and denote by τ_m the length of the period $[T_m, T_{m+1}]$, expressed in year fractions. Denote the forward LIBOR rate over $[T_i, T_{i+1}]$ as of time t by $F_i(t) := F(t; T_i, T_{i+1})$ in the SC setup and by $F_i^x(t) := F^x(t; T_i, T_{i+1})$ in the MC framework. Let $\mathbf{F}(t) = (F_0(t), \ldots, F_{N-1}(t))^\top$ and $\mathbf{F}^x(t) = \left(F_0^x(t), \ldots, F_{N-1}^x(t)\right)^\top$ be N-dimensional vectors of forward rates in the SC and MC case, respectively. Note that $F_i(t)$ and $F_i^x(t)$ solely exist when $0 \le t \le T_i$.
Furthermore, for simplicity of notation, denote by $P_i(t) := P(t, T_i)$ the time t value in the SC setup of a zero coupon bond with maturity T_i, for $i \in \{0, \ldots, N\}$, where $t \le T_i$. Similarly, $P_i^d(t) := P^d(t, T_i)$. Define the $N+1$-dimensional vectors $\mathbf{P}(t) = (P_0(t), \ldots, P_N(t))^\top$ and $\mathbf{P}^d(t) = \left(P_0^d(t), \ldots, P_N^d(t)\right)^\top$ for, respectively, the SC and MC frameworks.

2.5.1. PLAIN VANILLA INTEREST RATE SWAPS

An *interest rate swap* is a contract in which two parties agree to exchange streams of cash flows at future predefined dates. These streams are known as the *legs of the swap*. A plain vanilla fixed-for-floating swap, from now on referred to as a swap, involves a leg consisting of fixed rate payments and a leg of floating rate payments. Throughout this thesis the floating leg will be indexed to the LIBOR rate.

The frequency of the payment periods of the legs can be different but for simplicity of notation it is assumed that the frequency is the same. In this thesis the generalization is made that the payments are denoted in the same currency and that all cash flow exchange dates of the fixed and floating legs coincide. Furthermore the legs are based on the same notional amount which is never physically exchanged but serves as a basis for determining the interest payments. Moreover, in practice only the difference of the two cash flows at each payment date is paid out by one of the two parties.

The terminology of a swap refers to the fixed leg. The contract in which a fixed leg is paid and a floating leg is received is referred to as a *payer interest rate swap*, while the opposite case is known as a *receiver interest rate swap*.

Consider a swap over the time interval $[T_r, T_N]$, with payment dates T_{i+1}, $i \in \{r, \ldots, N-1\}$. At each time instant T_{i+1} the fixed leg pays an interest on the notional M based on the fixed rate K while the floating leg payments rest on the LIBOR rate set at the previous time instant T_i. The LIBOR rate resets at dates $T_r, \ldots, T_{N-1}$ and the payments occur at dates $T_{r+1}, \ldots, T_N$. The swap tenor is defined as the time distance between T_r and T_N, expressed in year fractions. Commonly, a $T_r \times (T_N - T_r)$ swap refers to a swap with settlement date T_r and swap tenor $T_N - T_r$.

Let T_m, T_r and T_N be time instants such that $T_m \le T_r < T_N$. In the MC framework, the value of an interest rate swap over $[T_r, T_N]$ at T_m, depending on the states $\mathbf{P}^d(T_m)$and $\mathbf{F}^x(T_m)$, is determined by summing over all the swap's payments and discounting the cash flows to time T_m:

$$\begin{aligned} S_{[r,N]}\left(T_m, \mathbf{P}^d(T_m), \mathbf{F}^x(T_m)\right) &= \sum_{j=r}^{N-1} P_{j+1}^d(T_m)\, \mathbb{E}_{T_m}^{\mathbb{Q}_d^{T_{j+1}}}\left[M\tau_j\, w\left(L^x\left(T_j, T_{j+1}\right) - K\right)\right], \\ &= M\sum_{j=r}^{N-1} \tau_j P_{j+1}^d(T_m)\, w\left(\mathbb{E}_{T_m}^{\mathbb{Q}_d^{T_{j+1}}}\left[L^x\left(T_j, T_{j+1}\right)\right] - K\right), \\ &= M\sum_{j=r}^{N-1} \tau_j P_{j+1}^d(T_m)\, w\left(F_j^x(T_m) - K\right), \end{aligned} \tag{2.13}$$

where $\mathbb{Q}_d^{T_{j+1}}$ is the T_{j+1}-forward measure related to numéraire $P_{j+1}^d(t)$ and w is an indicator function with $w = 1$ denoting a payer swap and $w = -1$ a receiver swap. Note from (2.13) that the value of a swap at time T_m is solely dependent on the term structure of interest rates observed at that time. Expression (2.13) can be

rewritten as

$$S_{[r,N]}\left(T_m,\mathbf{P}^d(T_m),\mathbf{F}^x(T_m)\right)=M\sum_{j=r}^{N-1}\tau_j P_{j+1}^d(T_m)\,w\left(\frac{\sum_{j=r}^{N-1}\tau_j P_{j+1}^d(T_m)}{\sum_{j=r}^{N-1}\tau_j P_{j+1}^d(T_m)}F_j^x(T_m)-K\right),$$
$$=MA_{[r,N]}\left(T_m,\mathbf{P}^d(T_m)\right)w\left(R_{[r,N]}\left(T_m,\mathbf{P}^d(T_m),\mathbf{F}^x(T_m)\right)-K\right), \tag{2.14}$$

where

$$A_{[r,N]}\left(T_m,\mathbf{P}^d(T_m)\right)=\sum_{j=r}^{N-1}\tau_j P_j^d(T_m),$$

is known as the *annuity* of the swap and

$$R_{[r,N]}\left(T_m,\mathbf{P}^d(T_m),\mathbf{F}^x(T_m)\right)=\frac{\sum_{j=r}^{N-1}\tau_j P_{j+1}^d(T_m)}{\sum_{j=r}^{N-1}\tau_j P_{j+1}^d(T_m)}F_j^x(T_m),$$
$$=\frac{\sum_{j=r}^{N-1}\tau_j P_{j+1}^d(T_m)}{A_{[r,N]}\left(T_m,\mathbf{P}^d(T_m)\right)}F_j^x(T_m), \tag{2.15}$$

is called the *swap rate*. The latter is interpreted as the fixed rate K such that the value of the swap at time T_m is equal to 0. It can be seen as the weighted average of the forward LIBOR rates. Furthermore, the swap rate is a martingale under the annuity measure $\mathbb{Q}_d^{r,N}$, induced by $A_{[r,N]}\left(t,\mathbf{P}^d(t)\right)$.

In the SC framework, equation (2.13) can be simplified as the forward LIBOR rate can be replicated by zero-coupon bonds. The adapted formulation becomes:

$$S_{[r,N]}(T_m,\mathbf{P}(T_m),\mathbf{F}(T_m))=M\sum_{j=r}^{N-1}\tau_j P_{j+1}(T_m)\,w\left(F_j(T_m)-K\right),$$
$$=M\sum_{j=r}^{N-1}\tau_j P_{j+1}(T_m)\,w\left(\frac{1}{\tau_j}\left(\frac{P_j(T_m)-P_{j+1}(T_m)}{P_{j+1}(T_m)}\right)-K\right),$$
$$=M\sum_{j=r}^{N-1}w\left(P_j(T_m)-P_{j+1}(T_m)-\tau_j K P_{j+1}(T_m)\right),$$
$$=Mw\left(P_r(T_m)-P_N(T_m)-K\sum_{j=r}^{N-1}\tau_j P_{j+1}(T_m)\right), \tag{2.16}$$

where the second equality follows from (2.9). Note from (2.16) that the floating leg of the swap is independent from the LIBOR rate tenor, contrary to the floating leg in the MC case. Furthermore, the swap rate expression in the SC framework assumes the following form:

$$R_{[r,N]}(T_m,\mathbf{P}(T_m),\mathbf{F}(T_m))=\frac{P_r(T_m)-P_N(T_m)}{A_{[r,N]}(T_m,\mathbf{P}(T_m))}.$$

2.5.2. EUROPEAN SWAPTIONS

The actively traded swap options, commonly referred to as *swaptions*, are a large class of vanilla interest rate derivatives. As the name does suggest, swaptions are options on interest rate swaps. A European swaption is an option granting its holder the right, but not the obligation, to enter into a plain vanilla interest rate swap at a future date, the swaption's settlement date, at a given fixed rate. The market distinguishes *payer* and *receiver swaptions*, which have, respectively, payer and receiver swaps as underlying securities.

Consider a $T_r\times(T_N-T_r)$ swaption with notional M and fixed strike K, where $T_r<T_N$. The holder of a swaption will exercise the option at time T_r if the value of the underlying contract is positive, otherwise the swaption will expire without being exercised, resulting in a value equal to zero. In the MC framework, the value $\widetilde{S}_{[r,N]}\left(T_r,\mathbf{P}^d(T_r),\mathbf{F}^x(T_r)\right)$ of a European swaption over $[T_r,T_N]$ at time T_r , depending on the states $\mathbf{P}^d(T_r)$ and $\mathbf{F}^x(T_r)$, is determined using the result of (2.14):

$$\widetilde{S}_{[r,N]}\left(T_r,\mathbf{P}^d(T_r),\mathbf{F}^x(T_r)\right)=\left(S_{[r,N]}\left(T_r,\mathbf{P}^d(T_r),\mathbf{F}^x(T_r)\right)\right)^+,$$

$$= \left(MA_{[r,N]}\left(T_r, \mathbf{P}^d(T_r)\right) w\left(R_{[r,N]}\left(T_r, \mathbf{P}^d(T_r), \mathbf{F}^x(T_r)\right) - K\right)\right)^+,$$
$$= MA_{[r,N]}\left(T_r, \mathbf{P}^d(T_r)\right)\left(w\left(R_{[r,N]}\left(T_r, \mathbf{P}^d(T_r), \mathbf{F}^x(T_r)\right) - K\right)\right)^+,$$

with $w = 1$ denoting a payer swaption and $w = -1$ representing a receiver swaption. For any time T_m such that $T_0 \leq T_m \leq T_r$, the no-arbitrage relation (2.2) gives:

$$\widetilde{S}_{[r,N]}\left(T_m, \mathbf{P}^d(T_m), \mathbf{F}^x(T_m)\right) = A_{[r,N]}\left(T_m, \mathbf{P}^d(T_m)\right)\mathbb{E}_{T_m}^{\mathbb{Q}_d^{r,N}}\left[\frac{MA_{[r,N]}\left(T_r, \mathbf{P}^d(T_r)\right)\left(w\left(R_{[r,N]}\left(T_r, \mathbf{P}^d(T_r), \mathbf{F}^x(T_r)\right) - K\right)\right)^+}{A_{[r,N]}\left(T_r, \mathbf{P}^d(T_r)\right)}\right],$$
$$= MA_{[r,N]}\left(T_m, \mathbf{P}^d(T_m)\right)\mathbb{E}_{T_m}^{\mathbb{Q}_d^{r,N}}\left[\left(w\left(R_{[r,N]}\left(T_r, \mathbf{P}^d(T_r), \mathbf{F}^x(T_r)\right) - K\right)\right)^+\right]. \quad (2.17)$$

Clearly, a swaption depends on the joint distribution of the spanning forward LIBOR rates. Note that a payer swaption can be interpreted as a European call option on the swap rate with strike K. Likewise, a receiver swaption is expressed as a European put option on $R_{[r,N]}\left(T_r, \mathbf{P}^d(T_r), \mathbf{F}^x(T_r)\right)$ struck at K. Hence, the expectation of (2.17) can be computed by means of Bachelier's or Black's model, see Section 2.3. If $R_{[r,N]}\left(T_r, \mathbf{P}^d(T_r), \mathbf{F}^x(T_r)\right)$ is assumed to be normally distributed under $\mathbb{Q}_d^{r,N}$ with mean $R_{[r,N]}\left(T_m, \mathbf{P}^d(T_m), \mathbf{F}^x(T_m)\right)$ and standard deviation $\sigma_{[r,N]}\sqrt{T_r - T_m}$, it follows that

$$\widetilde{S}_{[r,N]}\left(T_m, \mathbf{P}^d(T_m), \mathbf{F}^x(T_m)\right) = MA_{[r,N]}\left(T_m, \mathbf{P}^d(T_m)\right)$$
$$Bachelier\left(T_m, T_r, R_{[r,N]}\left(T_m, \mathbf{P}^d(T_m), \mathbf{F}^x(T_m)\right), K, \sigma_{[r,N]}\sqrt{T_r - T_m}, w\right).$$

If, instead, the dynamics of the swap rate are assumed to be driven by a log-normal process under the measure induced by $A_{[r,N]}\left(t, \mathbf{P}^d(t)\right)$, the price of a European swaption is computed as

$$\widetilde{S}_{[r,N]}\left(T_m, \mathbf{P}^d(T_m), \mathbf{F}^x(T_m)\right) = MA_{[r,N]}\left(T_m, \mathbf{P}^d(T_m)\right)$$
$$Black\left(T_m, T_r, R_{[r,N]}\left(T_m, \mathbf{P}^d(T_m), \mathbf{F}^x(T_m)\right), K, \sigma_{[r,N]}\sqrt{T_r - T_m}, w\right).$$

In the SC framework, the pricing formula of a swaption is given by

$$\widetilde{S}_{[r,N]}\left(T_m, \mathbf{P}(T_m), \mathbf{F}(T_m)\right) = MA_{[r,N]}\left(T_m, \mathbf{P}(T_m)\right)$$
$$Bachelier\left(T_m, T_r, R_{[r,N]}\left(T_m, \mathbf{P}(T_m), \mathbf{F}(T_m)\right), K, \sigma_{[r,N]}\sqrt{T_r - T_m}, w\right),$$

or

$$\widetilde{S}_{[r,N]}\left(T_m, \mathbf{P}(T_m), \mathbf{F}(T_m)\right) = MA_{[r,N]}\left(T_m, \mathbf{P}(T_m)\right)$$
$$Black\left(T_m, T_r, R_{[r,N]}\left(T_m, \mathbf{P}(T_m), \mathbf{F}(T_m)\right), K, \sigma_{[r,N]}\sqrt{T_r - T_m}, w\right),$$

depending whether the swap rate follows, respectively, a normal or log-normal distribution.

The prices of the European swaptions can be expressed in terms of their implied Bachelier/Black volatilities $\widetilde{\sigma}_{[r,N]}$.

To define the *moneyness* of a swaption, let $K_{\text{ATM}} = R_{[r,N]}\left(T_0, \mathbf{P}(T_0), \mathbf{F}(T_0)\right)$ and $K_{\text{ATM}} = R_{[r,N]}\left(T_0, \mathbf{P}^d(T_0), \mathbf{F}^x(T_0)\right)$ in, respectively, the SC and MC frameworks. Both payer and receiver swaptions are said to be *at-the-money* (ATM) if $K = K_{\text{ATM}}$. When $w = 1$, the swaption is *in-the-money* (ITM) for $K < K_{\text{AMT}}$ and *out-of-the-money* (OTM) if $K > K_{\text{ATM}}$. The reverse is true for a receiver swaption.

The concept of *co-terminal swaptions* will be relevant in Chapter 4, when the approach for calibrating the MC LMM will be explained. It refers to a strip of swaptions $\left\{T_{r_i} \times \left(T_N - T_{r_i}\right) : i = 1, \ldots, n\right\}$, where $0 \leq T_{r_1} < \ldots < T_{r_n} < T_N$ and $\left\{T_{r_i}\right\}_{i=1}^{n} \subset \left\{T_p\right\}_{p=0}^{N}$. These instruments have the same maturity T_N but different settlement dates T_{r_i}.

2.5.3. CAPS AND FLOORS

Another class of liquid interest rate vanilla options are caps and floors. These instruments may be used for calibration purposes. An *interest rate cap* is a financial security that allows the holder of an asset paying the floating rate to benefit from floating rates below a certain reference rate and to protect the holder from higher rates. For an investor with an asset receiving the floating rate, an *interest rate floor* is designed to protect him from rates under a predetermined fixed level and to allow him to benefit from higher rates.

A cap/floor can be decomposed into a series of European call/put options on successive LIBOR rates, known as *caplets/floorlets*, spanning the lifetime of the cap/floor in question. Consider a T_j-caplet/floorlet defined on the time interval $\left[T_j, T_{j+1}\right]$, for $j \in \{0,\ldots,N-1\}$. Furthermore, let M be the notional amount of the contract and K the predetermined fixed rate. Under the MC framework, the payoff at time T_{j+1} of the caplet/floorlet amounts to:

$$M\tau_j \left(w\left(L^x\left(T_j,T_{j+1}\right)-K\right)\right)^+,$$

where w is an indicator function with $w=1$ denoting a caplet and $w=-1$ a floorlet. The price of a caplet/floorlet at time T_n, where $T_n \leq T_j$, is determined by discounting the cash flow to T_n:

$$c_j\left(T_n,\mathbf{P}^d\left(T_n\right),\mathbf{F}^x\left(T_n\right)\right) = M\tau_j P^d_{j+1}\left(T_n\right)\mathbb{E}^{\mathbb{Q}^{T_{j+1}}_d}_{T_n}\left[\left(w\left(L^x\left(T_j,T_{j+1}\right)-K\right)\right)^+\right].$$

Now consider three time instants T_m, T_r and T_N such that $T_m \leq T_r < T_N$. As mentioned before, a cap/floor is a strip of caplets/floorlets on successive LIBOR rates, each with notional M and same strike K. Hence, the value $C_{[r,N]}\left(T_m,\mathbf{P}^d\left(T_m\right),\mathbf{F}^x\left(T_m\right)\right)$ of a cap/floor over $[T_r,T_N]$ at time T_m, depending on the states $\mathbf{P}^d\left(T_m\right)$ and $\mathbf{F}^x\left(T_m\right)$, is given by the sum of the individual caplets/floorlets at T_m:

$$\begin{aligned} C_{[r,N]}\left(T_m,\mathbf{P}^d\left(T_m\right),\mathbf{F}^x\left(T_m\right)\right) &= \sum_{j=r}^{N-1} c_j\left(T_m,\mathbf{P}^d\left(T_m\right),\mathbf{F}^x\left(T_m\right)\right), \\ &= M\sum_{j=r}^{N-1}\tau_j P^d_{j+1}\left(T_m\right)\mathbb{E}^{\mathbb{Q}^{T_{j+1}}_d}_{T_m}\left[\left(w\left(L^x\left(T_j,T_{j+1}\right)-K\right)\right)^+\right]. \end{aligned} \tag{2.18}$$

The marginal distributions of the forward LIBOR rates spanning the lifetime of the derivative security are sufficient to establish the price of caps/floors. In contrast to European swaptions, their joint distribution does not play a role in computing the expectation. Recalling that $L^x\left(T_j,T_{j+1}\right) = F^x_j\left(T_j\right)$, (2.18) can be expressed as

$$C_{[r,N]}\left(T_m,\mathbf{P}^d\left(T_m\right),\mathbf{F}^x\left(T_m\right)\right) = M\sum_{j=r}^{N-1}\tau_j P^d_{j+1}\left(T_m\right)\mathbb{E}^{\mathbb{Q}^{T_{j+1}}_d}_{T_m}\left[\left(w\left(F^x_j\left(T_j\right)-K\right)\right)^+\right]. \tag{2.19}$$

This expectation can be computed by means of Bachelier's model when assuming normal dynamics for all forward LIBOR rates $F^x_j\left(T_j\right)$, $j \in \{r,\ldots,N-1\}$, with respective means $F^x_j\left(T_m\right)$ and standard deviations $\sigma_j\sqrt{T_j-T_m}$. The price of a cap/floor then becomes

$$C_{[r,N]}\left(T_m,\mathbf{P}^d\left(T_m\right),\mathbf{F}^x\left(T_m\right)\right) = M\sum_{j=r}^{N-1}\tau_j P^d_{j+1}\left(T_m\right) Bachelier\left(T_m,T_j,F^x_j\left(T_m\right),K,\sigma_j\sqrt{T_j-T_m},w\right).$$

If the forward rates are assumed to follow a log-normal distribution, the price of a cap/floor is given by

$$C_{[r,N]}\left(T_m,\mathbf{P}^d\left(T_m\right),\mathbf{F}^x\left(T_m\right)\right) = M\sum_{j=r}^{N-1}\tau_j P^d_{j+1}\left(T_m\right) Black\left(T_m,T_j,F^x_j\left(T_m\right),K,\sigma_j\sqrt{T_j-T_m},w\right).$$

The price at time T_m of a cap/floor over $[T_r,T_N]$ evaluated under the SC setup can be determined by either

$$C_{[r,N]}\left(T_m,\mathbf{P}\left(T_m\right),\mathbf{F}\left(T_m\right)\right) = M\sum_{j=r}^{N-1}\tau_j P_{j+1}\left(T_m\right) Bachelier\left(T_m,T_j,F_j\left(T_m\right),K,\sigma_j\sqrt{T_j-T_m},w\right),$$

or

$$C_{[r,N]}\left(T_m,\mathbf{P}\left(T_m\right),\mathbf{F}\left(T_m\right)\right) = M\sum_{j=r}^{N-1}\tau_j P_{j+1}\left(T_m\right) Black\left(T_m,T_j,F_j\left(T_m\right),K,\sigma_j\sqrt{T_j-T_m},w\right),$$

depending whether normality or log-normality of the forward LIBOR rates is assumed.

Let $\widetilde{\sigma}_j$ denote the implied Bachelier/Black volatility corresponding to the j^{th} caplet/floorlet. A cap/floor can be quoted in terms of its implied flat volatility $\widetilde{\sigma}$. This is the constant implied volatility that provides the exact market price of the option when inserted for $\widetilde{\sigma}_j,\ j \in \{r,\ldots,N-1\}$, in each caplet/floorlet valuation formula. This flat volatility is constant for each caplet/floorlet and varies per cap/floor depending on the maturity of the derivative.

To define the moneyness of a cap and a floor, let $K_{\text{ATM}} = R_{[r,N]}\left(T_0, \mathbf{P}\left(T_0\right), \mathbf{F}\left(T_0\right)\right)$ and $K_{\text{ATM}} = R_{[r,N]}\left(T_0, \mathbf{P}^d\left(T_0\right), \mathbf{F}^x\left(T_0\right)\right)$ in, respectively, the SC and MC frameworks. Both instruments are said to be ATM when $K = K_{\text{ATM}}$. In the case of $w = 1$, the cap is ITM when $K < K_{\text{ATM}}$ and OTM if $K > K_{\text{ATM}}$. For the floor the reverse is true.

3

THE LIBOR MARKET MODEL

This chapter is devoted to an extensive discussion on the LIBOR Market Model (LMM). The classical, single-curve LMM will firstly be introduced in Section 3.1 as its model formulation will later be extended in order to accommodate the use of multiple curves. The SC LMM models the dynamics of the forward LIBOR rates, which are fully characterized by the specification of the correlation and instantaneous volatility functions. Possible parametrizations of these structures are treated in Subsection 3.2.1. To be able to simulate the forward LIBOR rates in practice, their dynamics have to be specified under one common measure. In Section 3.3 the characterization of the LMM under the spot measure is presented, whereafter the rank reduction technique to speed up the simulations is introduced in Section 3.4. Section 3.5 presents the formulation of the LMM in the multi-curve framework. A complete description of the application of the Monte Carlo method to price interest rate instruments is given in Section 3.6, together with an empirical test on the identification of the appropriate time step and a suitable number of simulations. In order to be able to calibrate the MC LMM to the swaption market, it is important to price swaptions under the model. To this end, an approximation formula for the swap rate volatilitiy is derived in Section 3.7, whose accuracy is tested in Section 3.8. For completeness, the valuation formulas for caps/floors under the MC LMM are included in Section 3.7 as well.

3.1. MODEL DYNAMICS

Consider a finite set of tenor dates $\{T_m\}_{m=0}^{N}$ such that $0 = T_0 < T_1 < \ldots < T_N$, and denote by τ_m the length of the interval $[T_m, T_{m+1}]$, expressed in year fractions. Let $F_k(t)$ be the forward LIBOR rate prevailing over the interval $[T_k, T_{k+1}]$, where $0 \leq t \leq T_k$, and denote by $\mathbf{F}(t) = (F_0(t), \ldots, F_{N-1}(t))^\top$ the N-dimensional vector consisting of these rates. Introduce $\alpha(t)$ as the time index such that $\alpha(t) = \min(k : T_k \geq t)$ holds. Hence, $T_{\alpha(t)-1} < t \leq T_{\alpha(t)}$ with $T_{-1} = 0$ is valid. This parameter represents the first upcoming reset moment with respect to time t, if t is not equal to a fixing date. In the case of t coinciding with a reset date T_k, $\alpha(t)$ represents this particular fixing date.

Once the fixing time T_k, $k \in \{1, \ldots, N-1\}$, of a certain rate $F_k(t)$ has been reached, the forward rate will remain constant for all $t \geq T_k$. Consequently, there is no need to model the rates the fixing date of which has already expired. Only the forward rates $F_{\alpha(t)}(t), F_{\alpha(t)+1}(t), \ldots, F_{N-1}(t)$ need to be simulated. As shown in Section 2.4, the forward LIBOR rate $F_k(t)$ has to be a martingale in the T_{k+1}-forward measure $\mathbb{Q}^{T_{k+1}}$. According to the Martingale Representation Theorem (Shreve, 2004), it then holds that

$$dF_k(t) = \phi(F_k(t))\,\mathbf{s}_k(t)^\top\, d\mathbf{W}^{\mathbb{Q}^{T_{k+1}}}(t), \quad 0 \leq t \leq T_k, \quad k \in \{\alpha(t), \ldots, N-1\},$$

where $\mathbf{W}^{\mathbb{Q}^{T_{k+1}}}(t)$ is a $\mathbb{R}^h$-valued, element-wise independent Brownian motion under $\mathbb{Q}^{T_{k+1}}$ and $\mathbf{s}_k(t,)$ is a h-dimensional vector that is allowed to depend on the current time t, but that has to be deterministic and bounded.[1] The function $\phi(F_k(t))$ appears in different parametrizations, depending on the desired distribution of the forward LIBOR rate dynamics. The formulation $\phi(F_k(t)) = 1$ models normally distributed forward

[1] In theory, $\mathbf{s}_k(t)$ can be a stochastic process. This type of diffusion coefficient give rise to the so-called stochastic volatility market models, whose main advantage is the capacity to reproduce the implied volatility smiles and skews as can be seen in the market. However, this is not the scope of this thesis and therefore a deterministic function $\mathbf{s}_k(t)$ will be considered throughout this thesis.

rates, while $\phi(F_k(t)) = F_k(t)$ specifies log-normal dynamics. The value h, $1 \le h \le N$, represents the number of independent driving Brownian Motions, also called factors. If $h = N$, the forward rates are said to be modeled under *full rank*, whereas for $h < N$ they are modeled under *reduced rank*.

Under the measure $\mathbb{Q}^{T_{k+1}}$ only the forward LIBOR rate $F_k(t)$ will be a martingale. In order to develop an arbitrage-free framework, it is required that all forward rates are martingales under a specific measure. When modeling the forward rate processes in $\mathbb{Q}^{T_{k+1}}$, the dynamics must be described as

$$dF_i(t) = \phi(F_i(t))\,\mathbf{s}_i(t)^\top \left(\mu_i(t,\mathbf{F}(t))\,dt + d\mathbf{W}^{\mathbb{Q}^{T_{k+1}}}(t)\right), \quad 0 \le t \le T_i, \quad i \in \{\alpha(t),\ldots,N-1\}, \tag{3.1}$$

with the drift parameters given by

$$\mu_i(t,\mathbf{F}(t)) \begin{cases} -\sum_{j=i+1}^{k} \frac{\tau_j \phi(F_j(t))\mathbf{s}_j(t)}{1+\tau_j F_j(t)}, & \text{for } i < k, \\ 0, & \text{for } i = k, \\ \sum_{j=i+1}^{k} \frac{\tau_j \phi(F_j(t))\mathbf{s}_j(t)}{1+\tau_j F_j(t)}, & \text{for } i > k. \end{cases}$$

See (Brigo and Mercurio, 2007) for a proof.

The term $\mathbf{s}_i(t)$ in (3.1) determines both the volatility and the correlation structure. A common representation for the diffusion coefficient is

$$\mathbf{s}_i(t) = \sigma_i(t)\,\boldsymbol{\lambda}_i(t), \tag{3.2}$$

where $\sigma_i(t)$ represents the total (deterministic) volatility of the i^{th} forward LIBOR rate and $\boldsymbol{\lambda}_i(t)$ is a bounded, h- dimensional vector-valued deterministic function defined as $\boldsymbol{\lambda}_i(t) = \mathbf{s}_i(t) / \|\mathbf{s}_i(t)\|$ (a proof is found in (Rebonato, 2002)).

The correlation among two forward rate increments $dF_i(t)$ and $dF_m(t)$, where $i, m \in \{0,\ldots,N-1\}$, has the form[1]

$$\begin{aligned} \rho(dF_i(t), dF_m(t)) &= \frac{\mathbf{s}_i(t)^\top \mathbf{s}_m(t)}{\|\mathbf{s}_i(t)\|\,\|\mathbf{s}_m(t)\|}, \\ &= \boldsymbol{\lambda}_i(t)^\top \boldsymbol{\lambda}_m(t), \end{aligned}$$

with $\|\cdot\|$ representing the Euclidean norm. For simplicity of notation, let $\rho_{i,m}(t) := \rho(dF_i(t), dF_m(t))$. $\rho_{i,m}(t) = 1$ always holds for $h = 1$, resulting in perfectly correlated forward rates. When more Brownian motions are added, the ability to capture complicated correlated structures improves. This phenomenon is referred to as decorrelation. On the downside, the model becomes more complex and the computational effort increases.

The representation (3.2) formally separates the correlation and the volatility structures. To fully characterize the dynamics of the forward rates in the LMM, the function $\sigma_i(t)$ and the matrix $\boldsymbol{\rho}(t)$, whose entries are given by $\rho_{i,m}(t)$, have to be exogenously specified. A choice for a possible volatility and correlation parametrization is given in Section 3.2, where $h = N$ is assumed. The implications of modeling the reduced rank dynamics for the correlation matrix are explained in Section 3.4.[2]

3.2. SPECIFICATION OF THE MODEL INPUTS

One of the main advantages of the LMM is the high degree of freedom to choose distinct volatility and correlation structures. Each characterization gives rise to a different version of the model. The simultaneous specification of the time-dependent volatility and correlation entirely determines the dynamics of the forward rates. In this chapter, a way to describe the instantaneous volatility function $\sigma_i(t)$ and the correlation function $\boldsymbol{\rho}(t)$ is presented.

[1] This expression follows from the correlation definition $\rho\left(dF_i(t), dF_m(t)\right) = \frac{\langle dF_i(t), dF_m(t)\rangle}{\sqrt{\langle dF_i(t)\rangle\langle dF_m(t)\rangle}}$.

[2] Simulating the forward LIBOR rates under reduced rank has no influence on the function $\sigma_i(t)$ as it does not depend on h.

3.2.1. INSTANTANEOUS VOLATILITY PARAMETRIZATION

A variety of choices and possibilities exists for modeling the instantaneous volatility $\sigma_i(t)$ of a specific forward rate $F_i(t)$. Volatilities show a complex functional dependence on a set of different drivers, the calendar time t and the expiry date T_i of the rate being the most common ones. Through the dependence on maturity T_i, different forward rates respond in distinct ways, at the same point in time, to the same Brownian shock. In a similar way, different values of $T_i - t$, representing the residual time to maturity, lead to distinct responses of one specific rate to Brownian shocks of the same magnitude.

When choosing a particular shape of the instantaneous volatility, it is important to have a view on the evolution of the term structure of the caplet implied Bachelier/Black volatilities $\widetilde{\sigma}_i(t)$, which are directly connected to the instantaneous volatilities $\sigma_i(t)$. This term structure is expressed at a particular time T_i by the graphical representation consisting of the points

$$\{(T_{i+1}, \widetilde{\sigma}_{i+1}(T_i)), (T_{i+2}, \widetilde{\sigma}_{i+2}(T_i)), \ldots, (T_{N-1}, \widetilde{\sigma}_{N-1}(T_i))\},$$

where

$$\widetilde{\sigma}_m(t) = \sqrt{\frac{\int_t^{T_m} (\sigma_m(s))^2 \, ds}{T_m - t}}, \quad m = i+1, \ldots, N-1,$$

represents the implied Bachelier/Black volatility. Hence, the term structure of volatilities at time T_i is the graphical representation of the reset dates T_m, $m = i+1, \ldots, N-1$, against the average volatilities $\widetilde{\sigma}_m(T_i)$ of the instantaneous volatilities $\sigma_m(t)$ over the period $[T_i, T_m]$. Figure 3.1 presents an example of a term structure of implied Bachelier volatilities at T_0. See (Brigo and Mercurio, 2007) for more details on this topic.

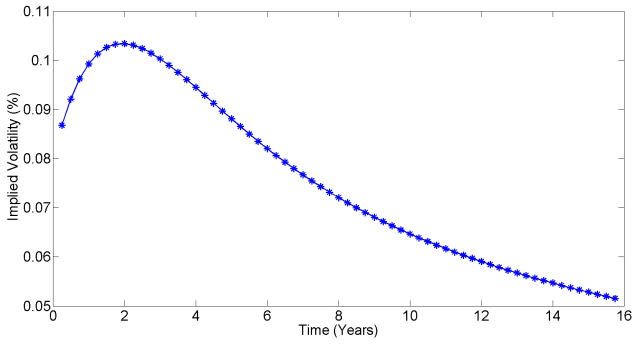

Figure 3.1: Example of the term structure of implied Bachelier volatilities.

According to Rebonato (2002), it is plausible to assume that the current term structure of implied Bachelier/Black volatilities can approximately be reproduced at a future date, meaning that its shape does not change significantly over time (see Figure 3.2). This phenomenon is known as time-homogeneity. The presence of this property in the term structure is a reason to impose a similar characteristic on the shape of the instantaneous volatility curve. A modeler thus believes that forward rates with a specific residual time to maturity have the same levels of volatility as forward rates at a future date with that same residual maturity time. Sporadically, the term structure of volatility can undergo some changes in its shape over time. The instantaneous volatility function should be flexible enough to take such changes into account.

Other noticeable features of the term structure of implied volatilities are the steep increase in implied volatilities from the very short maturities up to approximately 2 or 3 years and the monotonically decrease after this maturity. The volatility functions should have a flexible form in order to be able to reproduce either a humped or monotonically decreasing instantaneous volatility shape. The latter type of shape is appropriate if high levels of volatility are expected for the earliest-expiring rates in the near future. Note that the presence of a hump in the term structure of implied volatilities is not a direct reason for imposing a similar shape on the instantaneous volatility curve. Rebonato (2002, 2005) provides a financial justification for the humped-shaped instantaneous volatility.

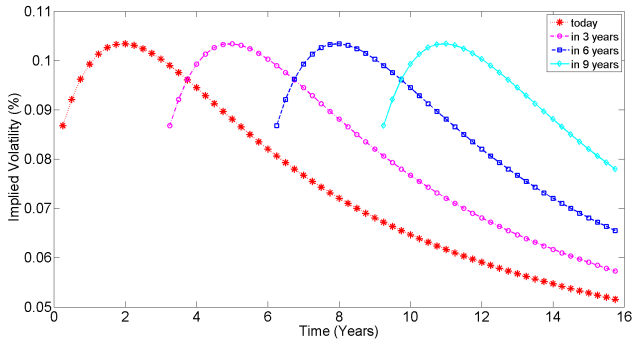

Figure 3.2: Example of the evolution of the term structure of implied Bachelier volatilities.

One distinguishes two main methods for specifying the instantaneous volatility. The first involves a piecewise-constant form where the instantaneous volatility of a particular forward rate is assumed to be constant between two reset dates. Usually, this type of volatility includes a number of parameters to be estimated that is many times larger than the number of instruments considered in the calibration set. The calibration procedure is said to be overparametrized, which may lead to an overfit of the volatility structure.

In order to avoid this problem, the instantaneous volatility function can be represented by some parametric form, thus reducing the number of parameters to be estimated. This will eventually result in a more stable calibration routine. Rebonato (2002) argues that functions of the general form

$$\sigma_i(t) = g(T_i) f(T_i - t),$$

display several desirable financial and computational features. The dependency on the remaining time to expiry $T_i - t$ of the forward rate $F_i(t)$ ensures that the instantaneous volatility behavior modeled today is the same as its behavior modeled in the future, satisfying the time-homogeneous property (see (Brigo and Mercurio, 2007)). In what follows, the actual functional forms of the different functions f and g will be specified.

CHARACTERIZATION OF THE FUNCTIONAL FORM OF $f(T_i - t)$

The time-homogeneous component f of the instantaneous volatility should conform to the following features:

- It should be flexible enough to be able to reproduce the humped or a monotonically decreasing shape.
- Its parameters should have a clear and transparent econometric interpretation.
- One should be able to easily integrate its square analytically, when evaluating the variance. In this way computationally expensive numerical integration schemes in the calibration procedures are avoided.

Rebonato (2002, 2005) proposes the parametric form

$$f(T_i - t) = (a + b(T_i - t))\, e^{-c(T_i - t)} + d, \tag{3.3}$$

where a, b, c and d are constant parameters, and shows that it satisfies the above criteria to an acceptable degree. Joshi (2003a) agrees that this functional form allows an initial steep rise followed by a slow decay, producing the most common shape observed in the market, the humped one.

Typically the parameters lie in the ranges $-0.02 \leq a \leq 0.02$, $-0.02 \leq b \leq 0.02$, $0 < c \leq 5$ and $0 < d \leq 0.01$.[1] To show the individual impact of the parameters on the instantaneous volatility curve, the base scenario

[1] See http://docs.fincad.com/support/ developerFunc/mathref/LIBORMarketModel.htm for the parameters' values in the log-normal LMM. In this model the diffusion coefficients $\mathbf{s}_i(t)$ are given by (3.2), with $\phi(F_i(t)) = F_i(t)$. In order to obtain the values in the normal LMM, where the diffusion coefficients are represented as (3.2) where $\phi(F_i(t)) = 1$, the function f obtained through the 'log-normal' values should be scaled down by a factor with the same order of magnitude of $F_i(t)$. This translates into scaling down a, b and d. Parameter c remains intact. In this way the levels of the diffusion coefficients in the normal and log-normal LMM are comparable. A scaling factor equal to 0.02 is chosen, representing the current approximated average level of the forward rates for the USD currency.

$a = -0.002$, $b = 0.003$, $c = 0.50$ and $d = 0.002$ is considered. Four cases are analyzed, each characterized by the alteration of one single parameter, see Figure 3.3. The parameter a influences the short end of the volatility curve, determining whether a humped or monotonically decreasing shape will occur. Parameter b primarily impacts the humped shape, where a greater value of b results in a more pronounced hump. The exponent decay parameter c controls both the magnitude of the hump and its position whereas d determines the level of the instantaneous volatilities.

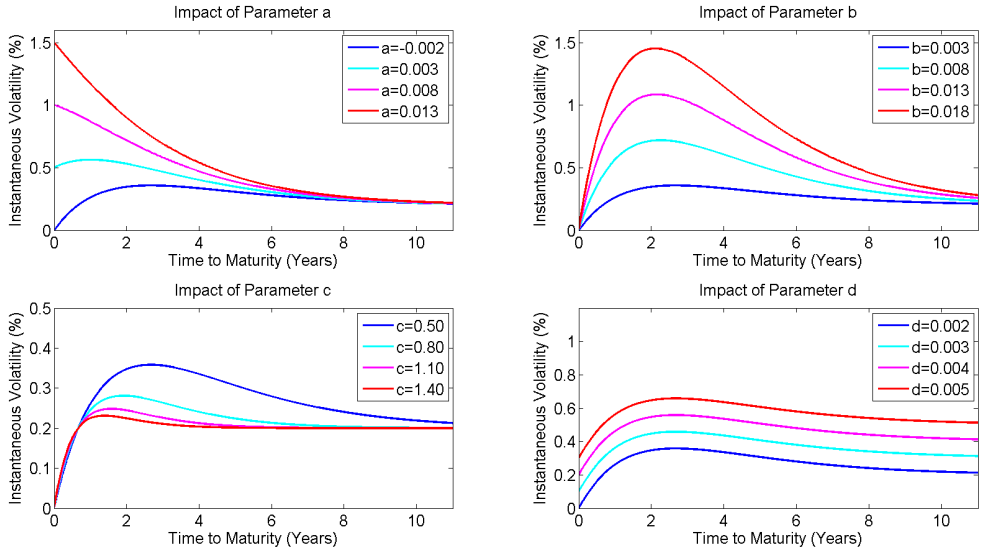

Figure 3.3: Impact of the instantaneous volatility parameters.

Note that $a+d$ reflects approximately the values given by the shortest-maturity implied volatilities since the instantaneous volatilities coincide with the average volatilities when $T_i - t$ converges to zero. Furthermore, parameter d represents the level of the longest-maturity implied volatilities as $f(T_i - t)$ tends to d when $T_i - t$ goes to infinity. It follows that, in order to preserve the desired short and long term behavior of the term structure and to assure a well-behaved instantaneous volatility function, the following constraints must be satisfied:

- $a + d > 0$,
- $d > 0$,
- $c > 0$.

Throughout this thesis it is assumed that the instantaneous volatility function will show a humped shape, more frequently observed in the market than the opposing monotonically decreasing form. In order to ensure this shape, it is necessary to take into account the first derivative of the function at the origin, given by $b - ac$, and the location of the extreme $(b - ac)/bc$, $bc \neq 0$. The extreme will be a maximum if and only if $b > 0$ holds. Furthermore, $a < b/c$ provides the function to rise for small values of $T_i - t$, given that $b > 0$. Usually, the top of the hump occurs in the last three years before maturity is reached, leading to the condition $(b - ac)/bc < 3$. Hence, the functional form f should also satisfy the additional constraints

- $b > 0$,
- $a < \frac{b}{c}$,
- $\frac{b-ac}{bc} < 3$.

The parametric specification f is then able to preserve the qualitative shape of the instantaneous volatility curve.

CHARACTERIZATION OF THE FUNCTIONAL FORM OF $g(T_i)$

Function (3.3) can be extended to a richer parametric form by multiplying it with a function g, which solely depends on the maturity date T_i. Rebonato (2002) and Brigo et al. (2005) model this functional form by

$$g(T_i) = k_i, \quad i = 0, \ldots, N-1,$$

where $k_i = 1+\epsilon(T_i)$ is positive and ideally close to one in order to preserve the time-homogeneous property of the instantaneous volatilities. The parameters k_i introduce a degree of flexibility that allow, in specific cases, an exact calibration to the swaption market, as shown in the next chapter.

The instantaneous volatility function

$$\sigma_i(t) = k_i\left((a+b(T_i-t))\,e^{-c(T_i-t)}+d\right), \tag{3.4}$$

is represented as a parametric core $f(T_i-t)$ that is locally altered by the parameter k_i at each maturity date T_i (Brigo and Mercurio, 2007). These modifications do not destroy the dependence on the time to maturity, providing they are small, and maintain the desirable qualitative features of the instantaneous volatility curve.

By introducing the parametric form (3.4) for the instantaneous volatilities, one succeeds to reduce the number of parameters to be estimated in the calibration routine. The set of volatility parameters that has to be determined is then limited to a, b, c, d and k_i, $i = 0, \ldots, N-1$.

An extensive overview of additional volatility functions used in practice can be found in (Brigo and Mercurio, 2007).

3.2.2. CORRELATION PARAMETRIZATION

Having specified the instantaneous volatilities of the forward rates in the previous subsection, one is half-way to fully describe their dynamics. What remains is the specification of the correlation structure between these forward rates.

Before explaining how $\boldsymbol{\rho}(t)$ can be constructed, it is important to mention that this matrix should satisfy some mathematical requirements in order to ensure that is a viable correlation structure. It should hold that:

(A1) $\rho_{i,i}(t) = 1 \quad$ for $i \in \{0, \ldots, N-1\}$,

(A2) $-1 \le \rho_{i,j}(t) \le 1 \quad$ for $i, j \in \{0, \ldots, N-1\}$,

(A3) $\rho_{i,j}(t) = \rho_{j,i}(t)$,

(A4) $\boldsymbol{\rho}(t)$ is positive definite.

Besides the above minimum requirements that must hold for any general valid correlation matrix, it is desirable that the forward rate correlation matrix exhibits the following features:

(B1) $i \mapsto \rho_{i,j}(t)$ is decreasing for $i \ge j$,

(B2) $i \mapsto \rho_{i+p,i}(t)$ is increasing for a fixed p.

The first property comes down to the observation that the farther apart two forward rates lie, the more decorrelated they should be. This results in a monotonically decreasing pattern when moving away from the '1' diagonal entry along any column or row. Furthermore, according to Brigo and Mercurio (2007) and Rebonato (2002), it is usually expected that the rates with a constant time distance between the fixing dates are more correlated on the long end of the curve compared to the short end. For example, the forward rates maturing in 1Y and 3Y should be more decorrelated than the rates expiring in 17Y and 20Y. This property leads to the second feature, stating that the entries along the sub- diagonals should increase.

Two different approaches exist to construct $\boldsymbol{\rho}(t)$. First, one can estimate the historical correlations, when possible. If time series of the forward rates are available, the correlations can be statistically estimated from these data sets using different basic techniques as explained in (Morini and Brigo, 2003), (Brigo and Mercurio,

2007) and (Andersen and Piterbarg, 2010b). Unfortunately, in practice this procedure often proves to contain noise in the data and it is difficult to use. Additionally, Rebonato and Jäckel (2011) point out that historically estimated correlations encounter problems caused by outliers and possible discontinuities in the correlation surfaces. Lastly, the $N-1 \times N-1$ historical correlation matrices have $(N-1)(N-2)/2$ entries that have to be estimated, taking into account symmetry and the ones on the diagonal. This number is often too high for practical purposes and generally, no reliable estimates are obtained (Brigo, 2002).

To overcome the complications mentioned above, Rebonato (2002) proposes the use of a parametric function to represent the correlations between the forward rates. This function must be able to reproduce the most salient correlation features seen in the market. By using a parametrization, the correlation surfaces are smoother and the number of parameters to be estimated is significantly reduced. Rebonato (2002) additionally points out that it is a realistic choice to impose dependency of the correlation matrix on the remaining time to maturity:

$$\rho_{i,j}(t) = \rho_{i,j}\left(T_i - t, T_j - t\right), \quad i,j \in \{0,\ldots,N-1\}.$$

According to Lutz (2010b), it is sufficient to consider the initial correlation matrix

$$\rho_{i,j}(t) = \rho_{i,j}(0),$$

for all $t \in [0, T_{N-1}]$. In other words, the correlation matrix is assumed to be constant across time. For simplicity of notation one can therefore define

$$\rho_{i,j} := \rho_{i,j}(t).$$

Throughout this thesis the so-called simple exponential parametric form

$$\begin{aligned} \rho_{i,j} &= e^{-\beta\left|(T_i - t) - (T_j - t)\right|}, \\ &= e^{-\beta\left|T_i - T_j\right|}, \end{aligned} \tag{3.5}$$

with $\beta > 0$, will be considered. Rebonato (2005) assures that matrix $\boldsymbol{\rho}$, whose entries are given by (3.5), satisfies requirements (A1)-(A4) for any positive β and hence, it is a valid correlation matrix. Furthermore, property (B1) is satisfied but unfortunately, parametrization (3.5) does not handle feature (B2) well as all entries of a particular sub-diagonal attain the same constant value. It does not give any information about the speed of decorrelation between two rates with a constant time distance $T_i - T_j$ between the fixing dates. Nevertheless, even though parametrization (3.5) does not satisfy property (B2), this function is often used in practice because of its flexible form involving one degree of freedom.

The simplicity of the parametric functions of $\sigma_i(t)$ and $\boldsymbol{\rho}$ allows analytical integration of the covariance integral $\int \sigma_i(t)\sigma_j(t)\rho_{i,j}dt$, where $\rho_{i,j}$ can be taken out of the integral since it does not depend on the calendar time. The precise evaluation can be found in (Rebonato, 2002). Since a closed form solution exists and no cumbersome numerical integration methods has to be applied, the computation of the indefinite integral will be significantly faster. This will have a computational advantage in the calibration routine, as the integral plays a crucial role in this procedure. This will become apparent in Chapter 4.

It is essential to specify the volatility and the correlation structures underlying the LMM realistically in order to obtain accurate exotic derivatives prices. While it is relatively easy to extract information about the rate volatilities from the market prices of caps and swaptions, this task is more delicate when dealing with correlations. For this reason it has been decided that throughout this thesis the parameter β will be fixed prior to calibration. This LMM formulation is sufficiently flexible to be able to be calibrated to a subset of the swaption market. The calibration procedure comes down to estimating volatility parameters a, b, c, d and k_i, $i = 0,\ldots,N-1$.

3.3. THE SPOT MEASURE

When simulating a set of forward rates in the LMM, it is required to specify their dynamics under one single measure. A convenient choice in practice is the spot measure $\mathbb{Q}^{B^*}$. Under this measure, the bias resulting from the discretization of the drift is more distributed among the different forward rates than when using other measures (Brigo and Mercurio, 2007). Furthermore, when simulating independent paths of a set of

forward rates through time, the drift terms can be implemented in a recursive fashion, thus reducing the computational effort. This will be explained in more detail in Subsection 3.6.2.

The spot measure is induced by the discrete-time equivalent of the continuously compounded money market account. The numéraire $B^*(T_m)$, called the rolling over bank account, is the value at time T_m, $m \in \{1,\dots,N\}$, of an investment of one unit of currency at T_0 and it is formed by the following trading strategy:

1. At time T_0, invest one unit of currency in $\frac{1}{P_1(T_0)}$ units of T_1-maturing zero coupon bonds.
2. At time T_1, receive $\frac{1}{P_1(T_0)}$ units of currency and reinvest in $\frac{1}{P_1(T_0)P_2(T_1)}$ units of T_2-maturing zero coupon bonds.
3. At time T_2, receive $\frac{1}{P_1(T_0)P_2(T_1)}$ units of currency and reinvest in $\frac{1}{P_1(T_0)P_2(T_1)P_3(T_2)}$ units of T_3-maturing zero coupon bonds.
4. Repeat this trading strategy at each date in the tenor structure up to time T_{m-1}.

Hence, by re-investing the received amount at each time instant T_i, $i \in \{0,\dots,m-1\}$ in zero coupon bonds maturing at the subsequent date T_{i+1}, the asset price process $B^*(T_m)$ can be defined as

$$B^*(T_m) = \frac{1}{\prod_{i=0}^{m-1} P_{i+1}(T_i)},$$

or equivalently as

$$B^*(T_m) \equiv B^*(\mathbf{F}(T_m)) = \prod_{i=0}^{m-1} (1+\tau_i F_i(t)),$$

with $B^*(T_0) = 1$.

Under the spot measure, the LMM specifies a system of stochastic differential equations of the form

$$dF_i(t) = \phi(F_i(t))\,\mathbf{s}_i(t)^\top \left(\mu_i(t,\mathbf{F}(t))\,dt + d\mathbf{W}^{\mathbb{Q}^{B^*}}(t)\right), \quad 0 \le t \le T_i, \quad i \in \{\alpha(t),\dots,N-1\}, \tag{3.6}$$

where $\mathbf{W}^{\mathbb{Q}^{B^*}}(t)$ is a $\mathbb{R}^h$-valued, element-wise independent Brownian motion under $\mathbb{Q}^{B^*}$, $\mathbf{s}_i(t)$ is defined as (3.2) and the drift parameter must be given by

$$\mu_i(t,\mathbf{F}(t)) = \sum_{j=\alpha(t)}^{i} \frac{\tau_j \phi(F_i(t))\,\mathbf{s}_j(t)}{1+\tau_j F_j(t)}.$$

See (Andersen and Piterbarg, 2010a) and (Fries, 2007) for a proof.

3.4. RANK REDUCTION

In practice, one aims for a fast and computationally viable simulation for the LMM. One way to achieve this is to diminish the number of driving Brownian motions. Formulations (3.1) and (3.6) allow the number of factors to be less than the number of forward LIBOR rates to be modeled. As explained in Section 3.1, reducing the number of driving factors decreases the ability to describe more complex correlation structures. Hence, the correlation matrix implied by the h, $h < N$, number of factors will differ from the full-rank correlation matrix. In this section it is shown how to use principal component analysis (PCA) to form such a reduced-rank correlation matrix, following the theory presented in (Andersen and Piterbarg, 2010b) and (Rebonato and Jäckel, 2011).

Consider a full-rank matrix $\boldsymbol{\rho} \in \mathbb{R}^{N\times N}$, whose entries are determined by (3.5) in this thesis. As $\boldsymbol{\rho}$ is symmetric and positive definite, it can be diagonalized as

$$\boldsymbol{\rho} = E\Lambda E^{-1},$$

where $\Lambda \in \mathbb{R}^{N\times N}$ is the diagonal matrix containing the eigenvalues of $\boldsymbol{\rho}$ in ascending order, $E \in \mathbb{R}^{N\times N}$ is the matrix composed by the corresponding eigenvectors and E^{-1} is the inverse matrix of E. If $\boldsymbol{\rho}$ is believed to be

well-represented by a rank-m representation, PCA can be applied to the correlation matrix, retaining the m largest eigenvalues and the corresponding vectors. This procedure yields:

$$\boldsymbol{\rho}_m = E_m \Lambda_m E_m^{-1},$$

with $E_m \in \mathbb{R}^{N\times m}$ and $\Lambda_m \in \mathbb{R}^{m\times m}$. However, the formulation of $\boldsymbol{\rho}_m$ does not ensure a unit diagonal, a necessary requirement for a correlation matrix. To achieve this, the entries of $\boldsymbol{\rho}_m$ are normalized. In this way, the rank-m reduced correlation matrix is a valid approximation of the full-rank matrix $\boldsymbol{\rho}$:

$$\begin{aligned}\boldsymbol{\rho} &\approx \widehat{\boldsymbol{\rho}}_m,\\ &:= e_m^{-1} E_m \Lambda_m E_m^{-1} e_m^{-1},\end{aligned}$$

where e_m is a $N\times N$ diagonal matrix with elements $(e_m)_{i,i} = \sqrt{\left(E_m \Lambda_m E_m^{-1}\right)_{i,i}}$, $i = 1,\dots,N$.

When assuming rank-reduced dynamics, the challenging task is choosing how many factors to retain such that the most salient features of the full-rank correlation matrix are preserved. To make this decision, the computational speed and the product to be priced have to be considered.[1]

3.5. MODEL FORMULATION IN THE MC FRAMEWORK

The classical SC LMM is based on modeling the joint evolution of a set of consecutive forward LIBOR rates corresponding to a given tenor structure under a common pricing measure. As Mercurio (2010a) explains, one encounters two types of complications when moving to a MC framework. The first is the need to jointly model as many forward LIBOR rates as forward curves together with the forward rates corresponding to the discount curve. The second is the non-validity of the classical assumption that forward LIBOR rates can be replicated by risk-free bonds.

The first issue is straightforward and can be tackled by adding multiple dimensions to the vector of rates to be modeled. The second point can be addressed by formulating a new definition of the forward LIBOR rates that is compatible with the existence of different curves. This extention of the definition to a MC setting is represented by (2.12).

For simplicity of notation, the theory of this subsection is restricted to the use of two curves, $\mathtt{C}^d$ and $\mathtt{C}^x$, but the concepts can be extended to a case considering n curves. Define a finite set of tenor dates $\{T_m\}_{m=0}^N$, compatible with curve $\mathtt{C}^x$ and where $0 = T_0 < T_1 < \ldots < T_N$. Denote by τ_m the length of the interval $[T_m, T_{m+1}]$, expressed in year fractions. Let the $N+1$-dimensional vector $\mathbf{P}^d(t) = \left(P_0^d(t),\dots,P_N^d(t)\right)^\top$ be composed by the zero coupon bonds computed on $\mathtt{C}^d$. Define the forward OIS rate over $[T_i, T_{i+1}]$ as of time t by $F_i^d(t)$, with $0 \le t \le T_i$, and write the N-dimensional vector of these rates as $\mathbf{F}^d(t) = \left(F_0^d(t),\dots,F_N^d(t)\right)^\top$. $\mathbf{F}^x(t) = \left(F_0^x(t),\dots,F_N^x(t)\right)^\top$ represents the N-dimensional vector of forward LIBOR rates.

3.5.1. POSSIBLE MC LMM EXTENSIONS

The MC LMM is characterized by the modeling of the joint evolution of the forward LIBOR rates and the forward rates corresponding to the discount curve. As mentioned in Section 2.4, the spread between the forward OIS and LIBOR rates referring to the same time interval widened after the credit crunch of 2007 and it became important to model those spreads in a realistic way, reflecting the current market conditions. Several types are proposed in literature:

- Additive spreads, as in Fujii et al. (2011), Mercurio and Xie (2012) and Mercurio (2010a):

$$G_i(t) := F_i^x(t) - F_i^d(t), \quad 0 \le t \le T_i, \quad i \in \{\alpha(t),\dots,N-1\}. \tag{3.7}$$

- Multiplicative spreads, as in Cuchiero et al. (2016b) and Henrard (2010):

$$G_i(t) := \frac{1+\tau_i F_i^x(t)}{1+\tau_i F_i^d(t)}, \quad 0 \le t \le T_i, \quad i \in \{\alpha(t),\dots,N-1\}. \tag{3.8}$$

[1] Interest rate instruments that have a high correlation sensitivity will require more factors than products that are less sensitive to the correlation structure.

- Instantaneous spreads, as in Andersen and Piterbarg (2010b):

$$P_i^x(t) = P_i^d(t)\, e^{\int_t^{T_i} g(u)du}, \quad 0 \le t \le T_i, \quad i \in \{\alpha(t), \ldots, N-1\}. \tag{3.9}$$

See (Castagna et al., 2015) for more details on the modeling of the basis spreads.

The MC LMM accommodates both deterministic and stochastic spreads. When considering stochastic spreads, the SC LMM can be extended to the MC setting in three different fashions, depending whether the spread is modeled implicitly of explicitly. These cases are characterized by:

1. Modeling the joint evolution of the forward LIBOR rates $F_i^x(t)$ and the OIS rates $F_i^d(t)$, where $0 \le t \le T_i$ and $i \in \{\alpha(t), \ldots, N-1\}$, as in (Mercurio, 2010a,b).

2. Modeling the joint evolution of the forward LIBOR rates $F_i^x(t)$ and the spreads $g(t)$ or $G_i(t)$ (depending on the definition of the spread), where $0 \le t \le T_i$ and $i \in \{\alpha(t), \ldots, N-1\}$.

3. Modeling the joint evolution of the OIS rates $F_i^d(t)$ and the spreads $g(t)$ or $G_i(t)$ (depending on the definition of the spread), where $0 \le t \le T_i$ and $i \in \{\alpha(t), \ldots, N-1\}$.

By modeling the dynamics of two out of the three processes $F_i^x(t)$, $F_i^d(t)$ and $g(t)$ or $G_i(t)$ (depending on the definition of the spread), the dynamics of the third process will be uniquely identified by one of the relations (3.7), (3.8) or (3.9). In the first possible extension of the LMM, the spreads are determined implicitly, while in the remaining two they are modeled explicitly. Mercurio (2010a) reflects on the advantages and drawbacks of the three different extensions.

In a deterministic basis spread model, a given forward or discount curve represents the reference curve. Its evolution is modeled by a stochastic process, as was done in the classical single-curve LMM. The other curve is consequently modeled at a deterministic spread over the reference curve.

3.5.2. MODEL DYNAMICS

For this particular extension of the LMM it is chosen to consider a constant spread and to model the forward OIS rates explicitly. The theory of Section 3.1-3.4 can now exclusively be applied to $F_k^d(t)$. Under the measure $\mathbb{Q}_d^{T_{k+1}}$ only the forward OIS rate $F_k^d(t)$ will be a martingale by definition, while others will not. In order for the LMM to be an arbitrage-free model, the dynamics of the other forward OIS rate processes under $\mathbb{Q}_d^{T_{k+1}}$ must be given by

$$dF_i^d(t) = \phi\left(F_i^d(t)\right)\mathbf{s}_i(t)^\top\left(\mu_i\left(t, \mathbf{F}^d(t)\right)dt + d\mathbf{W}^{\mathbb{Q}_d^{T_{k+1}}}(t)\right), \quad 0 \le t \le T_i, \quad i \in \{\alpha(t), \ldots, N-1\}, \tag{3.10}$$

with the drift parameters defined as

$$\mu_i\left(t, \mathbf{F}^d(t)\right)\begin{cases} -\sum_{j=i+1}^{k} \frac{\tau_j \phi\left(F_j^d(t)\right)\mathbf{s}_j(t)}{1+\tau_j F_j^d(t)}, & \text{for } i < k, \\ 0, & \text{for } i = k, \\ \sum_{j=i+1}^{k} \frac{\tau_j \phi\left(F_j^d(t)\right)\mathbf{s}_j(t)}{1+\tau_j F_j^d(t)}, & \text{for } i > k, \end{cases}$$

where

$$\mathbf{s}_i(t) = \sigma_i(t)\,\boldsymbol{\lambda}_i(t), \quad \boldsymbol{\lambda}_i(t) = \mathbf{s}_i(t) / \|\mathbf{s}_i(t)\|.$$

As mentioned earlier in Section 3.3, the simulation of a set of forward OIS rates requires the specification of their dynamics under one single measure. To this end, define the spot measure $\mathbb{Q}_d^{B^*}$, induced by the numéraire $B^*\left(\mathbf{F}^d(t)\right)$. Under this measure, the MC LMM specifies a system of stochastic differential equations of the form

$$dF_i^d(t) = \phi\left(F_i^d(t)\right)\mathbf{s}_i(t)^\top\left(\mu_i\left(t, \mathbf{F}^d(t)\right)dt + d\mathbf{W}^{\mathbb{Q}_d^{B^*}}(t)\right), \quad 0 \le t \le T_i, \quad i \in \{\alpha(t), \ldots, N-1\}, \tag{3.11}$$

where the drift parameter must be given by

$$\mu_i\left(t,\mathbf{F}^d(t)\right)=\sum_{j=\alpha(t)}^{i}\frac{\tau_j\phi\left(F_j^d(t)\right)\mathbf{s}_j(t)}{1+\tau_i F_j^d(t)}.$$

This system is equivalent to the one in the SC framework defined by (3.6).

The selection of the spread will influence the type of distribution of the forward LIBOR rates. In Chapter 4 and Chapter 5 the normal forward OIS rates are modeled and hence it is desirable to use Bachelier's model to price caps/floors and swaptions. Bachelier's model can be applied in the MC framework if the forward LIBOR rates are also normally distributed, as is shown in Section 3.7. This can be achieved by considering the constant additive spread defined by (3.7). Throughout this thesis the spread assumes the form

$$\begin{aligned}G_i(t)&\approx G_i(T_0),\\&=F_i^x(T_0)-F_i^d(T_0),\quad 0\le t\le T_i,\quad i\in\{\alpha(t),\ldots,N-1\}.\end{aligned}\tag{3.12}$$

The evolution of the forward LIBOR rate process is then uniquely identified by (3.7) and it is represented by the relation

$$F_i^x(t)=F_i^d(t)+G_i(T_0),\quad 0\le t\le T_i,\quad i\in\{\alpha(t),\ldots,N-1\}.\tag{3.13}$$

$F_i^d(t)$ is a martingale under $\mathbb{Q}_d^{T_{i+1}}$ since, recalling definition (2.11), it is deflated by $P_{i+1}^d(t)$. With this choice of spread, the same is true for $F_i^x(t)$.

3.6. MONTE CARLO IMPLEMENTATION

In Subsection 3.5.2 the arbitrage-free simultaneous dynamics of a set of forward OIS rates under the spot measure were presented. These forward rates are related to the forward LIBOR rates through the spread defined in (3.12). Ideally, it is desirable to find a closed-form solution to the differential equation that can be used to price a derivative security, but in some cases this equation may be too complex to solve analytically.

In general, when it is not possible to find an analytical solution to a differential equation, one can resort to two different ways of computing a derivative security price:

1. Using Monte Carlo simulation to generate paths of the underlying securities under a specific measure and estimating the expected discounted payoff under the same measure using these paths.

2. Solving numerically a partial differential equation, for example using finite differences.

See (Shreve, 2004) for more details on both methods.

The LMM involves a large number of forward rates to be modeled. Because of the high dimensionality and the stochastic drift, finite differences are rarely applicable and the model is typically implemented using the Monte Carlo method. In order to apply the latter, it is necessary to simulate all rates under a common measure. Throughout this thesis the spot measure will be considered because of its advantages mentioned in Section 3.3.

3.6.1. DISCRETIZATION OF THE FORWARD RATE DIFFERENTIAL EQUATION

As mentioned in Subsection 3.5.2, in this specific MC extension of the LMM the forward OIS rates are simulated as stochastic processes. In order to evolve the discount curve in time, the differential equation (3.11) has to be discretized. In particular, suppose one stands at time t, having the knowledge of all forward rates with maturity dates $T_{\alpha(t)}$, $T_{\alpha(t)+1}$, ..., T_{N-1}. To generate the forward OIS rate paths, the corresponding curve has to be moved to time $t+dt$, $dt>0$, by creating the samples

$$F_{\alpha(t+dt)}^d(t+dt),F_{\alpha(t+dt)+1}^d(t+dt),\ldots,F_{N-1}^d(t+dt).$$

The Euler scheme is applied to discretize (3.11) as this method is straightforward and easy to implement. The approximated dynamics are given by

$$\widehat{F}_i^d(t+dt) = \widehat{F}_i^d(t) + \phi\left(\widehat{F}_i^d(t)\right)\mathbf{s}_i(t)^\top\left(\mu_i\left(t,\mathbf{F}^d(t)\right)dt + \sqrt{dt}\boldsymbol{\epsilon}\right), \quad 0 \le t \le T_{i-1}, \quad i \in \{\alpha(t+dt),\ldots,N-1\}, \tag{3.14}$$

where $\boldsymbol{\epsilon}$ is an h-dimensional standard normal random variable, i.e. $\boldsymbol{\epsilon} \sim \mathcal{N}(\mathbf{0}, I)$ with $\mathbf{0}$ an h-dimensional zero vector and I the $h \times h$ identity matrix, and with

$$\mu_i\left(t,\mathbf{F}^d(t)\right) = \sum_{j=\alpha(t)}^{i} \frac{\tau_j \phi\left(\widehat{F}_j^d(t)\right)\mathbf{s}_j(t)}{1+\tau_j \widehat{F}_j^d(t)}.$$

In Chapter 4 and Chapter 5 the forward OIS rates will be specified by the normal formulation of (3.11), which also admits non-positive solutions of the SDE. The Euler scheme is a suitable discretization method as the the increments of this scheme are Gaussian, implying a non-zero probability of the rates crossing zero and becoming negative.

After determining $\mathbf{F}^d(t+dt)$, the forward LIBOR rates still existing at time $t+dt$ are obtained by

$$\widehat{F}_i^x(t+dt) = \widehat{F}_i^d(t+dt) + G_i(T_0), \quad 0 \le t \le T_{i-1}, \quad i \in \{\alpha(t+dt),\ldots,N-1\}. \tag{3.15}$$

The possibility exists that $\alpha(t+dt)$ exceeds $\alpha(t)$. In that case, a particular set of rates on the front-end of the forward OIS and LIBOR yield curve will expire. Consequently, there is no need to model these rates, as they will drop off the curves when moving to time $t+dt$.

Given the initial forward curves $\mathbf{F}^d(T_0)$ and $\mathbf{F}^x(T_0)$, the full paths $\{\mathbf{F}^d(T_i) : i = 0,\ldots,N-1\}$ and $\{\mathbf{F}^x(T_i) : i = 0,\ldots, N-1\}$ are created by repeating the single-period stepping scheme introduced above on a time-grid $t_0, t_1, \ldots$. This time line is referred to as the simulation grid and it can possibly be non-equidistant. In this thesis, however, a grid is considered with a constant time step dt. In Subsection 3.6.4 it is explained how to choose dt. As the forward OIS rates are modeled under the spot measure, it is desirable that the simulation grid include the tenor structure dates $T_0, T_1, \ldots, T_{N-1}$. In this way one can keep track of the spot numéraires computed on the curve without having to use inter- or extrapolation.

Keeping the forward rates between two subsequent simulation grid points constant will give rise to a discretization error. Making the grid finer by adding more simulation points will decrease this error to the expense of an increased computational load. According to Andersen and Piterbarg (2010b), considering a simulation grid that exactly coincides with the tenor structure, i.e. which $t_i = T_i$ holds for all $i \in \{0,\ldots,N-1\}$, gives an acceptable discretization error, unless the accrual periods τ_i are unusually long or the volatilities reach unusually high levels.

3.6.2. ANALYSIS OF THE COMPUTATIONAL EFFORT

The computational effort involved in advancing the forward OIS and LIBOR rates one step forward in time is dominated by the computation of the drift coefficients of (3.11). To evolve the forward OIS rates one single time step, these drift coefficients have to be determined for each forward rate i, $i \in \{\alpha(t+\Delta),\ldots,N-1\}$. Since the terms in the summation of the drift depend on $\alpha(t)$ and i, one needs to compute $i-\alpha(t)+1$ terms for every value of i. Each of these terms consists of roughly h multiplications. Consequently, the computation of a drift term involves approximately $h(i-\alpha(t)+1) = \mathcal{O}(hi)$ operations for a given i.

Advancing all $N-\alpha(t+\Delta)$ forward OIS rates still alive across a step requires $\mathcal{O}\left(hN^2\right)$ operations. The computational effort of generating a full path of yield curves scenarios from time 0 to time T_{N-1} amounts to $\mathcal{O}\left(hN^3\right)$, assuming that the simulation grid precisely coincides with the tenor structure. Hence, the drift computations are growing at rate hN^3, rapidly becoming the main bottleneck in terms of computational time when N is large. The simple application of the first-order Euler scheme requires considerable computing resources in these cases.

A way exists, though, next to the rank reduction technique to reduce the computational effort since there is no need to perform $\mathcal{O}(hN)$ operations on the computation of each drift coefficient. All drift terms can

be determined by an $\mathcal{O}(hN)$-step iteration, invoking the following recursive relationship for $\mu_i\left(t,\mathbf{F}^d(t)\right)$, $i\in\{\alpha(t+\Delta),\ldots,N-1\}$:

$$\mu_i\left(t,\mathbf{F}^d(t)\right)=\mu_{i-1}\left(t,\mathbf{F}^d(t)\right)+\frac{\tau_i\phi\left(\widehat{F}_i^d(t)\right)\mathbf{s}_i(t)}{1+\tau_i\widehat{F}_i^d(t)}, \tag{3.16}$$

starting from

$$\mu_{\alpha(t+\Delta)}\left(t,\mathbf{F}^d(t)\right)=\sum_{j=\alpha(t)}^{\alpha(t+\Delta)}\frac{\tau_j\phi\left(\widehat{F}_j^d(t)\right)\mathbf{s}_j(t)}{1+\tau_j\widehat{F}_j^d(t)}.$$

Moving the OIS yield curve across a single time step requires now $\mathcal{O}(hN)$ operations and, consequently, the computational effort of advancing the full OIS and LIBOR curves from time 0 to time T_{N-1} will be $\mathcal{O}\left(hN^2\right)$ compared to the $\mathcal{O}\left(hN^3\right)$ operations needed without using (3.16).

For more details on this topic, see (Joshi, 2003b), (Joshi and Liesch, 2007) and (Andersen and Piterbarg, 2010b).

3.6.3. PRICING FINANCIAL INSTRUMENTS

This subsection illustrates how the Monte Carlo method is used to determine the price of an interest rate instrument. Let $V\left(T_r,\mathbf{F}^d(T_r),\mathbf{F}^x(T_r)\right)$ be the price of this instrument at time T_r, $r\in\{1,\ldots,N-1\}$, depending on $\mathbf{F}^d(T_r)$ and $\mathbf{F}^x(T_r)$. When working in the spot measure, the value of the product at time T_0 is given by

$$V\left(T_0,\mathbf{F}^d(T_0),\mathbf{F}^x(T_0)\right)=\mathbb{E}_{T_0}^{\mathbb{Q}_d^{B^*}}\left[\frac{V\left(T_r,\mathbf{F}^d(T_r),\mathbf{F}^x(T_r)\right)}{B^*\left(\mathbf{F}^d(T_r)\right)}\right]. \tag{3.17}$$

To determine the Monte Carlo price of (3.17), the following steps are performed:

1. Draw an h-dimensional vector $\boldsymbol{\epsilon}$ from the multivariate standard normal distribution.
2. Simulate the sample paths $\left\{\mathbf{F}_p^d(T_i):i=0,\ldots,r\right\}$ and $\left\{\mathbf{F}_p^x(T_i):i=0,\ldots,r\right\}$ using (3.14) and (3.15), respectively.[1]
3. Compute the value of the interest rate security at T_0 as
$$V\left(T_0,\mathbf{F}_p^d(T_0),\mathbf{F}_p^x(T_0)\right)=\frac{V\left(T_r,\mathbf{F}_p^d(T_r),\mathbf{F}_p^x(T_r)\right)}{B^*\left(\mathbf{F}_p^d(T_r)\right)}.$$
4. Repeat steps 1-3 for $p=1,\ldots,H$ and form the Monte Carlo estimate
$$\widetilde{V}\left(T_0,\mathbf{F}^d(T_0),\mathbf{F}^x(T_0)\right)=\frac{1}{H}\sum_{p=1}^{H}V\left(T_0,\mathbf{F}_p^d(T_0),\mathbf{F}_p^x(T_0)\right), \tag{3.18}$$
which is an approximation of (3.17).

Optionally, one can construct the 95% confidence interval of the Monte Carlo price by

$$\left[\widetilde{V}\left(T_0,\mathbf{F}^d(T_0),\mathbf{F}^x(T_0)\right)-1.96\frac{\text{Std}}{\sqrt{H}},\quad\widetilde{V}\left(T_0,\mathbf{F}^d(T_0),\mathbf{F}^x(T_0)\right)+1.96\frac{\text{Std}}{\sqrt{H}}\right], \tag{3.19}$$

with Std representing the sample standard deviation, computed as

$$\text{Std}=\sqrt{\frac{1}{H-1}\sum_{p=1}^{H}\left(V\left(T_0,\mathbf{F}_p^d(T_0),\mathbf{F}_p^x(T_0)\right)-\widetilde{V}\left(T_0,\mathbf{F}^d(T_0),\mathbf{F}^x(T_0)\right)\right)^2}.$$

In this setting one is exposed to a second type of error, the statistical Monte Carlo error, which depends on the number of Monte Carlo iterations H. The bias of the estimator (3.18) decreases, and consequently the accuracy of the approximation increases, for larger values of H. Subsection 3.6.4 shows how to select a suitable value for H.

See (Glasserman, 2003) for more information about the application of Monte Carlo in the field of Financial Engineering.

[1] For clarity, the subscript p does not refer to a specific forward rate. It is linked to a particular simulated path.

3.6.4. DETERMINATION OF THE TIME STEP AND THE NUMBER OF SIMULATIONS

Smaller step sizes result in lower discretization errors and with higher numbers of simulations a more accurate Monte Carlo price (3.18) is achieved. However, these desirable features come at the price of a higher computational effort. Hence, a trade-off between accuracy and speed has to be made when establishing dt and H. In this subsection suitable values for dt and H are chosen that will be used throughout this thesis. To this end, the following test is carried out.

1. The finite set of tenor dates $\{T_m\}_{m=0}^{65}$ is considered, such that $0 = T_0 < T_1 < \ldots < T_{65}$ and $\tau_m = 0.25$ for all m. The instantaneous volatility parametrization (3.4) is used with $a = 0.0013$, $b = 0.0145$, $c = 0.5028$, $d = 0.0056$ and $k_i = 1.13$, $i \in \{0, \ldots, 64\}$.[1] These values are chosen to ensure a realistic evolution of the term structure of volatilities. The correlation among the distinct forward rates is given by (3.5) with $\beta = 0.20$.

2. The dynamics of the forward OIS rates (3.11) are assumed to be driven by a normal process, with as many driving Brownian motions as forward rates to be modeled. Given the initial OIS and LIBOR rate curves presented in Appendix A, a Monte Carlo evaluation of the strip of co-terminal, quarterly-annual paying swaptions {1Y15Y, 2Y14Y, 3Y13Y, 4Y12Y, 5Y11Y, 6Y10Y, 7Y9Y, 8Y8Y, 9Y7Y, 10Y6Y, 11Y5Y, 12Y4Y, 13Y3Y, 14Y2Y, 15Y1Y} with strike $K = 2.1\%$ is performed according to the methodology explained in Subsections 3.6.1-3.6.3 for a particular dt and H. The values of the swaptions are expressed in terms of their implied Bachelier volatilities. The 95% confidence intervals of these 15 Monte Carlo implied volatilities are computed and the width of the intervals is calculated. The total CPU time needed to perform this step is recorded.

3. Step 2 is performed for the three step sizes $dt = 0.25$, $dt = 0.1$ and $dt = 0.01$ and for the eight numbers of simulations $H = 500$, $H = 1{,}000$, $H = 5{,}000$, $H = 10{,}000$, $H = 50{,}000$, $H = 100{,}000$, $H = 500{,}000$ and $H = 1{,}000{,}000$.[2] Hence, 18 distinct cases are considered in total.[3]

Tables B.1-B.3 in Appendix B present the results for $dt = 0.25$, $dt = 0.10$ and $dt = 0.010$, respectively. For each specific H, the Monte Carlo implied Bachelier volatilities of the swaptions contained in the strip are denoted, together with their 95% confidence intervals and the corresponding interval widths. The results are expressed in terms of basis points. The required CPU time for each case, measured in hours, is listed. Furthermore, for a given step size, the impact of increasing the number of simulations on the accuracy of the Monte Carlo implied volatility estimates is analyzed. This is done by calculating the percentage change of the implied volatilities of the swaptions, determined using a specific H, with respect to the implied volatilities corresponding to the 'previous' H. If the percentage change of a specific swaption tends to 0%, the Monte Carlo implied volatility is considered to be an accurate estimate of the true, unknown, implied Bachelier volatility, as the Monte Carlo estimate is almost fully converged to this value.

From the tables in Appendix B one can see that, for a given H, the use of very small step sizes does not improve the accuracy of the Monte Carlo estimates. In fact, considering a value of $dt = 0.25$ results in a discretization error of the same order of magnitude as the ones corresponding to step sizes of 0.10 and of 0.010, which is in line with the observation of Andersen and Piterbarg (2010b) that a simulation grid consisting of exactly the tenor dates is sufficient. From an initial analysis the value of 0.01 has equally proven not to lead to an increased accuracy, while, on the other hand, requiring extremely long computational times. In view of the current high volatility environment considered in this study, a step size of 0.10 has been selected in order to ensure that it would be applicable to all cases under consideration.
Furthermore, since, for a given step size, the percentage variation of the Monte Carlo implied volatility value tends to zero for a large number of simulations, the corresponding estimates are considered to bear a high degree of accuracy. In particular, the Monte Carlo prices generated with $1{,}000{,}000$ simulations are considered to be almost fully converged, as the widths of the corresponding Monte Carlo windows are remarkably small. For this reason the value of $H = 1{,}000{,}000$ is used in all simulations, despite the drawback on the computational load.

[1] See Subsection 4.4.3 for a justification of the choice of the values of a, b, c and d. The constant value 1.13 of the parameters k_i is the average over the corresponding parameters presented in that same subsection.

[2] The simulation grid corresponding to each of the three step sizes include the dates on which the payments of the swaptions take place so that no inter- or extrapolation is required.

[3] To make a fair comparison of the required CPU time, the same PC is used for each case.

3.7. VALUATION OF INTEREST RATE DERIVATIVES IN THE MC LMM

In this section it is shown how to price interest rate caps/floors and European swaption in the MC LMM.

3.7.1. PRICING OF CAPS AND FLOORS

The pricing of caps and floors in the MC LMM is straightforward. As mentioned in Subsection 2.5.3, the value $C_{[r,N]}\left(T_m, \mathbf{P}^d(T_m), \mathbf{F}^x(T_m)\right)$ of a cap/floor over $[T_r, T_N]$ at time T_m, with $T_m \leq T_r < T_N$, is given by

$$C_{[r,N]}\left(T_m, \mathbf{P}^d(T_m), \mathbf{F}^x(T_m)\right) = M \sum_{j=r}^{N-1} \tau_j P^d_{j+1}(T_m) \mathbb{E}^{\mathbb{Q}^{T_{j+1}}_d}_{T_m}\left[\left(w\left(F^x_j(T_j) - K\right)\right)^+\right],$$

where $w = 1$ represents a cap and $w = -1$ denotes a floor. If the LMM assumes either normal or log-normal dynamics of the forward LIBOR rates, this expectation can be computed by, respectively, Bachelier's or Black's model:

$$C^{LMM}_{[r,N]}\left(T_m, \mathbf{P}^d(T_m), \mathbf{F}^x(T_m)\right) = M \sum_{j=r}^{N-1} \tau_j P^d_{j+1}(T_m)\, Bachelier\left(T_m, T_j, F^x_j(T_m), K, \sqrt{\int_{T_m}^{T_j} \sigma^2_j(t)\, dt}, w\right),$$

or

$$C^{LMM}_{[r,N]}\left(T_m, \mathbf{P}^d(T_m), \mathbf{F}^x(T_m)\right) = M \sum_{j=r}^{N-1} \tau_j P^d_{j+1}(T_m)\, Black\left(T_m, T_j, F^x_j(T_m), K, \sqrt{\int_{T_m}^{T_j} \sigma^2_j(t)\, dt}, w\right),$$

with $\sigma_j(t)$ characterizing the instantaneous volatility corresponding to $F^d_j(t)$. The implied Bachelier/Black volatility corresponding to the j^{th} caplet or floorlet is determined as

$$\widetilde{\sigma}_j = \sqrt{\frac{\int_{T_m}^{T_j} \sigma^2_j(t)\, dt}{T_j - T_m}}.$$

3.7.2. PRICING EUROPEAN SWAPTIONS

In Subsection 2.5.2 it is discussed that the value $\widetilde{S}_{[r,N]}\left(T_m, \mathbf{P}^d(T_m), \mathbf{F}^x(T_m)\right)$ of a European swaption over $[T_r, T_N]$ at time T_m, with $T_m \leq T_r < T_N$, is determined as

$$\widetilde{S}_{[r,N]}\left(T_m, \mathbf{P}^d(T_m), \mathbf{F}^x(T_m)\right) = MA_{[r,N]}\left(T_m, \mathbf{P}^d(T_m)\right) \mathbb{E}^{\mathbb{Q}^{r,N}_d}_{T_m}\left[\left(w\left(R_{[r,N]}\left(T_r, \mathbf{P}^d(T_r), \mathbf{F}^x(T_r)\right) - K\right)\right)^+\right], \quad (3.20)$$

with $w = 1$ denoting a payer swaption and $w = -1$ representing a receiver swaption. To compute the expectation by means of either Bachelier's or Black's model, it is required that the swap rate be, respectively, normally or log-normally distributed. However, if the LMM assumes that the forward OIS/LIBOR rates are (log-)normally distributed, resulting in non (log-)normal swap rate dynamics by definition (2.15). It is inconsistent to jointly model the forward rates and the swap rates as if they both derived from a (log-)normal distribution.[1] Nevertheless, multiple empirical studies in literature have shown that swap rates obtained from (log-)normal forward OIS/LIBOR rates are not far from being (log-)normal themselves under their relevant measure. In the LMM, the swap rate dynamics under the corresponding swap measure can be accurately approximated by exact (log-)normal dynamics. Mercurio (2009) proposes an approach for achieving this in the MC framework. The rest of this subsection is devoted to the derivation of the approximated swap rate dynamics in the MC LMM.

Let $T_0 \leq t \leq T_r < T_N$. The swap rate is represented as a weighted average of the underlying forward LIBOR rates

$$R_{[r,N]}\left(t, \mathbf{P}^d(t), \mathbf{F}^x(t)\right) = \frac{\sum_{j=r}^{N-1} \tau_j P^d_{j+1}(t)}{A_{[r,N]}\left(t, \mathbf{P}^d(t)\right)} F^x_j(t),$$

[1] The interested reader can find a more in depth discussion about the importance of the inconsistent distributional assumptions in (Brace et al., 2001), (Brigo and Liinev, 2005) and (Rebonato, 1999).

$$= \sum_{j=r}^{N-1} w_j\left(t, \mathbf{P}^d(t)\right)\left(F_i^d(t) + G_i(T_0)\right), \tag{3.21}$$

with weights $w_j\left(t, \mathbf{P}^d(t)\right)$. To lighten the notation, the dependence of the swap rate on $\mathbf{P}^d(t)$ and $\mathbf{F}^x(t)$ is suppressed in this section. Recall that $R_{[r,N]}(t)$ is a martingale under $\mathbb{Q}_d^{r,N}$, by definition. The application of Itô's lemma to (3.21) yields

$$\begin{aligned} dR_{[r,N]}(t) &= \sum_{j=r}^{N-1} \frac{\partial R_{[r,N]}(t)}{\partial F_j^d(t)} dF_j^d(t), \\ &= \phi\left(R_{[r,N]}(t)\right) \sum_{j=r}^{N-1} \frac{\partial R_{[r,N]}(t)}{\partial F_j^d(t)} \frac{\phi\left(F_j^d(t)\right)}{\phi\left(R_{[r,N]}(t)\right)} \sigma_j(t) \boldsymbol{\lambda}_j(t)^\top d\mathbf{W}^{\mathbb{Q}_d^{r,N}}(t), \end{aligned}$$

where $\phi(x) = 1$ specifies the normal model formulation, whereas $\phi(x) = x$ defines the log-normal formulation. The swap rate instantaneous volatility is clearly a stochastic quantity and consequently, the swap rate is not (log-)normally distributed.[1] In order to approximate this diffusion coefficient by a deterministic, time-depending variant, the following approximation is performed:

$$\frac{\partial R_{[r,N]}(t)}{\partial F_j^d(t)} \approx w_j\left(t, \mathbf{P}^d(t)\right).$$

Strictly speaking, this is not correct since the weights $w_j\left(t, \mathbf{P}^d(t)\right)$ depend on the forward OIS rates. However, in practice this has proven to be an acceptable approximation for yield curves that are not remarkably steep (see (Jäckel and Rebonato, 2000) and (Rebonato, 2002)). The weights are then frozen at their time T_m, $T_0 \le T_m \le T_r$, value. This is admissible since the variability of the weights is significantly lower than the one of the forward rates (see (Brigo and Mercurio, 2007) and (Rebonato, 2002)). Furthermore, according to Andersen and Andreasen (1998), for considerably flat curves it is reasonable to assume that the ratio $\phi\left(F_j^d(t)\right)/\phi\left(R_{[r,N]}(t)\right)$ is nearly constant.[2] For this reason, it is also justified to freeze the ratio at its time T_m value. One obtains the approximated (log-)normal swap rate dynamics

$$dR_{[r,N]}(t) \approx \phi\left(R_{[r,N]}(t)\right) \sum_{j=r}^{N-1} w_j\left(T_m, \mathbf{P}^d(T_m)\right) \frac{\phi\left(F_j^d(T_m)\right)}{\phi\left(R_{[r,N]}(T_m)\right)} \sigma_j(t) \boldsymbol{\lambda}_j(t)^\top d\mathbf{W}^{\mathbb{Q}_d^{r,N}}(t),$$

where the swap rate instantaneous volatility is deterministic and time-dependent. The expectation of (3.20) can now be computed by means of Bachelier's model if the forward OIS rates are modeled as coming from a normal distribution:

$$\widetilde{S}_{[r,N]}^{LMM}\left(T_m, \mathbf{P}^d(T_m), \mathbf{F}^x(T_m)\right) = MA_{[r,N]}\left(T_m, \mathbf{P}^d(T_m)\right) Bachelier\left(T_m, T_r, R_{[r,N]}\left(T_m, \mathbf{P}^d(T_m), \mathbf{F}^x(T_m)\right), K, v_{[r,N]}, w\right), \tag{3.22}$$

while, if the forward rates are log-normally distributed, Black's formula can be applied, yielding

$$\widetilde{S}_{[r,N]}^{LMM}\left(T_m, \mathbf{P}^d(T_m), \mathbf{F}^x(T_m)\right) = MA_{[r,N]}\left(T_m, \mathbf{P}^d(T_m)\right) Black\left(T_m, T_r, R_{[r,N]}\left(T_m, \mathbf{P}^d(T_m), \mathbf{F}^x(T_m)\right), K, v_{[r,N]}, w\right), \tag{3.23}$$

where

$$\begin{aligned} v_{[r,N]} &= \sqrt{\int_{T_m}^{T_r} \sum_{i=r}^{N-1} \sum_{j=r}^{N-1} w_i\left(T_m, \mathbf{P}^d(T_m)\right) w_j\left(T_m, \mathbf{P}^d(T_m)\right) \phi\left(F_i^d(T_m)\right) \phi\left(F_j^d(T_m)\right) \sigma_i(t) \sigma_j(t) \boldsymbol{\lambda}_i(t)^\top \boldsymbol{\lambda}_j(t) dt} \Big/ \phi\left(R_{[r,N]}(T_m)\right), \\ &= \sqrt{\sum_{i=r}^{N-1} \sum_{j=r}^{N-1} w_i\left(T_m, \mathbf{P}^d(T_m)\right) w_j\left(T_m, \mathbf{P}^d(T_m)\right) \phi\left(F_i^d(T_m)\right) \phi\left(F_j^d(T_m)\right) \rho_{i,j} \int_{T_m}^{T_r} \sigma_i(t) \sigma_j(t) dt} \Big/ \phi\left(R_{[r,N]}(T_m)\right), \end{aligned} \tag{3.24}$$

with the second equality following from $\rho_{i,j} = \boldsymbol{\lambda}_i(t)^\top \boldsymbol{\lambda}_j(t)$. This correlation term is taken out of the integral as it does not depend on the calendar time t. In practice, (3.24) is known as the Rebonato's swap rate volatility

[1] The swap rate instantaneous volatility is given by $\sum_{j=r}^{N-1} \frac{\partial R_{[r,N]}(t)}{\partial F_j^d(t)} \frac{\phi\left(F_j^d(t)\right)}{\phi\left(R_{[r,N]}(t)\right)} \sigma_j(t)$.

[2] For the case in which $\phi(x) = 1$, the ratio is always constant by definition.

approximation. The implied Bachelier/Black volatility is determined by

$$\begin{aligned}\widetilde{\sigma}_{[r,N]} &= \sqrt{\frac{v_{[r,N]}}{T_r - T_m}}, \\ &= h\left(T_m, T_r, T_N, a, b, c, d, \beta, k_r, k_{r+1}, \ldots, k_{N-1}\right),\end{aligned} \tag{3.25}$$

where the notation $h\left(T_m, T_r, T_N, a, b, c, d, \beta, k_r, k_{r+1}, \ldots, k_{N-1}\right)$ is introduced to show the explicit dependence on the model parameters. This representation will be useful in Chapter 4.

Jäckel and Rebonato (2000) have tested the accuracy of the SC variant of (3.24) by comparing the Monte Carlo prices of a particular strip of ATM co-terminal payer swaptions with the corresponding prices obtained using the approximation. This has been done for a flat yield curve at 7% and the GBP curve of August 10^{th}, 2000. The results corresponding to the flat yield curve show that the swaptions are priced with a remarkable degree of accuracy when using the approximation: the maximum difference between the prices determined by Monte Carlo and by Rebonato's approximation amounts to 2.50 basis points (bp). When considering the non-flat GBP curve, the approximation worsens and the price obtained using Rebonato's swap rate diverges from the Monte Carlo price up to 10 bp. In Section 3.8 a similar test to the one of (Jäckel and Rebonato, 2000) will be performed to analyze the accuracy of (3.24) in the MC LMM.

3.8. TESTING THE ACCURACY OF REBONATO'S APPROXIMATION

3.8.1. TEST DESCRIPTION

In the previous section the MC variant of Rebonato's swap rate approximation was derived, which depended only on the forward OIS rate curve at time T_m. In this section a proof of the validity of (3.24) is given by checking actual European swaption prices. The following test is carried out.

1. The finite set of tenor dates $\{T_m\}_{m=0}^{45}$ is considered, such that $0 = T_0 < T_1 < \ldots < T_{45}$ and $\tau_m = 0.25$ for all m. The instantaneous volatility parametrization (3.4) is used with $a = 0.0013$, $b = 0.0145$, $c = 0.5028$, $d = 0.0056$ and $k_i = 1.13$, $i \in \{0, \ldots, 44\}$.[1] These values are chosen so that the current levels of volatilities can be reproduced by the model. The correlation among the distinct forward rates is given by (3.5) with $\beta = 0.20$.

2. The dynamics of the forward OIS rates (3.11) are assumed to be driven by a normal process, where as many driving Brownian motions are retained as forward rates to be modeled. The implied Bachelier volatilities (3.25) of the strip of co-terminal, quarterly-annual paying ATM swaptions {1Y10Y, 2Y9Y, 3Y8Y, 4Y7Y, 5Y6Y, 6Y5Y, 7Y4Y, 8Y3Y, 9Y2Y, 10Y1Y} are determined, whereafter the corresponding approximated Bachelier payer swaption prices are computed.

3. Given the initial OIS and LIBOR rate curves presented in Appendix A, a Monte Carlo evaluation of the chosen payer swaption prices is carried out with $dt = 0.1$ and $H = 1,000,000$.

4. The Bachelier payer swaption prices obtained using (3.25) are compared to the corresponding Monte Carlo prices.

The setup considered in steps 1-3 specifies the reference scenario.[2] As, in Chapter 4, Rebonato's swaption volatility approximation will be applied to price swaptions involving other underlying swap tenors and strikes, it is of interest to analyze if (3.24) also performs well under these circumstances. The individual impact of these two elements on the approximation is identified by creating new scenarios, in which only one single element at a time is modified with respect to the reference setup. Steps 1-4 are again performed, considering these new scenarios. The additional setups involve the following sets of payer swaptions to be priced:

- Scenario 1: ATM swaption strip {1Y5Y, 2Y4Y, 3Y3Y, 4Y2Y, 5Y1Y},
- Scenario 2: ATM swaption strip {1Y15Y, 2Y14Y, 3Y13Y, 4Y12Y, 5Y11Y, 6Y10Y, 7Y9Y, 8Y8Y, 9Y7Y, 10Y6Y, 11Y5Y, 12Y4Y, 13Y3Y, 14Y2Y, 15Y1Y},

[1] The same values of a, b, c and d are chosen as the ones presented in Subsection 4.4.3. The constant value 1.13 of the parameters k_i is the average over the corresponding parameters shown in that same subsection.

[2] For clarity, the reference scenario involves the ATM swaption strip {1Y10Y, 2Y9Y, 3Y8Y, 4Y7Y, 5Y6Y, 6Y5Y, 7Y4Y, 8Y3Y, 9Y2Y, 10Y1Y}.

- Scenario 3: ATM − 1% swaption strip {1Y10Y, 2Y9Y, 3Y8Y, 4Y7Y, 5Y6Y, 6Y5Y, 7Y4Y, 8Y3Y, 9Y2Y, 10Y1Y},
- Scenario 4: ATM + 1% swaption strip {1Y10Y, 2Y9Y, 3Y8Y, 4Y7Y, 5Y6Y, 6Y5Y, 7Y4Y, 8Y3Y, 9Y2Y, 10Y1Y},
- Scenario 5: ATM + 2% swaption strip {1Y10Y, 2Y9Y, 3Y8Y, 4Y7Y, 5Y6Y, 6Y5Y, 7Y4Y, 8Y3Y, 9Y2Y, 10Y1Y},
- Scenario 6: ATM + 3% swaption strip {1Y10Y, 2Y9Y, 3Y8Y, 4Y7Y, 5Y6Y, 6Y5Y, 7Y4Y, 8Y3Y, 9Y2Y, 10Y1Y}.

In Subsection 3.8.2 the empirical results of the reference scenario are presented, while the ones of the other setups can be found in Appendix C. The results come in the form of a table, in which the approximated Bachelier prices for all payer swaptions in the considered strip are shown, together with the corresponding Monte Carlo prices. The difference between these two prices are included as well. All prices and differences are expressed in basis points, choosing a notional of 10,000 units of currency.

3.8.2. EMPIRICAL RESULTS FOR THE REFERENCE SCENARIO

Maturity (in years)	Tenor (in years)	Strike	LMM Rebonato price (in bp)	LMM MC price (in bp)	Difference (in bp)
1	10	0.01974	364.61	359.42	−5.19
2	9	0.02092	473.03	468.77	−4.26
3	8	0.02170	521.30	517.92	−3.38
4	7	0.02224	533.14	530.63	−2.51
5	6	0.02265	518.97	516.32	−2.65
6	5	0.02298	483.47	481.34	−2.14
7	4	0.02323	428.20	426.37	−1.82
8	3	0.02342	352.64	351.48	−1.16
9	2	0.02354	255.58	255.19	−0.39
10	1	0.02369	136.99	137.09	0.10

Table 3.1: Results for reference scenario, K = ATM.

3.8.3. DISCUSSION OF THE EMPIRICAL RESULTS

From the results shown in Table 3.1 one can see that shorter underlying swaps produce better results, as the approximation involves less forward OIS rates. In the most unfavorable cases of the 1Y10Y and 2Y9Y, with respectively 40 and 36 forward rates in the underlying swap, the differences between the Monte Carlo prices and and the approximated Bachelier prices increase, with a maximum error amounting to 5.19 bp. For the current test, a USD LIBOR yield curve has been used, that is relatively flat. This has produced an error that is twice as large as that of the flat yield curve considered in (Jäckel and Rebonato, 2000) but that is closer to the results provided by the GBP non-flat curve, also addressed in the same article. Given the non perfectly flat nature of the USD LIBOR curve used, the results appear in line with those of the referenced paper.

Table C.1 and Table C.2, presented in Appendix C, form additional support to the conjecture that larger underlying swap tenors lead to a decrease in the accuracy of the approximation. Indeed, the maximum error of the strip involving swaptions with a maximum underlying tenor of 5Y amounts to −2.11 bp, whereas the errors observed for the strip of swaptions with a maximum underlying 15Y tenor are up to −7.59 bp. Furthermore, the results of both tables show larger errors for the first few swaptions of the strips.

Table C.3 shows that, for ITM strikes, the differences between the approximated prices and Monte Carlo prices at the front end of the strip are larger than those for the ATM strike. It is indeed seen that the approximated price diverges from the Monte Carlo price up to 8.60 bp for payer swaptions with strike ATM − 1%, while the maximum difference observed for the ATM case amounts to −5.19 bp.
For increasing OTM strikes, the differences at the front end of the strip first decrease significantly, compared to those in the ATM reference scenario, whereas they marginally increase afterwards. Table C.4 shows that the Rebonato approximation is extremely accurate when considering ATM + 1% payer swaptions, as the maximum difference amounts to 0.90 bp. For deeper OTM strikes this difference starts to increase, as is observed

for the ATM + 2% and ATM + 3% payer swaptions. In these cases the approximated Bachelier payer swaption prices differ from the Monte Carlo ones by a maximum of, respectively, 1.38 and 2.02 bp, but this can still be considered very accurate according to (Jäckel and Rebonato, 2000).
The above observations are in line with the consideration of Andersen and Piterbarg (2010b) that the Rebonato approximation is in general less accurate for strikes further away from the swap rate. Research on the cause of this behavior, though, is beyond the scope of this work.

4

CALIBRATION OF THE LMM IN THE MC FRAMEWORK

In order to use the MC LMM for option pricing, the model parameters have to be calibrated. A calibration procedure can be described as the routine in which the free parameters are estimated such that model-prices match the market quoted prices of specific instruments as closely as possible. It ensures that the set of *calibration instruments* is priced back by the the model. Calibration instruments are chosen that are closely related to the exotic derivatives to be priced. As, in this research, the ultimate goal is to value Bermudan swaptions, the MC LMM is calibrated to the underlying swaptions.

This chapter first presents the general calibration strategy for determining the model parameters, whereafter the minimization problem is introduced. Subsequently, it is explained how the MC LMM is calibrated to real market data, the results of which are given in Section 4.4. In Section 4.5, the calibration results are discussed, followed by a short conclusion of the chapter.

4.1. GENERAL CALIBRATION STRATEGY

In the calibration procedure the MC LMM swaption prices have to be determined in a quick and efficient way, after which they are compared to the corresponding market prices. The brute-force approach to determine these model prices involves carrying out a Monte Carlo simulation of the forward OIS rate processes, using an initial set of model parameters and varying these parameters until an optimal solution is reached. In practice this is not a viable method since the Monte Carlo method is computationally expensive. Instead, the analytical closed-form swap rate volatility approximation derived in Subsection 3.7.2 can be used for calibration purposes. Fixing the correlation parameter β in advance, the calibration procedure comes down to determining the model parameters a, b, c, d and k_i, $i \in \{0,\ldots,N-1\}$, such that the model implied volatilities of a certain set of European swaptions given by (3.25) are in line with their corresponding current market volatilities. Recalling from Subsection 2.5.2 that $\widetilde{\sigma}^{MKT}_{[r,N]}$ defines the $T_r \times (T_N - T_r)$ swaption implied Bachelier/Black volatility provided by the market, a, b, c, d and k_i, $i \in \{0,\ldots,N-1\}$, have to be found that solve

$$\widetilde{\sigma}^{MKT}_{[r,N]} = h\big(T_0, T_r, T_N, a, b, c, d, \beta, k_r, k_{r+1}, \ldots, k_{N-1}\big),$$

for each swaption in the set of calibration instruments.

The calibration routine can be divided into two different phases. During the first phase an optimal set of the parameters a, b, c and d is found that gives the best possible fit to a set of model implied volatilities of European swaptions to the market. Subsequently the parameters k_i, $i = 0,\ldots,N-1$ are determined in a bootstrap fashion such that the market implied volatilities of the calibration instruments can be priced back precisely by the MC LMM. This procedure constitutes the second phase.

This calibration strategy is outlined in the following general algorithm. Further details and a more in depth discussion on this routine can be found in the subsequent sections.

1. Choose a set of p co-terminal swaptions with maturities $0 < T_{m_1} < \ldots < T_{m_p}$, $\{T_{m_i}\}_{i=1}^{p} \subseteq \{T_i\}_{i=1}^{N-1}$, where the underlying swap corresponding to the i^{th} swaption, $i \in \{1,\ldots,p\}$, has strike K_i and final payment date T_N.[1]

2. Set $k_i = 1$ for all $i \in \{0,\ldots,N-1\}$.

3. Calibrate parameters a, b, c and d so that the model implied volatilities of the set of swaption instruments match the corresponding market volatilities as close as possible. Denote these optimal parameters a^*, b^*, c^* and d^*.

4. Consider the swaption corresponding to the last option maturity date T_{m_p}. Determine the parameters $\{k_i\}_{i=m_p}^{N-1}$ such that

$$\tilde{\sigma}^{MKT}_{[m_p,N]} - h\left(T_0, T_{m_p}, T_N, a^*, b^*, c^*, d^*, \beta, k_{m_p}, k_{m_p+1}, \ldots, k_{N-1}\right) = 0, \tag{4.1}$$

   under the constraint

$$k_{m_p} = k_{m_p+1} = \ldots = k_{N-1}.$$

   Equation (4.1) is solved using a numerical root-finding algorithm.[2] Let $\{k_i^*\}_{i=m_p}^{N-1}$ be the set of parameters that gives an exact fit to the market implied swaption volatilities.

5. To determine the parameters k_i for the remaining maturities, proceed according to the following. Assume that the MC LMM is able to exactly price back the swaptions with maturities $\{T_{m_i}\}_{i=n}^{p}$, i.e. one has the knowledge of $\{k_i^*\}_{i=m_n}^{N-1}$. In order to match the model implied volatility of the $T_{m_{n-1}} \times \left(T_N - T_{m_{n-1}}\right)$ swaption to its corresponding market volatility, find $\{k_i\}_{i=m_{n-1}}^{m_n-1}$ such that

$$\tilde{\sigma}^{MKT}_{[m_{n-1},N]} - h\left(T_0, T_{m_{n-1}}, T_N, a^*, b^*, c^*, d^*, \beta, k_{m_{n-1}}, k_{m_{n-1}+1}, \ldots, k_{m_n-1}, k^*_{m_n}, \ldots, k^*_{N-1}\right) = 0,$$

   under the constraint

$$k_{m_{n-1}} = k_{m_{n-1}+1} = \ldots = k_{m_n-1}.$$

   Define these parameters as $\{k_i^*\}_{i=m_{n-1}}^{m_n-1}$.

6. Repeat the previous step until the first swaption can exactly be priced back by the model, i.e. until $n = 2$ is reached.

Note that, following this procedure, the set $\{k_i\}_{i=0}^{m_1-1}$ will remain equal to 1.

4.2. MINIMIZATION PROBLEM

A key element of the calibration procedure is the algorithm for identifying the values of the parameters a, b, c and d from the market data. This consists in the determination of the set of model parameters that minimizes the difference between the market volatilities of the swaptions in the calibration set and the corresponding implied volatilities predicted by the model.[3] It is chosen to consider volatilities rather than outright prices from a time-saving perspective as this avoids the need to apply (3.22) or (3.23) in the calibration procedure. The most important advantage however is that the relative scaling of the individual swaptions is more natural when working with implied volatilities. If calibration was done to prices, long- dated trades would tend to be overweighted relative to short-dated trades. The difference between the model and market implied volatilities of the calibration instruments, measured in the Euclidean norm, represents the objective function that has to be minimized. By introducing the exogenously specified weights w_n, $n = 1,\ldots,p$, the function

[1] The MC LMM is calibrated to co-terminal swaptions as these instruments are the underlyings of a Bermudan swaption. The calibration approach described cannot be generalized for swaptions that do not have the same final payment date as it only works for co-terminal products.

[2] Throughout this thesis a combination of bisection, secant and inverse quadratic interpolation methods is used. See (Forsythe et al., 1977) for more details.

[3] This is done while keeping $k_i = 1$ for all $i \in \{0,\ldots,N-1\}$.

is flexible enough to include the possibility of assigning unequal weights to the distinct calibration instruments. Considering the above, the core of step 3 of the general calibration strategy is defined by the following minimization problem:

$$
\begin{aligned}
\underset{a,b,c,d}{\text{minimize}} \quad & \sum_{n=1}^{p} w_n \left(\tilde{\sigma}^{MKT}_{[m_n,N]} - h\left(T_0, T_{m_n}, T_N, a, b, c, d, \beta, k_{m_n}, k_{m_n+1}, \ldots, k_{N-1}\right)\right)^2, \\
\text{subject to} \quad & -0.02 \leq a \leq 0.016, \\
& 0 < b \leq 0.06, \\
& 0 < c \leq 1, \\
& 0 < d \leq 0.008, \\
& a + d > 0, \\
& a < \frac{b}{c}, \\
& \frac{b - ac}{bc} < 3.
\end{aligned}
$$

The appropriate constraints on the model parameters were discussed in Subsection 3.2.1. A note of precaution is due at this point: by imposing strict bounds on a, b, c and d, one can force the term structure of implied volatilities to adopt any desirable form, this however, will be at the expense of a good fit to the market volatilities. On the other hand, looser bounds will put more emphasis on obtaining an improved fit to the data than on recovering a realistic term structure. Considering the bounds described in the minimization problem, the MC LMM is in general able to fit the target prices to an acceptable degree of accuracy, while preserving a realistic term structure of volatilities.

Choosing the algorithm to solve the minimization problem requires a trade-off between the speed of the routine and the accuracy of the fit. As in this thesis a fast calibration is preferred, the local optimization method based on the interior-point algorithm as presented by Byrd et al. (2000) is chosen. This algorithm is a large-scale algorithm, meaning that it uses linear algebra that does not need to store, nor handles full matrices. Instead, sparse linear algebra is used for computation whenever possible and sparse matrices are internally stored. This leads to the most favorable characteristic of this method: low memory usage and the ability to solve this optimization problem quickly. This algorithm also guarantees that bounds and constraints are satisfied at all iterations. These desirable features were the decisive factors for choosing this interior point approach. Since the scope of this research does not include a thorough analysis of this algorithm, exact details are not presented in this text. The reader is referred to (Byrd et al., 1999) and (Waltz et al., 2006) for an extensive description of the method.

4.3. CALIBRATION TO MARKET DATA

In the previous sections a general calibration strategy of the MC LMM was presented together with a more detailed description of the minimization problem. The algorithm that solves this problem requires several inputs, such as the value of the constant parameter β and the initial estimate for the model parameters a, b, c and d. In Subsection 4.3.1 it is explained how to determine these values. Before starting the calibration routine, it is also essential to specify the set of calibration instruments the prices of which will serve as target values. This is done in Subsection 4.3.2. Furthermore, it is important to determine which degree of influence each of those instrument should have on the outcome of the calibration. To this end, the weight factors have to be carefully assigned, see Subsection 4.3.3 for more details. At this point, one is ready to calibrate the model to real market data. Subsection 4.3.4 explains how the calibration procedure is carried out and presents the format in which the results are recorded.

4.3.1. CHOICE OF PARAMETERS

CHOICE OF CONSTANT PARAMETER β

The decay constant β reflects the sensitivity of the correlation between two forward rates to the difference between their fixing dates. According to Rebonato (2002), European swaptions are mildly dependent on the

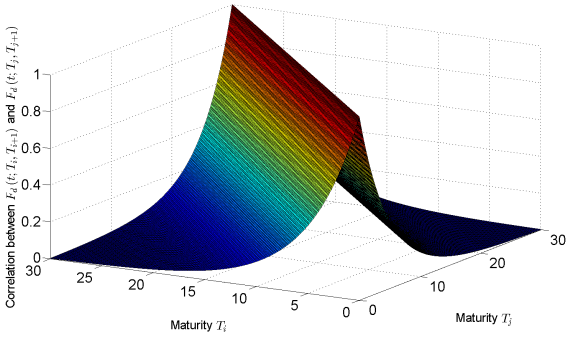

Figure 4.1: Correlation surface for $\beta = 0.20$.

intricate features of the shape of the correlation surface and consequently, calibration to the swaption market is not suitable for determining β. For this reason, it is chosen to fix β prior to calibration. As mentioned in Subsection 3.2.2, it is required that $\beta > 0$ in order to have a valid correlation matrix. From literature it is seen that $\beta \in [0.05, 0.35]$ is a common choice. Unless otherwise stated, $\beta = 0.20$ will be selected. Figure 4.1 shows the correlation surface generated with this value of β.

CHOICE OF INITIAL ESTIMATES FOR THE MODEL PARAMETERS

The interior point algorithm discussed in Section 4.2 requires initial estimates for the volatility parameters a, b, c and d. As this algorithm is a local optimizer method, it is possible for the algorithm to converge to a local optimum. From our experience, the initial guesses

$$a^{\text{init}} = \frac{1}{2}(a_{\min} + a_{\max}), \quad b^{\text{init}} = \frac{1}{2}(b_{\min} + b_{\max}), \quad c^{\text{init}} = \frac{1}{2}(c_{\min} + c_{\max}), \quad d^{\text{init}} = \frac{1}{2}(d_{\min} + d_{\max}),$$

where $a_{\min}, \ldots, d_{\max}$ represent the lower- and upper bounds on the corresponding parameters, have proved to be adequate starting points.[1] With this choice of initial values, the algorithm converged to an optimum that resulted in a good fit of the calibration instruments and that retrieved a realistic term structure of the implied volatilities. There exists a probability that the algorithm may have not reached the global minimum but, as the results obtained using the calibrated parameters are satisfactory, this is not considered relevant.

4.3.2. CHOICE OF CALIBRATION INSTRUMENTS

Three distinct strips of co-terminal swaptions are considered, each characterized by a different maximum underlying tenor. These strips are composed of the following swaptions:

Strip 1: {1Y5Y, 2Y4Y, 3Y3Y, 4Y2Y, 5Y1Y},
Strip 2: {1Y10Y, 2Y9Y, 3Y8Y, 4Y7Y, 5Y6Y, 6Y5Y, 7Y4Y, 8Y3Y, 9Y2Y, 10Y1Y},
Strip 3: {1Y15Y, 2Y14Y, 3Y13Y,4Y12Y, 5Y11Y, 6Y10Y, 7Y9Y, 8Y8Y, 9Y7Y, 10Y6Y, 11Y5Y, 12Y4Y, 13Y3Y, 14Y2Y, 15Y1Y}.

5 different strike levels are considered for each strip. Defining the at-the-money level of the xYzY swaption as $\text{ATM}_{x\text{Y}}^{z\text{Y}}$, the fixed strikes of the swaptions to which the model is calibrated are:

Strikes of strip 1: $\text{ATM}_{1\text{Y}}^{5\text{Y}} + \{-100, 0, +100, +200, +300\}$ bp,
Strikes of strip 2: $\text{ATM}_{1\text{Y}}^{10\text{Y}} + \{-100, 0, +100, +200, +300\}$ bp,
Strikes of strip 3: $\text{ATM}_{1\text{Y}}^{15\text{Y}} + \{-100, 0, +100, +200, +300\}$ bp.

The MC LMM is calibrated for each different strip and distinct strike, resulting in 15 calibration procedures. Each of these requires the market volatilities of the swaptions contained in the respective strip and with the corresponding strike. In Chapter 5 the reader will see that these sets of co-terminal swaptions are related to the swaps underlying the Bermudan swaptions under consideration. In order for the MC LMM to realistically price these exotic interest rate derivatives, it must be able to price back the underlying swaptions with a certain degree of accuracy and, for this reason, the model is calibrated to these instruments.

[1] $a_{\min}, \ldots, d_{\max}$ can be found in Section 4.2.

4.3.3. CHOICE OF THE WEIGHT FACTORS

As mentioned previously, it is possible to attribute more emphasis to certain calibration instruments in the objective function, such that these instruments have more weight in the optimization. This is done by assigning the weights $\{w_i\}_{i=1}^{p}$, where p represents the number of swaptions contained in the calibration set. As all swaptions underlying the Bermudan swaptions considered in Chapter 5 should be priced back as accurately as possible by the MC LMM, in this research it is chosen to use equal weight factors:

$$w_1 = w_2 = \ldots = w_p = 1.$$

4.3.4. CALIBRATION OF THE MC LMM TO REAL MARKET DATA

In this subsection the model will be calibrated to real market data. The most liquid tenor for quoting prices of vanilla instruments for the USD currency is the 3M index. Throughout this research, the USD 3M LIBOR rate will represent the floating benchmark rate. The historical data of 30 January 2015 is considered. The 3M OIS discount curve and the 3M forward LIBOR curve, both as of this date, are shown in Appendix A. For a graphical representation, see Figure 4.2 and Figure 4.3.

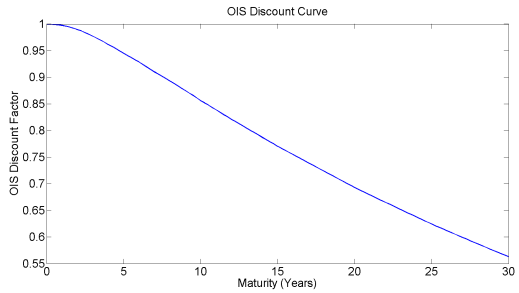

Figure 4.2: OIS discount curve.

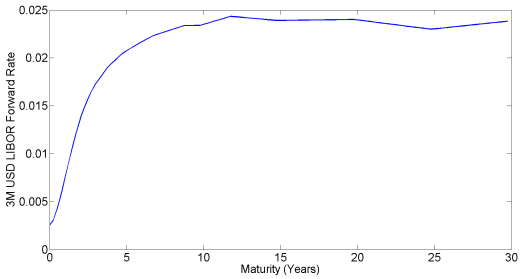

Figure 4.3: 3M USD LIBOR curve.

The past years are marked by a sharp decline in interest rates resulting in exceptionally low, and even negative rates these days. This decline has caused the log-normal volatilities to surge to high levels, as the uncertainties in the market have increased. The usual convention to quote prices in terms of implied Black volatilities has become obsolete, since negative interest rates cause a break down of this model. The quoting convention for implied volatilities has now shifted to, for example, Bachelier implied volatilities (Cuchiero et al., 2016a). Simulating normal dynamics rather than log-normal under the MC LMM reflects the reality of today in a more accurate way, partly because the rates are allowed to become negative. For the calibration this means that model parameters a, b, c, d and k_i, $i = 0,\ldots,N-1$, are determined such that the market implied Bachelier volatilities of a set of specific instruments can be reproduced by the MC LMM.

The instruments in the calibration sets are priced back in two different ways using the calibrated model. First, the model implied volatilities are computed with the normal version of Rebonato's approximation (3.24) considering the full-rank correlation matrix given by (3.5). If the calibration approach is implemented correctly, these prices coincide with the market implied volatilities of the corresponding instruments. Second, the prices are determined using the full-rank, normal MC LMM, employing the Monte Carlo approach as described in Section 3.6. To ensure convergence of this method, an equidistant step size of 0.1 years is taken and 1,000,000 simulations are used.

In Section 4.4 the results of 3 out of the 15 different calibration procedures are presented. As mentioned previously, each calibration approach is characterized by the use of a different set of calibration instruments. To show the impact of the maximum underlying tenor on the calibration accuracy, the results corresponding to the sets consisting of the following swaptions are listed in Section 4.4:

- Strip 1 with fixed strike $\text{ATM}_{1\text{Y}}^{5\text{Y}}$,
- Strip 2 with fixed strike $\text{ATM}_{1\text{Y}}^{10\text{Y}}$,

- Strip 3 with fixed strike $\text{ATM}_{1\text{Y}}^{15\text{Y}}$.

The calibration results of the other cases are presented in Appendix D.

For each calibration procedure related to a specific set of instruments, a table with calibration results in terms of implied volatilities is included. In this table the observed market volatilities are listed for each instrument together with the corresponding volatilities computed with Rebonato's swap rate approximation. The differences between these two volatilities, expressed in basis points, can also be found in the results table. These differences are computed by:

$$\Delta_n^{Reb-MKT} = 10000 \times \left(h\left(T_0, T_{m_n}, T_N, a^*, b^*, c^*, d^*, \beta, k^*_{m_n}, \ldots, k^*_{N-1}\right) - \widetilde{\sigma}^{MKT}_{[m_n,N]} \right),$$

where $\Delta_n^{Reb-MKT}$ denotes the discrepancy between the two implied volatilities related to the n^{th}, $n = 1, \ldots, p$, instrument in the calibration set. Furthermore, the Monte Carlo implied volatilities are given together with the differences in basis points between these volatilities and the observed market volatilities, which are calculated as:

$$\Delta_n^{MC-MKT} = 10000 \times \left(\widetilde{\sigma}^{MC}_{[m_n,N]} - \widetilde{\sigma}^{MKT}_{[m_n,N]} \right).$$

To assess the degree of accuracy of the calibration results for each swaption type, these results are also expressed in terms of payer and receiver swaption prices that are included in a second and third table.[1] These tables are presented to demonstrate how well the MC LMM prices back the payer and receiver swaptions underlying, respectively, the payer and receiver Bermudan swaptions considered in Chapter 5. A notional of 10,000 units of currency is considered so that all prices and differences are expressed in basis points.
Additionally to these tables another table is included, listing the calibrated values of the volatility parameters a, b, c and d. A graphical representation of k_i is given. Moreover, to see if the instantaneous volatilities, with the set of calibrated parameters, show a humped shape and feature the time-homogeneous property, the evolution of a selected set of volatilities $\sigma_n(t)$, $t \in [0, T_n]$, is plotted against the residual maturity time $T_n - t$ of the respective forward OIS rate. The extent to which the time-homogeneous property is present is identified by inspecting if the distinct instantaneous volatility curves coincide. If this is the case, the forward OIS rates with a specific residual time to maturity have the same levels of volatility as OIS rates at a future date with that same residual maturity time, satisfying the time- homogeneous property. Furthermore, a plot of the term structure of implied Bachelier volatilities is included to evaluate if it can be approximately reproduced across time and to analyze if the curve steeply increases for the very short maturities up to 2 years and monotonically decreases after this maturity.

[1] For clarification, the payer and receiver swaption prices are obtained by inserting the implied volatilities of the first table into (3.22) together with the inputs $w = 1$ and $w = -1$, respectively.

4.4. CALIBRATION RESULTS

4.4.1. STRIP 1 WITH STRIKE $\mathbf{ATM}^{\mathbf{5Y}}_{\mathbf{1Y}}$

Maturity (in years)	Tenor (in years)	Market vol.	LMM Rebonato vol.	Difference (in bp)	LMM MC vol.	Difference (in bp)
1	5	0.00838	0.00838	0.0	0.00826	−1.2
2	4	0.00864	0.00864	0.0	0.00853	−1.2
3	3	0.00902	0.00902	0.0	0.00891	−1.1
4	2	0.00917	0.00917	0.0	0.00907	−1.0
5	1	0.00937	0.00937	0.0	0.00932	−0.5

Table 4.1: Strip 1 with strike $K = 1.679\%$: calibration results in terms of implied volatilities.

Maturity (in years)	Tenor (in years)	Market price (in bp)	LMM Rebonato price (in bp)	Difference (in bp)	LMM MC price (in bp)	Difference (in bp)
1	5	161.41	161.41	0.00	159.12	2.29
2	4	223.04	223.04	0.00	220.51	2.53
3	3	222.81	222.81	0.00	220.75	2.06
4	2	176.14	176.14	0.00	174.67	1.47
5	1	100.03	100.03	0.00	99.61	0.43

Table 4.2: Strip 1 with strike $K = 1.679\%$: calibration results in terms of payer swaption prices.

Maturity (in years)	Tenor (in years)	Market price (in bp)	LMM Rebonato price (in bp)	Difference (in bp)	LMM MC price (in bp)	Difference (in bp)
1	5	161.41	161.41	0.00	159.68	1.73
2	4	155.06	155.06	0.00	153.24	1.82
3	3	139.19	139.19	0.00	137.39	1.81
4	2	105.70	105.70	0.00	104.65	1.05
5	1	59.57	59.57	0.00	59.36	0.21

Table 4.3: Strip 1 with strike $K = 1.679\%$: calibration results in terms of receiver swaption prices.

a	b	c	d
0.0030	0.0187	0.7611	0.0033

Table 4.4: Strip 1 with strike $K = 1.679\%$: calibrated parameters a, b, c, d.

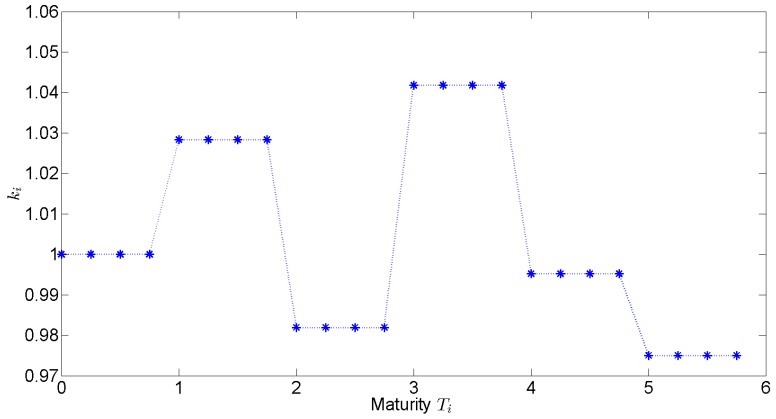

Figure 4.4: Strip 1 with strike $K = 1.679\%$: representation of k_i.

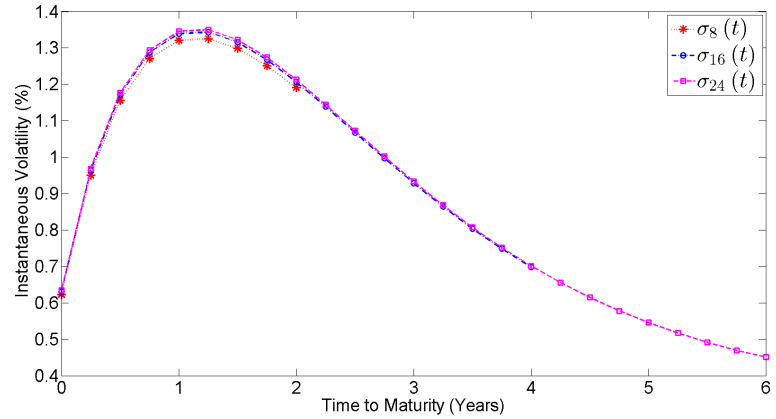

Figure 4.5: Strip 1 with strike $K = 1.679\%$:
evolution of the instantaneous volatility.

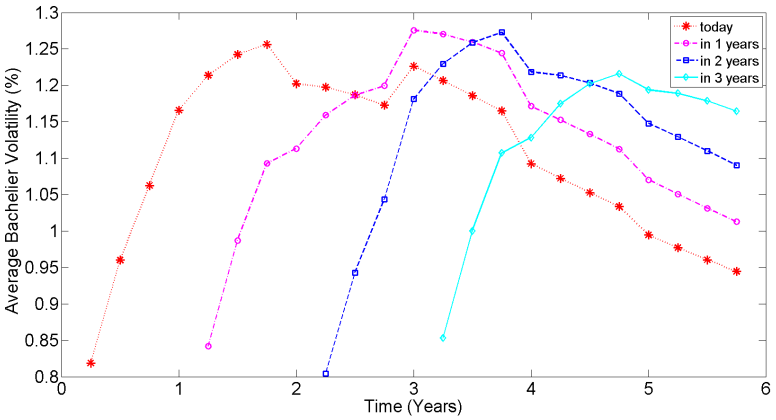

Figure 4.6: Strip 1 with strike $K = 1.679\%$:
evolution of the term structure of implied Bachelier volatilities.

4.4.2. STRIP 2 WITH STRIKE ATM_{1Y}^{10Y}

Maturity (in years)	Tenor (in years)	Market vol.	LMM Rebonato vol.	Difference (in bp)	LMM MC vol.	Difference (in bp)
1	10	0.00833	0.00833	0.0	0.00822	−1.1
2	9	0.00839	0.00839	0.0	0.00829	−1.0
3	8	0.00850	0.00850	0.0	0.00842	−0.8
4	7	0.00858	0.00858	0.0	0.00851	−0.8
5	6	0.00865	0.00865	0.0	0.00858	−0.8
6	5	0.00859	0.00859	0.0	0.00851	−0.8
7	4	0.00859	0.00859	0.0	0.00853	−0.7
8	3	0.00861	0.00861	0.0	0.00856	−0.6
9	2	0.00864	0.00864	0.0	0.00861	−0.3
10	1	0.00874	0.00874	0.0	0.00873	−0.1

Table 4.5: Strip 2 with strike $K = 1.974\%$: calibration results in terms of implied volatilities.

Maturity (in years)	Tenor (in years)	Market price (in bp)	LMM Rebonato price (in bp)	Difference (in bp)	LMM MC price (in bp)	Difference (in bp)
1	10	307.00	307.00	0.00	303.09	3.91
2	9	440.87	440.87	0.00	436.05	4.82
3	8	501.50	501.50	0.00	497.28	4.22
4	7	514.56	514.56	0.00	510.67	3.89
5	6	494.69	494.69	0.00	491.14	3.55
6	5	445.84	445.84	0.00	442.24	3.60
7	4	381.22	381.22	0.00	378.80	2.43
8	3	302.15	302.15	0.00	300.75	1.40
9	2	211.12	211.12	0.00	210.55	0.57
10	1	110.85	110.85	0.00	110.75	0.11

Table 4.6: Strip 2 with strike $K = 1.974\%$: calibration results in terms of payer swaption prices.

Maturity (in years)	Tenor (in years)	Market price (in bp)	LMM Rebonato price (in bp)	Difference (in bp)	LMM MC price (in bp)	Difference (in bp)
1	10	307.00	307.00	0.00	301.82	5.18
2	9	343.57	343.57	0.00	338.17	5.40
3	8	359.57	359.57	0.00	354.46	5.11
4	7	357.24	357.24	0.00	353.10	4.14
5	6	339.25	339.25	0.00	336.41	2.85
6	5	303.26	303.26	0.00	301.18	2.08
7	4	259.53	259.53	0.00	257.82	1.71
8	3	206.86	206.86	0.00	205.93	0.93
9	2	146.26	146.26	0.00	145.72	0.54
10	1	77.51	77.51	0.00	77.31	0.20

Table 4.7: Strip 2 with strike $K = 1.974\%$: calibration results in terms of receiver swaption prices.

a	b	c	d
0.0018	0.0180	0.6116	0.0048

Table 4.8: Strip 2 with strike $K = 1.974\%$: calibrated parameters a, b, c, d.

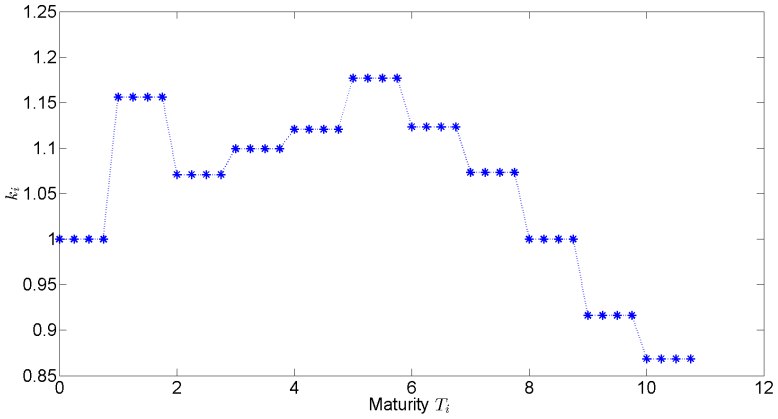

Figure 4.7: Strip 2 with strike $K = 1.974\%$: representation of k_i.

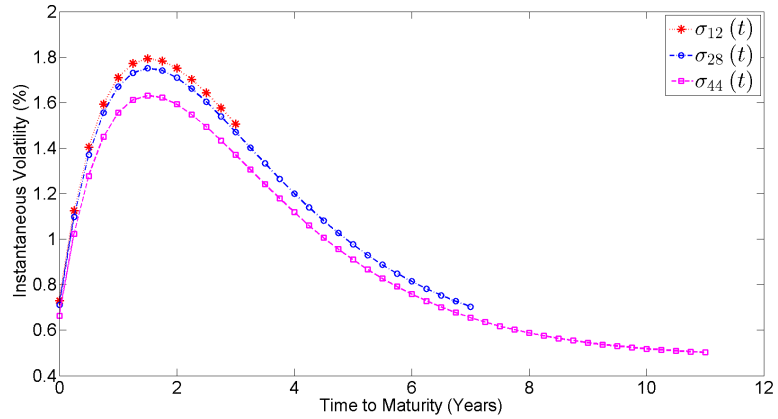

Figure 4.8: Strip 2 with strike $K = 1.974\%$:
evolution of the instantaneous volatility.

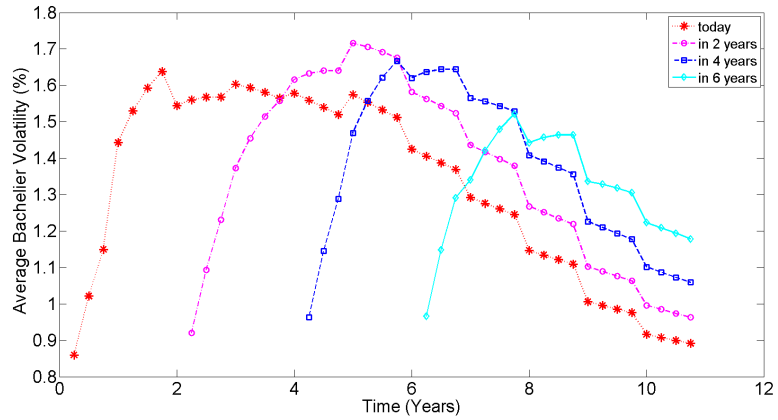

Figure 4.9: Strip 2 with strike $K = 1.974\%$:
evolution of the term structure of implied Bachelier volatilities.

4.4.3. STRIP 3 WITH STRIKE ATM_{1Y}^{15Y}

Maturity (in years)	Tenor (in years)	Market vol.	LMM Rebonato vol.	Difference (in bp)	LMM MC vol.	Difference (in bp)
1	15	0.00823	0.00823	0.0	0.00807	−1.5
2	14	0.00818	0.00818	0.0	0.00805	−1.2
3	13	0.00815	0.00815	0.0	0.00803	−1.2
4	12	0.00821	0.00821	0.0	0.00810	−1.1
5	11	0.00827	0.00827	0.0	0.00816	−1.0
6	10	0.00822	0.00822	0.0	0.00814	−0.8
7	9	0.00815	0.00815	0.0	0.00808	−0.7
8	8	0.00806	0.00806	0.0	0.00799	−0.7
9	7	0.00797	0.00797	0.0	0.00790	−0.7
10	6	0.00789	0.00789	0.0	0.00782	−0.7
11	5	0.00775	0.00775	0.0	0.00768	−0.6
12	4	0.00767	0.00767	0.0	0.00761	−0.5
13	3	0.00754	0.00754	0.0	0.00750	−0.4
14	2	0.00739	0.00739	0.0	0.00736	−0.3
15	1	0.00738	0.00384	0.0	0.00736	−0.2

Table 4.9: Strip 3 with strike $K = 2.105\%$: calibration results in terms of implied volatilities.

Maturity (in years)	Tenor (in years)	Market price (in bp)	LMM Rebonato price (in bp)	Difference (in bp)	LMM MC price (in bp)	Difference (in bp)
1	15	433.48	433.48	0.00	425.45	8.04
2	14	620.33	620.33	0.00	611.57	8.76
3	13	720.10	720.10	0.00	710.99	9.11
4	12	774.82	774.82	0.00	766.09	8.73
5	11	794.84	794.84	0.00	786.28	8.57
6	10	780.92	780.92	0.00	774.06	6.86
7	9	744.60	744.60	0.00	739.14	5.45
8	8	691.88	691.88	0.00	686.92	4.96
9	7	627.12	627.12	0.00	622.56	4.56
10	6	554.23	554.23	0.00	549.77	4.46
11	5	470.09	470.09	0.00	466.85	3.25
12	4	382.44	382.44	0.00	380.31	2.13
13	3	288.92	288.92	0.00	287.58	1.34
14	2	192.84	192.84	0.00	192.03	0.80
15	1	98.16	98.16	0.00	97.88	0.28

Table 4.10: Strip 3 with strike $K = 2.105\%$: calibration results in terms of payer swaption prices.

Maturity (in years)	Tenor (in years)	Market price (in bp)	LMM Rebonato price (in bp)	Difference (in bp)	LMM MC price (in bp)	Difference (in bp)
1	15	433.48	433.48	0.00	426.69	6.80
2	14	510.06	510.06	0.00	501.68	8.38
3	13	552.37	552.37	0.00	543.99	8.38
4	12	579.06	579.06	0.00	570.22	8.84
5	11	588.54	588.54	0.00	580.32	8.22
6	10	575.26	575.26	0.00	568.94	6.32
7	9	547.84	547.84	0.00	541.94	5.91
8	8	509.78	509.78	0.00	504.51	5.27
9	7	463.93	463.93	0.00	460.02	3.91
10	6	411.27	411.27	0.00	408.55	2.72
11	5	349.43	349.43	0.00	347.03	2.40
12	4	287.55	287.55	0.00	285.91	1.64
13	3	220.03	220.03	0.00	219.07	0.96
14	2	148.26	148.26	0.00	147.71	0.55
15	1	76.27	76.27	0.00	76.11	0.17

Table 4.11: Strip 3 with strike $K = 2.105\%$: calibration results in terms of receiver swaption prices.

a	b	c	d
0.0013	0.0145	0.5028	0.0056

Table 4.12: Strip 3 with strike $K = 2.105\%$: calibrated parameters a, b, c, d.

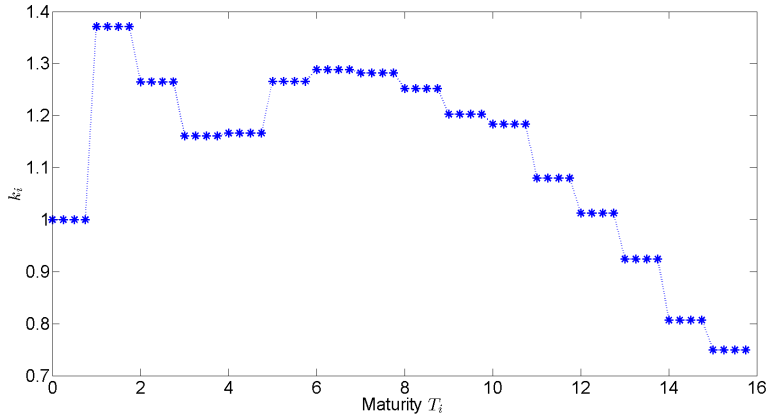

Figure 4.10: Strip 3 with strike $K = 2.105\%$: representation of k_i.

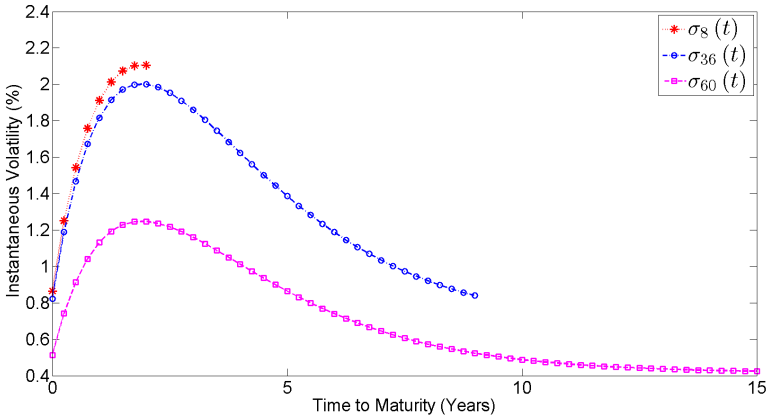

Figure 4.11: Strip 3 with strike $K = 2.105\%$:
evolution of the instantaneous volatility.

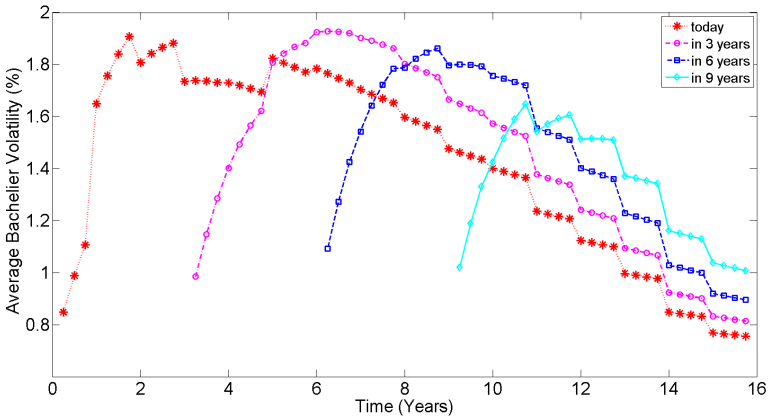

Figure 4.12: Strip 3 with strike $K = 2.105\%$:
evolution of the term structure of implied Bachelier volatilities.

4.5. DISCUSSION OF THE CALIBRATION RESULTS

In the previous section and in Appendix D the calibration results of the MC LMM were presented for 15 different sets of implied swaption volatilities. In this section we will take a closer look at these results, evaluating the effectiveness of the calibration routines considered. This means analyzing whether the generated values of the model parameters give a good fit to the market prices of the calibration instruments and inspecting whether the instantaneous volatility curves feature the humped shape and possess the time-homogeneous property. Additionally, it will be observed if the term structure of implied Bachelier volatilities can be reproduced across time and if it shows a steep increase at the front end of the curve, followed by a monotonic decrease.

4.5.1. QUANTITATIVE ASSESSMENT

It can be noted that larger differences between the implied volatilities determined by (3.24) do not necessarily result in larger differences in terms of payer or receiver swaption prices. Since it is of importance for the MC LMM to price back the swaptions underlying the Bermudan swaptions considered in Chapter 5, the analysis will be done in terms of prices rather than implied volatilities. As it was expected beforehand, the market prices of all payer and receiver swaptions are exactly fitted by the model, when using Rebonato's volatility approximation. However, when pricing these swaptions with the MC LMM using Monte Carlo, it can be seen from the various calibration results that some errors between the Monte Carlo prices and the market prices are present. From now on, these errors will be referred to as calibration errors. Note that, in general, the calibration error becomes larger as the underlying tenor increases. This translates into (3.24) becoming a less accurate approximation for prices of the payer and receiver swaptions with long tenors, as the double sum in (3.24) contains more terms involving approximated values. In particular, when considering a specific strip at a fixed strike, Monte Carlo usually prices the first swaptions of this strip with the greatest degree of inaccuracy, as they have the longest tenors. This phenomenon becomes particularly noticeable for strips 2 and 3, strip 1 shows some exceptions as it contains swaptions with relatively short tenors.

Furthermore, the results for the first strip clearly show that payer and receiver swaptions are priced very accurately with calibration errors up to 2.5 bp for all strikes. When considering the second strip, one sees that the MC LMM prices the swaptions with a reasonable degree of accuracy. In general, the maximum calibration errors lie between 1.7 and 3.7 bp. Some outliers are seen for strikes $K = \text{ATM}_{1\text{Y}}^{10\text{Y}}$ and $K = \text{ATM}_{1\text{Y}}^{10\text{Y}} - 1\%$ where the maximum errors are in the range of 4.8 and 6.5 bp. The calibration errors related to the swaptions contained in strip 3 increase, with maximum errors between 8.0 and 17.5 bp. An extreme case is observed for the payer and receiver swaptions struck at $K = \text{ATM}_{1\text{Y}}^{15\text{Y}} + 3\%$, where the approximated Bachelier prices diverge from the Monte Carlo prices up to 20.9 bp. Only the payer and receiver swaptions with strike $K = \text{ATM}_{1\text{Y}}^{15\text{Y}} + 1\%$ are priced accurately by the MC LMM as the corresponding maximum errors are, respectively, 3.5 and 2.6 bp. Overall, it can be observed that the Rebonato approximation achieves the highest degree of accuracy for strikes close to the ATM level of the first swaption of the strip. As one moves away from these strikes, the calibration errors increase. Improving the accuracy of the Rebonato approximation, though, is beyond the scope of this research.

4.5.2. REALIZED INSTANTANEOUS VOLATILITY CURVES AND TERM STRUCTURES OF IMPLIED VOLATILITIES

For every strip and strike, the calibrated model parameters result in a humped-shape instantaneous volatility curve and a term structure of implied volatilities that features a steep increase for the early maturities, followed by a monotonic decrease. Regarding the preservation of the time-homogeneous property, the values of k_i, $i = 0, \ldots, N-1$, oscillate neatly around 1 for strip 1 with values between 0.9 and 1.2. For strips 2 and 3 the parameters k_i are in the ranges $0.8 - 1.9$ and $0.7 - 2.0$, respectively, and are thus farther away from the desired level of 1. The number of instruments in the calibration sets can be accounted for this phenomenon. When the LMM is calibrated to a larger number of swaptions, the calibrated parameters a, b, c and d will in general result in a less accurate global fit to the market prices of the swaptions in question. Therefore, the values of k_i have to be adjusted more with respect to their original levels of 1 in order to ensure an exact fit. Including more swaptions in the calibration sets, consequently, leads to a loss of the time-homogeneity. This becomes apparent in the plots showing the evolution of the instantaneous volatilities and the evolu-

tions of the term structures of implied Bachelier volatilities. Consider for example the extreme case of strip 3 and strike $K = \text{ATM}_{1\text{Y}}^{15\text{Y}} + 3\%$, the results of which are given in Appendix D.12. Figure D.34 shows that the parameters k_i can attain values between 0.7 and 2.0. Figure D.35 presents the evolution of the instantaneous volatilities $\sigma_n(t)$, $n = 8, 36, 60$ and $t \in [0, T_n]$, corresponding to the OIS rates $F^d(t : 2.00, 2.25)$, $F^d(t : 9.00, 9.25)$ and $F^d(t : 15.00, 15.25)$, respectively. Note that the curves do not coincide, meaning that these OIS rates for a given residual time to maturity do not have the same level of volatility. Furthermore, Figure D.36 shows that the term structure is not equally reproduced across time as its shape changes and the top of the hump decreases. This indicates that, in this particular case, adjusting the values of k_i in order to ensure an exact market fit destroys the essential dependence on the time to maturity. Opposite observations can be made for strip 1 and strike $K = \text{ATM}_{1\text{Y}}^{5\text{Y}}$, see Subsection 4.4.1 for the corresponding results. The values of k_i oscillate around 1, and consequently the instantaneous volatility curves of, for example, $\sigma_8(t)$, $\sigma_{16}(t)$ and $\sigma_{24}(t)$belonging to the OIS rates $F^d(t : 2.00, 2.25)$, $F^d(t : 4.00, 4.25)$ and $F^d(t : 6.00, 6.25)$, respectively, coincide (see Figure 4.5). For the term structure of implied volatilities shown in Figure 4.6 this means that it can be correctly reproduced across time, as its hump shape is approximately preserved.

Note furthermore that, for a specific strip, the distances between the parameters k_i and the desirable value of 1 become larger as the strike moves away from the ATM level of the first swaption of that strip. Consequently, increasing and decreasing the strike with respect to this reference level destroys the dependence on the time to maturity. In particular, it can be seen that the case involving the strike $K = \text{ATM}_{x\text{Y}}^{y\text{Y}} + 3\%$ results in values of k_i, $i = 0, \ldots, N-1$ that lie the farthest away from 1 compared to the values determined for the other cases involving the strip in question. As an example consider the parameters k_i corresponding to strip 3 and strikes $K = \text{ATM}_{1\text{Y}}^{15\text{Y}}$ and $K = \text{ATM}_{1\text{Y}}^{15\text{Y}} + 3\%$. In the first case the values lie within the range $0.7 - 1.4$ while in the latter the parameters k_i assume values between 0.7 and 2.0 (as mentioned earlier). This phenomenon may be a consequence of Rebonato's approximation being less accurate for deeper ITM and OTM strikes.

4.6. SUMMARY

In this chapter the MC LMM is calibrated to 15 distinct sets of implied Bachelier swaption volatilities that correspond to the payer and receiver swaptions underlying the Bermudan swaptions analyzed in Chapter 5. The closed-form approximation (3.24) for the swaption volatility is used in the calibration procedure, which, in the single-curve framework, has proven to be remarkably accurate for yield curves that are (close to) flat (Jäckel and Rebonato, 2000). The correlation parameter β is fixed prior to calibration as swaptions have a low dependency on the correlation structure. The volatility parameters a, b, c and d are calibrated to the market implied volatilities contained in the calibration set, whereafter the parameters k_i are adjusted from their level of 1 to achieve an exact fit. The market payer and receiver prices corresponding to the implied swaption volatilities in the calibration sets are then compared to the MC LMM prices obtained using Monte Carlo.

We have seen from the calibration results that, in all 15 cases considered, the instantaneous volatility curves feature a humped shape and the term structures of implied volatilities show a steep increase for the early maturities, followed by a monotonic decrease. Furthermore, adding more instruments to the calibration sets leads to a loss of the time-homogeneous property.

The results also show that, for the cases of short underlying tenors and strikes near the ATM level, the calibrated model parameters give a good fit to the market prices of the payer and receiver swaptions contained in the calibration sets. The maximum observed calibration errors are up to 2.53 bp. However, the calibration performance decreases when considering swaptions having a combination of long underlying tenors and strikes that are deep ITM or OTM. The calibration error increases for these particular cases and can reach levels up to 20.85 bp. The errors will have an impact on the Bermudan swaption as the prices of the underlying swaptions are not in line with the corresponding market prices.

5

PRICING OF BERMUDAN SWAPTIONS

After successfully calibrating the MC LMM to the swaption market, as illustrated in Chapter 4, the model is now able to price more complex and exotic derivatives. This chapter is devoted to the pricing of Bermudan swaptions, an important subset of the Callable LIBOR Exotic (CLE) class. Bermudan swaptions are actively traded and among the most liquid exotic interest rate derivatives having an early exercise feature.

The main purpose of this chapter is to analyze the impact of the MC LMM on the option value of Bermudan swaptions. The pricing results will be compared to the one-factor Hull-White (1FHW) model. The most important advantage of the MC LMM above the 1FHW model is the ability to exhibit decorrelation among the forward rates and hence, to reproduce different modes of deformation of the yield curve. The 1FHW model, in contrast, assumes that the rates are perfectly correlated at every time instant and consequently only parallel movements of the interest rate curve can be achieved, a shock to the curve at time t being equally transmitted to all maturities. By calibrating both the MC LMM and the 1FHW model to the same set of underlying swaptions, a fair comparison can be made between the Bermudan prices generated by these models. One can then investigate the impact of the model selection.

This chapter starts with the definition of a Bermudan swaption, an explanation follows how these exotic instruments are valued. Subsequently, the test strategy is presented. In this section the details of the considered test deals are given, along with the identification of the numerical methods used for determining the Bermudan swaption prices. It is illustrated how the impact of the model choice on the Bermudan swaption prices can be assessed. In Section 5.3 the MC LMM and the 1FHW prices of the considered deals are highlighted and the pricing results are discussed. Finally, a short conclusion of the chapter is given.

5.1. DEFINITION AND VALUATION

Consider the finite set of tenor dates $\mathcal{T} := \{T_m\}_{m=0}^{N}$, such that $0 = T_0 < T_1 < \ldots < T_N$ and denote by τ_m the year fraction corresponding to the time interval $[T_m, T_{m+1}]$. A *Bermudan swaption* allows the holder to enter into a swap at different times.[1] The set of possible exercise dates is denoted as $\mathcal{E} := \{E_i\}_{i=1}^{s}$, such that $E_1 < \ldots < E_s$ and where $\mathcal{E} \subseteq \mathcal{T} \setminus \{T_0, T_N\}$. The final payment of all swaps takes place at T_N. The *non-call period* refers to the interval $[T_0, E_1)$ in which the holder is not allowed to exercise the Bermudan.[2] The *tenor of the option* is defined as $\tau(E_1, E_s)$.

To determine the optimal exercise strategy, at each exercise time the holder of the Bermudan must decide whether to exercise or keep the option. This decision is based on the comparison between the payoff from immediate exercise with the expected payoff from continuation. The Bermudan is exercised at a certain *call date* if the hold value is greater than or equal to the continuation value. To value a Bermudan at time T_0, the

[1] This right to exercise is referred to as the *call right*.
[2] For simplicity, a Bermudan refers to a Bermudan swaption.

optimal stopping time E_τ, with $E_\tau \in \mathscr{E}$, has to be found that maximizes the expected payoff of the option;

$$V(T_0) = \max_{E_\tau \in \mathscr{E}} \mathbb{E}_{T_0}^{\mathbb{Q}_d^{B^*}} \left[\frac{S_{[\tau,N]}\left(E_\tau, \mathbf{P}^d(E_\tau), \mathbf{F}^x(E_\tau)\right)}{B^*\left(\mathbf{F}^d(E_\tau)\right)} \right].$$

In this thesis the optimal stopping time is estimated within the Monte Carlo framework by the Longstaff & Schwartz (LS) algorithm, in which the difference between the hold and continuation value is regressed along a path on a set of monomials evaluated in a selection of explanatory variables. The accuracy of the approximation depends on the choice of the explanatory variables and on the degree of the monomials. As this method is extensively discussed in literature, a detailed description is not given here. The interested reader is referred to (Longstaff and Schwartz, 2001).

5.2. TEST STRATEGY

This section is devoted to a description of the test strategy. First, the trade characteristics of 30 test deals are given. Subsequently, the models used to price the Bermudans are discussed and the set of calibration instruments are identified. Thereafter, the numerical methods for pricing the interest rate derivatives are determined. In the last subsection, the impact on the model choice on the Bermudans is assessed.

5.2.1. TRADE CHARACTERISTICS

To value the Bermudans under consideration, the market data of 30 January 2015 is used. Further characteristics of the test deals are shown in Table 5.1. The payment schedules treated in the MC LMM are based on calendar days, while the ones considered in the 1FHW model take into account business days. In total 30 deals are in scope. Each payer and receiver Bermudan starting in 1Y and with a specific tenor zY, $z \in \{5, 10, 15\}$, is valued for the following fixed payment rates K:

$$K \in \mathrm{ATM}_{1\mathrm{Y}}^{z\mathrm{Y}} + \{-100, 0, +100, +200, +300\}\,\mathrm{bp}, \tag{5.1}$$

where $\mathrm{ATM}_{1\mathrm{Y}}^{z\mathrm{Y}}$ represents the swap rate of the plain vanilla swap with the same start date (in the considered cases always 1Y) and tenor as the deal.[1]

Currency	USD
Product	Bermudan swaption
Notional	10000
Start date in	1Y
Tenor	5Y, 10Y or 15Y
Swap type	Payer or receiver
Fixed leg	
Payment index	Fixed K
Coupon frequency	Quarterly
Day count convention	Actual 365
# coupons	20, 40 or 60
Floating leg	
Coupon type	Floating
Payment index	LIBOR
Coupon frequency	Quarterly
Day count convention	Actual 365
# coupons	20, 40 or 60
Callable right	
Exercise schedule	Annual

Table 5.1: Trade characteristics.

[1] A payer/receiver Bermudan swaption refers to a Bermudan swaption with underlying payer/receiver swaps.

5.2.2. MODELS AND CALIBRATION

All Bermudan deals are priced using the MC LMM and the 1FHW model, for the latter a fixed mean reversion rate is used together with a piecewise constant volatility. For a detailed description of the 1FHW model, the reader is referred to (Brigo and Mercurio, 2007). Prior to pricing these interest rate derivatives, the model parameters have to be calibrated. In order to make a fair comparison between the Bermudan prices obtained under the MC LMM and under the 1FHW model, the two models are calibrated to the same set of instruments. As the co-terminal swaptions matching the time to maturity on each exercise date and with the same strike as a particular test trade are the natural hedging instruments of that Bermudan, these swaptions are selected as the calibration instruments. Since the models are calibrated to implied volatilities instead of prices, no distinction is made between underlying payer and receiver swaptions.[1] Consequently, 15 calibration procedures are carried out, each characterized by a distinct set of calibration volatilities.[2] Chapter 4 and Appendix D present the calibration results of the MC LMM.

5.2.3. VALUATION

To value the Bermudans with the MC LMM, the Monte Carlo method based on the LS algorithm is used. A time step of 0.10 is considered and 1,000,000 simulations are performed. The forward OIS rates are modeled with normal, full rank dynamics, which are discretized by means of the Euler scheme. The initial OIS and LIBOR curves, both from 30 January 2015, are presented in Appendix A. The Bermudan prices computed with the 1FHW model are externally provided.

5.2.4. IMPACT ANALYSIS

For each test deal, the impact of the MC LMM is analyzed. To this end, the difference between the Bermudan prices computed under the MC LMM and the 1FHW model is determined by

$$\text{Difference} = V^{\text{MC LMM}}(T_0) - V^{\text{1FHW}}(T_0). \tag{5.2}$$

This difference may contain some noise factors and it can be decomposed into the following three components:

1. A contribution from the choice of the model,
2. A contribution from the slightly different payment schedules,
3. A contribution from the calibration error in the MC LMM.

A clarification on component 3 is in order here. As mentioned in Subsection 5.2.2, it is desired that the MC LMM and the 1FHW prices of the swaption underlying the Bermudans coincide. However, Rebonato's approximation is not always accurate, as was seen in Chapter 4, and consequently the MC LMM using Monte Carlo does not always price back the calibration instruments' market prices consistent with the corresponding market prices. These sets of calibration instruments are priced differently by both models, leading to a noise component in (5.2). In this research it has been decided not to take into account noise component 2 as the differences between the payment dates corresponding to the MC LMM and the 1FHW model are only marginal, see Appendix E. The payment schedules corresponding to Bermudans with a 5Y tenor show differences that lie in the range of $0.001 - 0.005$ (expressed in year fractions), while the maximum observed difference related to the MC LMM and the 1FHW model schedules of Bermudans with a 10Y tenor is 0.011. The differences in the payment schedules of Bermudans with a tenor of 15Y are in general between 0.001 and 0.012, with two outliers of 0.014 and 0.016. From these results it can be seen that the payment schedules considered in the MC LMM and in the 1FHW model only slightly differ.

Furthermore, the MC LMM impact on the option value can be compared to the 1FHW vega of the option

[1] As in the current low volatility environment swaption volatilities should be interpreted as normal volatilities, the models are calibrated to implied Bachelier volatilities rather than to implied Black volatilities.

[2] To clarify, the calibrated model parameters obtained by a specific calibration procedure can be used to price both a payer and receiver Bermudan swaption, which, respectively, have the payer and receiver swaptions, whose implied volatilities are contained in the calibration set, as underlyings.

value. The 1FHW vega is computed by a 1 bp parallel shift of the implied volatilities corresponding to the swaptions underlying the Bermudan:

$$\text{vega 1FHW} = V_{1\,\text{bp}}^{\text{1FHW}}(T_0) - V_{0\,\text{bp}}^{\text{1FHW}}(T_0). \tag{5.3}$$

$V_{x\,\text{bp}}^{\text{1FHW}}(T_0)$ represents the Bermudan price at time T_0 determined by the 1FHW model, the model parameters of which are calibrated to a set of implied swaption volatilities that have undergone a parallel shift of x bp. Using (5.3), the MC LMM impact on the Bermudans can be expressed in terms of multiplier × vega.

5.3. EMPIRICAL RESULTS OF THE TEST DEALS

In this section the results of the test deals described in Section 5.2 are presented. For each test deal, the prices computed using the MC LMM and the 1FHW model are given, together with the difference between these prices as defined in (5.2). Additionally, the 1FHW vega is included along with the maximum underlying European swaption market price and the maximum observed absolute calibration error. All prices and differences are expressed in basis points. The results are shown in Table 5.2.[1]

Non-call period (in years)	Tenor (in years)	Fixed rate	ATM level (in %)	Rel strike (in %)	Abs strike (in %)	1FHW price	MC LMM price	Difference MC LMM-1FHW	Vega 1FHW	Max European	Max abs cal error
1	5	Pay	1.68	−1.00	0.68	544.72	568.93	24.21	1.94	496.66	2.00
1	5	Pay	1.68	0.00	1.68	282.04	308.50	26.46	2.71	223.04	2.53
1	5	Pay	1.68	+1.00	2.68	141.98	161.03	19.05	2.36	107.83	1.42
1	5	Pay	1.68	+2.00	3.68	71.52	83.16	11.64	1.64	53.19	0.89
1	5	Pay	1.68	+3.00	4.68	36.89	43.80	6.91	1.10	28.64	0.43
1	5	Receive	1.68	−1.00	0.68	55.51	63.16	7.65	1.81	38.01	1.36
1	5	Receive	1.68	0.00	1.68	217.81	237.24	19.43	2.71	161.41	1.82
1	5	Receive	1.68	+1.00	2.68	542.87	563.41	20.54	1.88	516.10	0.47
1	5	Receive	1.68	+2.00	3.68	979.22	990.57	11.35	0.73	971.19	1.14
1	5	Receive	1.68	+3.00	4.68	1452.47	1456.94	4.47	0.19	1449.60	0.80
1	10	Pay	1.97	−1.00	0.97	1128.03	1267.39	139.36	5.44	990.48	6.47
1	10	Pay	1.97	0.00	1.97	659.24	798.11	138.87	6.84	514.56	4.82
1	10	Pay	1.97	+1.00	2.97	389.00	508.63	119.63	6.22	285.13	2.56
1	10	Pay	1.97	+2.00	3.97	239.12	328.30	89.18	5.03	169.16	3.04
1	10	Pay	1.97	+3.00	4.97	156.27	226.33	70.06	3.94	110.45	3.68
1	10	Receive	1.97	−1.00	0.97	188.68	246.92	58.24	5.09	125.71	5.60
1	10	Receive	1.97	0.00	1.97	505.32	607.79	102.48	6.49	359.57	5.40
1	10	Receive	1.97	+1.00	2.97	1091.91	1206.38	114.47	4.81	988.44	1.68
1	10	Receive	1.97	+2.00	3.97	1898.17	1992.46	94.29	2.31	1861.23	2.58
1	10	Receive	1.97	+3.00	4.97	2790.16	2863.81	73.65	1.04	2774.99	2.41
1	15	Pay	2.10	−1.00	1.10	1680.33	1972.25	291.92	9.62	1440.68	14.50
1	15	Pay	2.10	0.00	2.10	1023.58	1316.88	293.30	11.84	794.84	9.11
1	15	Pay	2.10	+1.00	3.10	629.71	892.02	262.31	10.89	457.80	3.45
1	15	Pay	2.10	+2.00	4.10	413.12	642.44	229.32	9.10	283.83	12.25
1	15	Pay	2.10	+3.00	5.10	296.40	488.40	192.01	7.44	195.48	20.85
1	15	Receive	2.10	−1.00	1.10	334.72	473.52	138.80	8.84	228.49	10.75
1	15	Receive	2.10	0.00	2.10	794.91	1005.80	210.89	10.76	588.54	8.84
1	15	Receive	2.10	+1.00	3.10	1600.86	1836.96	236.10	7.98	1404.36	3.69
1	15	Receive	2.10	+2.00	4.10	2724.88	2936.59	211.71	3.87	2655.77	17.47
1	15	Receive	2.10	+3.00	5.10	3990.83	4131.94	141.11	1.32	3965.05	20.00

Table 5.2: Bermudan pricing results.

5.4. DISCUSSION OF THE RESULTS

In this section the pricing results presented in Section 5.3 are discussed. From Table 5.2 it is seen that the MC LMM overprices all Bermudan deals relative to the 1FHW prices. For increasing Bermudan tenors, the order of magnitude of the differences between the MC LMM and the 1FHW Bermudan prices becomes larger.

Furthermore, the impact of the choice of the model on the Bermudan price, considering the same tenor, is in general larger for strikes around the ATM level of the first underlying swap. This is expected since, for $K \to \infty$, the receiver Bermudan value will converge to its maximum underlying swap price, which, for this strike, will

[1] The third column identifies if the fixed rate K is payed or received by the swaps underlying the Bermudan. The fourth column refers to the ATM level of the underlying swap with the same start date and tenor of the deal. The relative strike is measured with respect to this ATM level and it assumes values in $\{-100, 0, +100, +200, +300\}$ bp. The absolute strike K is defined as in (5.1).

coincide with the maximum European swaption price. The price of a payer Bermudan will converge to zero for the strike going to infinity. This is also reflected in the behavior of the 1FHW vega, that converges to zero for $K \to \infty$. Consequently, in these extreme cases, the risk related to the model selection becomes very small and the Bermudans become more independent of the model choice. In these circumstances, for Bermudans that have low model risk, the difference between their MC LMM and 1FHW price should be around zero. Nevertheless, if this is not the case, this difference can be attributed to calibration errors of the underlying swaptions. If, however, a Bermudan is not fully converged to its maximum underlying European swaption or to zero and the underlying MC LMM swaptions are priced with a significant calibration error, it is difficult to discriminate the component related to the calibration errors from that of the selection of the model.

5.4.1. BERMUDANS WITH A TENOR OF 5 YEARS

Observing that the calibration errors of all swaptions underlying the Bermudan deals with a tenor of 5Y are smaller than or equal to 2.53 bp, it can be concluded that the differences between the prices of the MC LMM and 1FHW Bermudan prices, that lie in the range of 4.47 – 26.46 bp, are primarily related to the selection of the model. The model impact on the Bermudans in terms of vega is between 5 × vega and 10 × vega.

The results obtained for the receiver Bermudan with a 5Y tenor and with relative strike +3.00% show that this Bermudan has low model-risk. As the calibration errors are up to 0.80 bp, the MC LMM prices the underlying swaptions consistently with the 1FHW model. It can be seen from Table 5.2 that both MC LMM and 1FHW Bermudan prices (respectively, 1456.94 and 1452.47 bp) have almost completely converged to the underlying maximum European swaption market price (1449.60 bp). The choice of the model has an impact on the Bermudan price that is limited to 4.47 bp.

5.4.2. BERMUDANS WITH A TENOR OF 10 YEARS

Analyzing the Bermudans with a tenor of 10Y and relative strikes +1.00%, +2.00% and +3.00%, one sees that the MC LMM prices back the underlying swaptions with a high accuracy as the maximum observed calibration error amounts to 3.68 bp. The calibration error component of the difference between the MC LMM and 1FHW Bermudan prices is then considered to be marginal and the observed differences, that are in the range of 70.06 – 119.63 bp, primarily represent the impact of the model choice. In terms of vega, the impact of the model selection is around 20 × vega.

The swaptions underlying the ATM Bermudans and the Bermudans with relative strike −1.00% feature slightly larger calibration errors that reach a maximum value of 6.47 bp. As the calibration errors are relatively small compared to the observed differences between the MC LMM and the 1FHW Bermudan prices, which are between 58.24 and 139.36 bp, the errors will have a slight impact on the Bermudan prices.

5.4.3. BERMUDANS WITH A TENOR OF 15 YEARS

Looking at the Bermudans with a tenor of 15Y, it can be seen that only in the case of relative strike +1.00% the calibration errors corresponding to the underlying swaptions are small as they are up to 3.69 bp. For this reason the differences between the MC LMM and 1FHW prices of the payer and receiver Bermudans (respectively, 262.31 bp and 236.10 bp) are primarily attributed to the impact of the model choice. The model impacts on these two deals expressed in vega are 25 × vega and 30 × vega.

When looking at different strikes, though, the calibration errors reach higher levels up to 20.85 bp and consequently it is expected that the differences between the MC LMM and the 1FHW Bermudan prices, which are in the range of 138.80 – 291.92 bp, do include a more substantial noise component related to these errors. Considering for example the extreme case of the deep ITM receiver Bermudan with relative strike +3.00%, the maximum observed calibration error related to the underlying swaptions amounts to 20.00 bp. As the 1FHW Bermudan price (3990.83 bp) is not yet fully converged to the maximum underlying European swaption price (3965.05 bp), the price of the exotic derivative is not independent of the model choice. Hence, the difference of 141.11 bp between the MC LMM and the 1FHW Bermudan price can be decomposed into an element related to the selection of the model and one due to the calibration errors. As the model impact on the Bermudan with a tenor of 10Y and with the same moneyness amounted to approximately 73.65 bp, by extrapolation it is expected that the model choice explains at least half of the amount of 141.11 bp.

5.5. SUMMARY

In this chapter the impact of the model selection on the Bermudan swaption prices is investigated. 30 deals are considered, each characterized by a different tenor, strike and underlying swap type. The impact is assessed by comparing the MC LMM prices to the corresponding prices computed with the 1FHW model. Both models are calibrated to the co-terminal swaptions underlying the Bermudans. The difference between the Bermudan prices determined under the two models can be decomposed into three components related to the model choice, the calibration errors in the MC LMM and the slightly different payment schedules used by the models. The impact of the latter component on the Bermudan prices is not taken into account in this research as the differences between the payment dates are only marginal, with a maximum discrepancy of 0.016 (expressed in year fractions).

It is seen that the MC LMM always overprices the Bermudans relative to the 1FHW prices. For increasing Bermudan tenors, the difference between the MC LMM and the 1FHW Bermudan prices increases.

All differences between the MC LMM and the 1FHW Bermudans with a tenor of 5Y, which are in the range of $4.47 - 26.46$ bp, are primarily explained by the model choice, as the calibration errors related to the underlying swaptions are small (up to 2.53 bp). The model impact on these Bermudans expressed in terms of vega is between $5 \times$ vega and $10 \times$ vega. For the Bermudans related to swaptions priced with a small calibration error (up to 3.68 bp), the model selection will have an impact of $70.06 - 119.63$ bp on the prices of the exotic instruments. This is equivalent to a model impact of approximately $20 \times$ vega. Considering Bermudans with a tenor of 15Y, the MC LMM in general prices the underlying swaptions with a significant calibration error up to 20.85 bp. These errors will have an impact on the Bermudan prices. Only two Bermudans are observed that are accurately valued by the MC LMM with a maximum error of 3.69 bp. The differences 236.10 and 262.31 bp between the MC LMM and the 1FHW Bermudan prices principally reflect the impact of the model choice. In terms of vega, the model selection impacts for these Bermudans are $25 \times$ vega and $30 \times$ vega.

6

CONCLUSION

The main objectives of this research are to extend the classical LMM to a multi-curve framework and to investigate the impact of this extended model on exotic interest rate derivatives. It is chosen to analyze the impact of the model selection on Bermudan swaptions, as these instruments are actively traded and among the most liquid exotic IR derivatives with an early exercise feature. In order to be able to price Bermudan swaptions, the extended LMM is calibrated to the swaption market.

In Chapter 3 the SC LMM is extended by assuming a constant additive spread between the OIS and the LIBOR curves, with the former used for discounting cash flows as this thesis only considers fully collateralized derivatives. The adapted model formulation is derived, in which the evolution of the forward OIS rates is modeled. The instantaneous forward rate volatility and the correlation structure are assumed to be specified by two parametric functions. The volatility function involves four constant parameters, which are calibrated to the swaption market. By introducing the additional volatility parameters k_i, depending on the maturity T_i of the forward OIS rate, one assures a perfect fit of the swaption prices contained in the calibration set. The volatility parameters control the shape of the term structure of implied volatilities and the instantaneous volatility curve and the values of k_i regulate the extend to which this time-homogeneous property is preserved. The choice of the correlation parametrization takes into account the fact that swaptions are only mildly dependent on the shape of the correlation structure, making the swaption market not suitable for the calibration of correlation parameters. For this reason a parametrization is chosen involving one constant parameter that is fixed prior to calibration.

The extended LMM assumes (log-)normal dynamics for the forward OIS rates. Consequently, the swap rates cannot follow simultaneously a (log-)normal distribution under this model. In order to ensure a fast calibration, an analytical, closed-form approximation for the swaption volatility is derived. The approximated prices, obtained by inserting the swaption volatility approximation into Bachelier's or Black's model, are an approximation of the true model implied swaption prices. The closed-form swaption volatility is based on the assumption that the swap rate is well-approximated by a weighted sum of the underlying forward rates, with constant weights. The accuracy of the approximation formula is tested by comparing the closed-form swaption price with the Monte Carlo swaption price. This is done for different sets of swaptions, characterized by distinct underlying tenors and strikes. It is shown that the approximation reaches its highest degree of accuracy for swaptions with shorter underlying tenor and with strikes around the swap rate.

In Chapter 4 the extended LMM is calibrated to market data from the the USD market using the closed-form swaption volatility approximation. The model is calibrated to fifteen different sets of implied Bachelier swaption volatilities, where each volatility is related to a swaption characterized by a distinct underlying tenor and strike. Three different strips are considered and five distinct strikes. The payer/receiver swaptions related to the volatilities contained in each set are exactly the swaptions underlying a specific Bermudan swaption that is analyzed in Chapter 5. First the parameters a, b, c and d are calibrated to the market implied swaption volatilities contained in a set, whereafter the parameters k_i are adjusted from their level of 1 to ensure a perfect fit. The calibration results show that the instantaneous volatility curves and the term structures of implied volatilities obtained feature a humped shape, which is often seen in the market. Adding more instru-

ments to the calibration set leads to a loss of the time-homogeneity of the instantaneous volatilities and term structures. Furthermore, in some cases the swaptions are priced accurately, with calibration errors up to 2.5 bp. This is especially apparent for swaptions with shorter underlying tenors and with strikes near the ATM level. For swaptions with longer underlying tenors and with strikes not close to the ATM level, the accuracy of the approximation decreases. In the extreme cases of deep OTM payer and deep ITM receiver swaptions with a maximum underlying tenor of 15Y, calibration errors up to 20.9 bp are observed.

In Chapter 5 the impact of the normal MC LMM on the Bermudan swaption prices is investigated. This is done by comparing the prices of these instruments computed using the MC LMM and the one-factor Hull-White model. Thirty different deals are considered, each characterized by a distinct tenor, fixed strike and underlying swap type. The difference between the Bermudan swaption prices computed by both models can be decomposed into three components related to the model selection, the calibration errors and the slightly different payment schedules used by the models. In this thesis, the impact of the third component is not taken into account as the difference between the payment dates exhibits a maximum discrepancy of 0.016 (expressed in year fractions).

The pricing results show that the MC LMM overprices all Bermudan deals relative to the 1FHW prices. This overprice increases for increasing Bermudan tenors. Furthermore, as the swaptions underlying the Bermudans with a tenor of 5Y feature small calibration errors up to 2.53 bp, the differences between the MC LMM and the 1FHW Bermudan prices, that lie between 4.47 bp and 26.46 bp, are primarily explained by the model selection. In terms of vega, the model impact on these Bermudans is between 5 × vega and 10 × vega. Considering Bermudans with a 10Y tenor, for some deals it is seen that the calibration errors related to the underlying swaptions are between 4.82 and 6.47 bp. Part of the differences between the Bermudans determined by the two models, which are in the range of 58.24 – 139.36 bp, is attributed to these errors. For the other 10Y tenor Bermudan cases, which have maximum calibration errors in the range of 1.68 – 3.68 bp, the component related to the calibration error will have a smaller impact on the Bermudan prices. The differences of the MC LMM and the 1FHW Bermudan prices, lying between 70.06 and 119.63 bp, are primarily explained by the model choice. This is equivalent to a model impact of approximately 20 × vega. The calibration error of the swaptions underlying the Bermudan deals with a tenor of 15Y increase and can reach levels up to 20.85 bp. The calibration errors will have an impact on the MC LMM Bermudan price. Hence, part of the differences between the MC LMM and the 1FHW Bermudan prices, which are in the range of 138.80 – 291.92 bp, is explained by these errors. Only two deals with a tenor of 15Y feature small calibration errors up to 3.69 bp. The differences of the Bermudan prices computed under both models (262.31 and 236.10 bp) are primarily attributed to the selection of the model. Expressed in terms of vega, the model impacts on these Bermudans are 25 × vega and 30 × vega.

POINTS OF FURTHER RESEARCH

During the execution of this thesis, it became apparent that some elements could not be fully addressed, as they were beyond the scope of the present work. A list of these topics is provided, that could be used to further expand this research.

- **Improvement of the calibration accuracy**.
  In order to be able to price swaptions in the MC LMM, a former industry standard swaption volatility approximation is extended to accommodate the MC framework. It is observed that the performance of this approximation decreases for swaptions with longer underlying tenors and with strikes that are not close to the swap rate. Consequently, these swaptions are priced by the MC LMM with a calibration error. The investigation on a method to improve the calibration error is suggested. As part of this research, alternative swaption volatility approximations could be extended to the MC framework and their accuracy could be analyzed. The refined approximation discussed in (Jäckel and Rebonato, 2000) could, for example, be considered.

- **Modeling different tenors simultaneously**.
  In this research the dynamics of the forward OIS rates presented in Section 3.5 were specified for one particular tenor. By simulating the forward OIS rates with a given length, the implications on other tenors were not considered. When modeling multiple tenors simultaneously, possible no-arbitrage

relations that hold across different time-intervals have to be taken into account and the forward OIS rates with different tenors cannot be simulated as being unrelated to each other. An investigation on the joint simulation of forward OIS rates with different tenors is advised. The theory given in (Mercurio, 2010a) could provide a good starting point.

- **Analysis of the impact of rank reduction on Bermudan swaption prices**.
  In this thesis a full-rank correlation matrix is considered. However, in practice, considering as many driving Brownian motions as the number of forward rates to be modeled may result in extremely time-consuming computations. To overcome this problem, the number of factors can be decreased. An investigation is proposed on the impact of rank reduction on the prices of Bermudan swaptions. In Section 3.4 the popular rank reduction technique, the principal component analysis, is introduced. The analysis of the influence of distinct rank reduction methods on the Bermudan swaptions is suggested. (Andersen and Andreasen, 2001) and (Lutz, 2010b) could serve as starting points for this research topic.

- **Analysis of the impact of the correlation parametrization on Bermudan swaption prices**.
  Throughout this thesis, one of the most basic correlation parametrizations, involving a single constant parameter, is considered. The correlation structure generated with this parametrization does not have the property that rates with a constant time distance between the fixing dates are more correlated on the long end of the curve compared to the short end. A more realistic correlation surface could be obtained by considering more complex correlation parametrizations involving multiple parameters. A research is proposed on the impact of different correlation parametrizations on the prices of the Bermudan swaptions. The parametrizations discussed in (Lutz, 2010a) and (Schoenmakers and Coffey, 2005) could be taken into account.

BIBLIOGRAPHY

Andersen, L. and Andreasen, J. (1998). Volatility skews and extensions of the libor market model. *Available at SSRN 111030*.

Andersen, L. and Andreasen, J. (2001). Factor dependence of bermudan swaptions: fact or fiction? *Journal of Financial Economics*, 62(1):3–37.

Andersen, L. B. and Piterbarg, V. V. (2010a). *Interest Rate Modeling, volume I: Foundations and Vanilla Models*. Atlantic Financial Press London.

Andersen, L. B. and Piterbarg, V. V. (2010b). *Interest Rate Modeling, volume II: Term Structure Models*. Atlantic Financial Press London.

Benninga, S., Björk, T., and Wiener, Z. (2002). On the use of numeraires in option pricing. *The Journal of Derivatives*, 10(2):43–58.

Brace, A., Dun, T., and Barton, G. (2001). Towards a central interest rate model. *Option Pricing, Interest Rates and Risk Management*, pages 278–313.

Brace, A., Gatarek, D., and Musiela, M. (1997). The market model of interest rate dynamics. *Mathematical Finance*, 7(2):127–155.

Brigo, D. (2002). A note on correlation and rank reduction. *Available at damianobrigo.it*.

Brigo, D. and Liinev, J. (2005). On the distributional distance between the lognormal libor and swap market models. *Quantitative Finance*, 5(5):433–442.

Brigo, D. and Mercurio, F. (2007). *Interest Rate Models - Theory and Practice: With Smile, Inflation and Credit*. Springer Science & Business Media.

Brigo, D., Mercurio, F., and Morini, M. (2005). The libor model dynamics: Approximations, calibration and diagnostics. *European Journal of Operational Research*, 163(1):30–51.

Byrd, R. H., Gilbert, J. C., and Nocedal, J. (2000). A trust region method based on interior point techniques for nonlinear programming. *Mathematical Programming*, 89(1):149–185.

Byrd, R. H., Hribar, M. E., and Nocedal, J. (1999). An interior point algorithm for large-scale nonlinear programming. *SIAM Journal on Optimization*, 9(4):877–900.

Castagna, A., Cova, A., and Camelia, M. (2015). Modelling of libor-ois basis. *Available at SSRN 2577710*.

Cuchiero, C., Fontana, C., and Gnoatto, A. (2016a). Affine multiple yield curve models. *arXiv preprint arXiv:1603.00527*.

Cuchiero, C., Fontana, C., and Gnoatto, A. (2016b). A general hjm framework for multiple yield curve modelling. *Finance and Stochastics*, 20(2):267–320.

Forsythe, G. E., Moler, C. B., and Malcolm, M. A. (1977). *Computer Methods for Mathematical Computations*. Prentice-Hall.

Fries, C. (2007). *Mathematical Finance: Theory, Modeling, Implementation*. John Wiley & Sons.

Fujii, M., Shimada, Y., and Takahashi, A. (2011). A market model of interest rates with dynamic basis spreads in the presence of collateral and multiple currencies. *Wilmott*, 2011(54):61–73.

Glasserman, P. (2003). *Monte Carlo Methods in Financial Engineering*, volume 53. Springer Science & Business Media.

Grbac, Z., Papapantoleon, A., Schoenmakers, J., and Skovmand, D. (2015). Affine libor models with multiple curves: Theory, examples and calibration. *SIAM Journal on Financial Mathematics*, 6(1):984–1025.

Henrard, M. (2010). The irony in derivatives discounting part ii: The crisis. *Wilmott Journal*, 2(6):301–316.

Jäckel, P. and Rebonato, R. (2000). Linking caplet and swaption volatilities in a bgm/j framework: Approximate solutions. *Quantitiative Research Centre, The Royal Bank of Scotland*.

Joshi, M. S. (2003a). *The Concepts and Practice of Mathematical Finance*, volume 1. Cambridge University Press.

Joshi, M. S. (2003b). Rapid computation of drifts in a reduced factor libor market model. *Wilmott Magazine*, 5:84–85.

Joshi, M. S. and Liesch, L. (2007). Effective implementation of generic market models. *Astin Bulletin*, 37(02):453–473.

Longstaff, F. A. and Schwartz, E. S. (2001). Valuing american options by simulation: A simple least-squares approach. *Review of Financial studies*, 14(1):113–147.

Lutz, M. (2010a). Extracting correlations from the market: New correlation parameterizations and the calibration of a stochastic volatility lmm to cms spread options. *SSRN Working Paper Series*.

Lutz, M. (2010b). Fast rank reduction of parametric forward rate correlation matrices. *Available at SSRN 1711191*.

Mercurio, F. (2009). Interest rates and the credit crunch: New formulas and market models. *Bloomberg Portfolio Research Paper*.

Mercurio, F. (2010a). Libor market models with stochastic basis. *Bloomberg Education and Quantitative Research Paper*.

Mercurio, F. (2010b). Modern libor market models: Using different curves for projecting rates and for discounting. *International Journal of Theoretical and Applied Finance*, 13(01):113–137.

Mercurio, F. and Xie, Z. (2012). The basis goes stochastic. *Risk*, 25(12):78.

Miltersen, K. R., Sandmann, K., and Sondermann, D. (1997). Closed form solutions for term structure derivatives with log-normal interest rates. *The Journal of Finance*, 52(1):409–430.

Morini, M. and Brigo, D. (2003). New developments on the analytical cascade swaption calibration of the libor market model. Technical report, Citeseer.

Pelsser, A. (2000). *Efficient Methods for Valuing Interest Rate Derivatives*. Springer Science & Business Media.

Rebonato, R. (1999). On the pricing implications of the joint lognormal assumption for the swaption and cap markets. *Journal of Computational Finance*, 2(3):57–76.

Rebonato, R. (2002). *Modern Pricing of Interest-Rate Derivatives: The LIBOR Market Model and Beyond*. Princeton University Press.

Rebonato, R. (2005). *Volatility and Correlation: the Perfect Hedger and the Fox*. John Wiley & Sons.

Rebonato, R. and Jäckel, P. (2011). The most general methodology to create a valid correlation matrix for risk management and option pricing purposes. *Available at SSRN 1969689*.

Schoenmakers, J. G. and Coffey, B. (2005). *Stable implied calibration of a multi-factor LIBOR model via a semi-parametric correlation structure*. Weierstrass Institute Berlin.

Shreve, S. E. (2004). *Stochastic Calculus for Finance II: Continuous-Time Models*, volume 11. Springer Science & Business Media.

Waltz, R. A., Morales, J. L., Nocedal, J., and Orban, D. (2006). An interior algorithm for nonlinear optimization that combines line search and trust region steps. *Mathematical programming*, 107(3):391–408.

A

MARKET DATA USED

A.1. 3M FORWARD LIBOR CURVE

$F^{3M}(0;0.00,0.25)$	0.0025
$F^{3M}(0;0.25,0.50)$	0.0031
$F^{3M}(0;0.50,0.75)$	0.0043
$F^{3M}(0;0.75,1.00)$	0.0058
$F^{3M}(0;1.00,1.25)$	0.0075
$F^{3M}(0;1.25,1.50)$	0.0092
$F^{3M}(0;1.50,1.75)$	0.0108
$F^{3M}(0;1.75,2.00)$	0.0123
$F^{3M}(0;2.00,2.25)$	0.0137
$F^{3M}(0;2.25,2.50)$	0.0148
$F^{3M}(0;2.50,2.75)$	0.0157
$F^{3M}(0;2.75,3.00)$	0.0166
$F^{3M}(0;3.00,3.25)$	0.0173
$F^{3M}(0;3.25,3.50)$	0.0179
$F^{3M}(0;3.50,3.75)$	0.0184
$F^{3M}(0;3.75,4.00)$	0.0190
$F^{3M}(0;4.00,4.25)$	0.0194
$F^{3M}(0;4.25,4.50)$	0.0198
$F^{3M}(0;4.50,4.75)$	0.0201
$F^{3M}(0;4.75,5.00)$	0.0205
$F^{3M}(0;5.00,5.25)$	0.0208
$F^{3M}(0;5.25,5.50)$	0.0210
$F^{3M}(0;5.50,5.75)$	0.0212
$F^{3M}(0;5.75,6.00)$	0.0215
$F^{3M}(0;6.00,6.25)$	0.0217
$F^{3M}(0;6.25,6.50)$	0.0219
$F^{3M}(0;6.50,6.75)$	0.0221
$F^{3M}(0;6.75,7.00)$	0.0223
$F^{3M}(0;7.00,7.25)$	0.0225
$F^{3M}(0;7.25,7.50)$	0.0226
$F^{3M}(0;7.50,7.75)$	0.0227
$F^{3M}(0;7.75,8.00)$	0.0229
$F^{3M}(0;8.00,8.25)$	0.0230
$F^{3M}(0;8.25,8.50)$	0.0231
$F^{3M}(0;8.50,8.75)$	0.0233
$F^{3M}(0;8.75,9.00)$	0.0234
$F^{3M}(0;9.00,9.25)$	0.0234
$F^{3M}(0;9.25,9.50)$	0.0234
$F^{3M}(0;9.50,9.75)$	0.0234
$F^{3M}(0;9.75,10.00)$	0.0234
$F^{3M}(0;10.00,10.25)$	0.0235
$F^{3M}(0;10.25,10.50)$	0.0236
$F^{3M}(0;10.50,10.75)$	0.0237
$F^{3M}(0;10.75,11.00)$	0.0239
$F^{3M}(0;11.00,11.25)$	0.0240
$F^{3M}(0;11.25,11.50)$	0.0241
$F^{3M}(0;11.50,11.75)$	0.0242
$F^{3M}(0;11.75,12.00)$	0.0243
$F^{3M}(0;12.00,12.25)$	0.0243
$F^{3M}(0;12.25,12.50)$	0.0243
$F^{3M}(0;12.50,12.75)$	0.0242
$F^{3M}(0;12.75,13.00)$	0.0242
$F^{3M}(0;13.00,13.25)$	0.0242
$F^{3M}(0;13.25,13.50)$	0.0241
$F^{3M}(0;13.50,13.75)$	0.0241
$F^{3M}(0;13.75,14.00)$	0.0241
$F^{3M}(0;14.00,14.25)$	0.0240
$F^{3M}(0;14.25,14.50)$	0.0240
$F^{3M}(0;14.50,14.75)$	0.0240
$F^{3M}(0;14.75,15.00)$	0.0239
$F^{3M}(0;15.00,15.25)$	0.0239
$F^{3M}(0;15.25,15.50)$	0.0239
$F^{3M}(0;15.50,15.75)$	0.0239
$F^{3M}(0;15.75,16.00)$	0.0239
$F^{3M}(0;16.00,16.25)$	0.0239
$F^{3M}(0;16.25,16.50)$	0.0239
$F^{3M}(0;16.50,16.75)$	0.0239
$F^{3M}(0;16.75,17.00)$	0.0240
$F^{3M}(0;17.00,17.25)$	0.0240
$F^{3M}(0;17.25,17.50)$	0.0240
$F^{3M}(0;17.50,17.75)$	0.0240
$F^{3M}(0;17.75,18.00)$	0.0240
$F^{3M}(0;18.00,18.25)$	0.0240
$F^{3M}(0;18.25,18.50)$	0.0240
$F^{3M}(0;18.50,18.75)$	0.0240
$F^{3M}(0;18.75,19.00)$	0.0240
$F^{3M}(0;19.00,19.25)$	0.0240
$F^{3M}(0;19.25,19.50)$	0.0240
$F^{3M}(0;19.50,19.75)$	0.0240
$F^{3M}(0;19.75,20.00)$	0.0240
$F^{3M}(0;20.00,20.25)$	0.0240
$F^{3M}(0;20.25,20.50)$	0.0239
$F^{3M}(0;20.50,20.75)$	0.0239
$F^{3M}(0;20.75,21.00)$	0.0238
$F^{3M}(0;21.00,21.25)$	0.0238
$F^{3M}(0;21.25,21.50)$	0.0237
$F^{3M}(0;21.50,21.75)$	0.0237
$F^{3M}(0;21.75,22.00)$	0.0236
$F^{3M}(0;22.00,22.25)$	0.0236
$F^{3M}(0;22.25,22.50)$	0.0235
$F^{3M}(0;22.50,22.75)$	0.0235
$F^{3M}(0;22.75,23.00)$	0.0234
$F^{3M}(0;23.00,23.25)$	0.0234
$F^{3M}(0;23.25,23.50)$	0.0233
$F^{3M}(0;23.50,23.75)$	0.0233
$F^{3M}(0;23.75,24.00)$	0.0232
$F^{3M}(0;24.00,24.25)$	0.0232
$F^{3M}(0;24.25,24.50)$	0.0231
$F^{3M}(0;24.50,24.75)$	0.0231
$F^{3M}(0;24.75,25.00)$	0.0230
$F^{3M}(0;25.00,25.25)$	0.0230
$F^{3M}(0;25.25,25.50)$	0.0231
$F^{3M}(0;25.50,25.75)$	0.0231
$F^{3M}(0;25.75,26.00)$	0.0232
$F^{3M}(0;26.00,26.25)$	0.0232
$F^{3M}(0;26.25,26.50)$	0.0232
$F^{3M}(0;26.50,26.75)$	0.0233
$F^{3M}(0;26.75,27.00)$	0.0233
$F^{3M}(0;27.00,27.25)$	0.0234
$F^{3M}(0;27.25,27.50)$	0.0234
$F^{3M}(0;27.50,27.75)$	0.0235
$F^{3M}(0;27.75,28.00)$	0.0235
$F^{3M}(0;28.00,28.25)$	0.0235
$F^{3M}(0;28.25,28.50)$	0.0236
$F^{3M}(0;28.50,28.75)$	0.0236
$F^{3M}(0;28.75,29.00)$	0.0237
$F^{3M}(0;29.00,29.25)$	0.0237
$F^{3M}(0;29.25,29.50)$	0.0238
$F^{3M}(0;29.50,29.75)$	0.0238
$F^{3M}(0;29.75,30.00)$	0.0238

Table A.1: 3M forward LIBOR curve as of 30 January 2015.

A.2. OIS DISCOUNT CURVE

$P^d(0,0.00)$	1.0000
$P^d(0,0.25)$	0.9997
$P^d(0,0.50)$	0.9993
$P^d(0,0.75)$	0.9986
$P^d(0,1.00)$	0.9976
$P^d(0,1.25)$	0.9962
$P^d(0,1.50)$	0.9943
$P^d(0,1.75)$	0.9922
$P^d(0,2.00)$	0.9896
$P^d(0,2.25)$	0.9869
$P^d(0,2.50)$	0.9839
$P^d(0,2.75)$	0.9805
$P^d(0,3.00)$	0.9769
$P^d(0,3.25)$	0.9734
$P^d(0,3.50)$	0.9697
$P^d(0,3.75)$	0.9658
$P^d(0,4.00)$	0.9617
$P^d(0,4.25)$	0.9578
$P^d(0,4.50)$	0.9537
$P^d(0,4.75)$	0.9495
$P^d(0,5.00)$	0.9451
$P^d(0,5.25)$	0.9411
$P^d(0,5.50)$	0.9370
$P^d(0,5.75)$	0.9328
$P^d(0,6.00)$	0.9285
$P^d(0,6.25)$	0.9241
$P^d(0,6.50)$	0.9196
$P^d(0,6.75)$	0.9150
$P^d(0,7.00)$	0.9103
$P^d(0,7.25)$	0.9061
$P^d(0,7.50)$	0.9019
$P^d(0,7.75)$	0.8976
$P^d(0,8.00)$	0.8932
$P^d(0,8.25)$	0.8888
$P^d(0,8.50)$	0.8844
$P^d(0,8.75)$	0.8799
$P^d(0,9.00)$	0.8753
$P^d(0,9.25)$	0.8707
$P^d(0,9.50)$	0.8660
$P^d(0,9.75)$	0.8613
$P^d(0,10.00)$	0.8565
$P^d(0,10.25)$	0.8522
$P^d(0,10.50)$	0.8478
$P^d(0,10.75)$	0.8434
$P^d(0,11.00)$	0.8390
$P^d(0,11.25)$	0.8346
$P^d(0,11.50)$	0.8301
$P^d(0,11.75)$	0.8257
$P^d(0,12.00)$	0.8212
$P^d(0,12.25)$	0.8170
$P^d(0,12.50)$	0.8128
$P^d(0,12.75)$	0.8086
$P^d(0,13.00)$	0.8044
$P^d(0,13.25)$	0.8002
$P^d(0,13.50)$	0.7959
$P^d(0,13.75)$	0.7917
$P^d(0,14.00)$	0.7875
$P^d(0,14.25)$	0.7832
$P^d(0,14.50)$	0.7789
$P^d(0,14.75)$	0.7747
$P^d(0,15.00)$	0.7704
$P^d(0,15.25)$	0.7665
$P^d(0,15.50)$	0.7626
$P^d(0,15.75)$	0.7587
$P^d(0,16.00)$	0.7548
$P^d(0,16.25)$	0.7509
$P^d(0,16.50)$	0.7470
$P^d(0,16.75)$	0.7431
$P^d(0,17.00)$	0.7393
$P^d(0,17.25)$	0.7354
$P^d(0,17.50)$	0.7315
$P^d(0,17.75)$	0.7277
$P^d(0,18.00)$	0.7238
$P^d(0,18.25)$	0.7199
$P^d(0,18.50)$	0.7161
$P^d(0,18.75)$	0.7122
$P^d(0,19.00)$	0.7084
$P^d(0,19.25)$	0.7045
$P^d(0,19.50)$	0.7007
$P^d(0,19.75)$	0.6968
$P^d(0,20.00)$	0.6930
$P^d(0,20.25)$	0.8522
$P^d(0,20.50)$	0.8478
$P^d(0,20.75)$	0.8434
$P^d(0,21.00)$	0.8390
$P^d(0,21.25)$	0.8346
$P^d(0,21.50)$	0.8301
$P^d(0,21.75)$	0.8257
$P^d(0,22.00)$	0.8212
$P^d(0,22.25)$	0.8170
$P^d(0,22.50)$	0.8128
$P^d(0,22.75)$	0.8086
$P^d(0,23.00)$	0.8044
$P^d(0,23.25)$	0.8002
$P^d(0,23.50)$	0.7959
$P^d(0,23.75)$	0.7917
$P^d(0,24.00)$	0.7875
$P^d(0,24.25)$	0.7832
$P^d(0,24.50)$	0.7789
$P^d(0,24.75)$	0.7747
$P^d(0,25.00)$	0.7704
$P^d(0,25.25)$	0.7665
$P^d(0,25.50)$	0.7626
$P^d(0,25.75)$	0.7587
$P^d(0,26.00)$	0.7548
$P^d(0,26.25)$	0.7509
$P^d(0,26.50)$	0.7470
$P^d(0,26.75)$	0.7431
$P^d(0,27.00)$	0.7393
$P^d(0,27.25)$	0.7354
$P^d(0,27.50)$	0.7315
$P^d(0,27.75)$	0.7277
$P^d(0,28.00)$	0.7238
$P^d(0,28.25)$	0.7199
$P^d(0,28.50)$	0.7161
$P^d(0,28.75)$	0.7122
$P^d(0,29.00)$	0.7084
$P^d(0,29.25)$	0.7045
$P^d(0,29.50)$	0.7007
$P^d(0,29.75)$	0.6968
$P^d(0,30.00)$	0.6930

Table A.2: OIS discount curve as of 30 January 2015.

B

MONTE CARLO TIME STEP AND NUMBER OF SIMULATIONS

H		1Y15Y	2Y14Y	3Y13Y	4Y12Y	5Y11Y	6Y10Y	7Y9Y	8Y8Y	9Y7Y	10Y6Y	11Y5Y	12Y4Y	13Y3Y	14Y2Y	15Y1Y	CPU Time
500	LMM MC	75.80	74.28	73.55	79.52	84.73	86.20	84.84	87.79	92.78	98.56	102.88	105.79	112.39	115.88	130.33	0.004
	% Vol Change	–	–	–	–	–	–	–	–	–	–	–	–	–	–	–	
	MC Window	[66.82 – 84.78]	[65.1483.42]	[64.31 – 82.77]	[69.80 – 89.22]	[74.96 – 94.48]	[76.78 – 95.61]	[75.23 – 94.43]	[77.89 – 97.68]	[82.39 – 103.17]	[87.88 – 109.22]	[92.06 – 113.68]	[94.18 – 117.38]	[100.33 – 124.44]	[102.82 – 128.94]	[115.46 – 145.21]	
	Width MC Window	17.96	18.28	18.46	19.42	19.52	18.83	19.20	19.79	20.78	21.34	21.62	23.20	24.11	26.12	29.75	
1,000	LMM MC	79.64	77.24	77.89	75.29	74.87	77.19	81.14	81.43	84.80	85.45	91.71	97.42	103.09	106.20	109.54	0.009
	% Vol Change	5.07	3.98	5.90	−5.31	−11.64	−10.45	−4.36	−7.25	−8.60	−13.29	−10.85	−7.91	−8.28	−8.36	−15.96	
	MC Window	72.78 – 86.50	70.61 – 83.87	71.22 – 84.55	68.75 – 81.83	68.27 – 81.45	70.59 – 83.79	74.45 – 87.81	74.69 – 88.16	77.83 – 91.77	78.15 – 92.75	84.12 – 99.30	89.44 – 105.39	94.62 – 111.55	97.34 – 115.05	99.87 – 119.20	
	Width MC Window	13.71	13.25	13.32	13.08	13.19	13.21	13.36	13.47	13.94	14.60	15.18	15.95	16.93	17.71	19.33	
5,000	LMM MC	76.47	77.45	76.44	76.76	77.40	78.53	80.21	81.98	86.50	90.62	95.26	99.36	104.77	109.03	114.15	0.049
	% Vol Change	−3.99	0.27	−1.86	1.95	3.39	1.73	−1.14	0.68	2.01	6.04	3.86	1.99	1.63	2.67	4.22	
	MC Window	[73.57 – 79.36]	[74.45 – 80.45]	[73.48 – 79.40]	[73.80 – 79.73]	[74.42 – 80.38]	[75.56 – 81.49]	[77.23 – 83.19]	[78.95 – 85.01]	[83.35 – 89.66]	[87.30 – 93.93]	[91.74 – 98.78]	[95.71 – 103.01]	[100.93 – 108.61]	[104.96 – 113.11]	[109.88 – 118.43]	
	Width MC Window	5.79	6.00	5.91	5.93	5.95	5.93	5.96	6.05	6.31	6.64	7.04	7.29	7.68	8.15	8.55	
10,000	LMM MC	74.97	75.55	76.54	76.64	76.54	78.14	79.84	83.02	86.02	88.09	91.69	96.19	100.36	103.62	108.16	0.116
	% Vol Change	−1.96	−2.45	0.13	−0.16	−1.12	−0.49	−0.46	1.27	−0.55	−2.79	−3.74	−3.19	−4.21	−4.96	−5.25	
	MC Window	72.97 – 76.97	73.46 – 77.65	74.44 – 78.64	74.56 – 78.72	74.47 – 78.60	76.06 – 80.23	77.72 – 81.97	80.84 – 85.20	83.78 – 88.26	85.78 – 90.40	89.24 – 94.14	93.62 – 98.77	97.66 – 103.07	100.79 – 106.45	105.18 – 111.14	
	Width MC Window	4.01	4.18	4.20	4.17	4.13	4.17	4.25	4.36	4.48	4.63	4.90	5.14	5.41	5.66	5.96	
50,000	LMM MC	75.60	76.21	75.96	76.42	77.19	78.34	80.22	82.21	84.84	87.81	92.26	97.07	101.67	107.09	111.31	0.614
	% Vol Change	0.84	0.87	−0.76	−0.29	0.85	0.25	0.47	−0.97	−1.38	−0.31	0.62	0.91	1.30	3.34	2.92	
	MC Window	74.69 – 76.51	75.27 – 77.14	75.02 – 76.89	75.49 – 77.35	76.26 – 78.12	77.40 – 79.28	79.27 – 81.16	81.24 – 83.18	83.84 – 85.83	86.78 – 88.85	91.18 – 93.34	95.93 – 98.20	100.47 – 102.88	105.82 – 108.36	109.98 – 112.65	
	Width MC Window	1.82	1.87	1.87	1.86	1.86	1.87	1.89	1.94	1.99	2.07	2.16	2.27	2.41	2.54	2.67	
100,000	LMM MC	75.25	76.11	76.60	77.23	77.40	78.43	79.77	82.03	84.56	87.56	91.21	95.33	100.26	105.06	109.73	1.158
	% Vol Change	−0.46	−0.13	0.84	1.07	0.28	0.11	−0.56	−0.22	−0.33	−0.29	−1.14	−1.79	−1.39	−1.90	−1.42	
	MC Window	74.61 – 75.88	75.45 – 76.77	75.94 – 77.26	76.57 – 77.89	76.74 – 78.06	77.76 – 79.09	79.10 – 80.44	81.35 – 82.72	83.85 – 85.26	86.83 – 88.29	90.45 – 91.97	94.53 – 96.13	99.41 – 101.10	104.16 – 105.95	108.80 – 110.67	
	Width MC Window	1.28	1.32	1.32	1.32	1.32	1.32	1.34	1.37	1.41	1.46	1.52	1.60	1.69	1.78	1.88	
500,000	LMM MC	74.99	76.05	76.34	76.96	77.77	78.91	80.50	82.46	85.01	88.48	92.25	96.65	101.38	106.33	110.95	6.022
	% Vol Change	−0.34	−0.08	−0.34	−0.35	0.47	0.62	0.92	0.52	0.54	1.05	1.15	1.39	1.12	1.22	1.10	
	MC Window	74.71 – 75.28	75.75 – 76.34	76.04 – 76.63	76.67 – 77.26	77.47 – 78.06	78.61 – 79.21	80.20 – 80.80	82.15 – 82.76	84.70 – 85.33	88.15 – 88.81	91.91 – 92.59	96.29 – 97.01	101.01 – 101.76	105.93 – 106.73	110.53 – 111.37	
	Width MC Window	0.57	0.59	0.59	0.59	0.59	0.59	0.60	0.61	0.63	0.65	0.68	0.72	0.76	0.80	0.84	
1,000,000	LMM MC	75.20	76.17	76.61	76.97	77.70	78.79	80.31	82.43	85.12	88.31	92.17	96.53	101.35	106.34	110.87	11.880
	% Vol Change	0.28	0.17	0.35	0.02	−0.09	−0.15	−0.25	−0.03	0.13	−0.19	−0.09	−0.13	−0.03	0.01	−0.06	
	MC Window	75.00 – 75.41	75.96 – 76.38	76.40 – 76.81	76.77 – 77.18	77.49 – 77.90	78.58 – 79.00	80.09 – 80.52	82.21 – 82.65	84.90 – 85.35	88.08 – 88.55	91.92 – 92.41	96.28 – 96.78	101.08 – 101.62	106.06 – 106.62	110.58 – 111.17	
	Width MC Window	0.40	0.42	0.42	0.42	0.42	0.42	0.42	0.43	0.45	0.46	0.48	0.51	0.53	0.57	0.60	

Table B.1: Results Monte Carlo test, $dt = 0.25$.

H		1Y15Y	2Y14Y	3Y13Y	4Y12Y	5Y11Y	6Y10Y	7Y9Y	8Y8Y	9Y7Y	10Y6Y	11Y5Y	12Y4Y	13Y3Y	14Y2Y	15Y1Y	CPU Time
500	LMM MC	75.73	76.41	77.61	78.84	74.94	76.46	76.33	77.21	77.43	79.27	83.57	94.88	98.03	103.15	105.26	0.017
	% Vol Change	–	–	–	–	–	–	–	–	–	–	–	–	–	–	–	
	MC Window	66.57 – 84.89	67.30 – 85.51	68.74 – 86.45	69.67 – 88.00	66.05 – 83.81	67.12 – 85.78	67.29 – 85.36	67.97 – 86.42	67.89 – 86.95	69.23 – 89.29	72.90 – 94.23	83.44 – 106.31	86.02 – 110.03	90.18 – 116.10	92.12 – 118.39	
	Width MC Window	18.32	18.21	17.71	18.33	17.76	18.66	18.07	18.46	19.06	20.06	21.33	22.87	24.01	25.92	26.28	
1,000	LMM MC	75.01	75.33	81.10	82.20	79.59	76.43	78.92	85.65	90.14	93.28	99.75	102.70	102.21	106.14	109.33	0.037
	% Vol Change	−0.96	−1.41	4.51	4.26	6.21	−0.04	3.38	10.94	16.41	17.67	19.35	8.24	4.27	2.90	3.87	
	MC Window	68.88 – 81.14	68.71 – 81.94	74.40 – 87.80	75.30 – 89.10	72.74 – 86.43	69.76 – 83.10	72.26 – 85.57	78.68 – 92.61	82.86 – 97.40	85.66 – 100.89	91.87 – 107.63	94.46 – 110.93	93.92 – 110.51	97.44 – 114.83	100.00 – 118.66	
	Width MC Window	12.26	13.22	13.40	13.80	13.70	13.34	13.31	13.93	14.54	15.24	15.76	16.47	16.59	17.38	18.66	
5,000	LMM MC	73.91	75.90	77.49	79.55	81.01	80.63	81.13	84.18	86.66	89.77	93.04	95.15	100.25	106.52	111.46	0.179
	% Vol Change	−1.46	0.76	−4.46	−3.23	1.79	5.49	2.81	−1.72	−3.85	−3.76	−6.73	−7.35	−1.92	0.36	1.95	
	MC Window	71.09 – 76.73	72.93 – 78.87	74.49 – 80.48	76.56 – 82.52	78.00 – 84.02	77.61 – 83.65	78.08 – 84.19	81.06 – 87.29	83.47 – 89.85	86.47 – 93.07	89.63 – 96.44	91.58 – 98.72	96.49 – 104.01	102.55 – 110.48	107.24 – 115.68	
	Width MC Window	5.65	5.94	5.99	5.96	6.02	6.05	6.11	6.23	6.38	6.60	6.82	7.15	7.51	7.94	8.44	
10,000	LMM MC	76.024	76.88	76.26	75.87	76.87	77.55	79.42	81.45	84.11	88.08	92.27	96.55	103.83	107.56	112.98	0.338
	% Vol Change	2.85	1.30	−1.58	−4.63	−5.11	−3.83	−2.12	−3.24	−2.94	−1.88	−0.82	1.47	3.57	0.98	1.36	
	MC Window	73.97 – 78.07	74.77 – 78.99	74.16 – 78.36	73.78 – 77.95	74.79 – 78.96	75.47 – 79.62	77.30 – 81.53	79.29 – 83.60	81.89 – 86.34	85.76 – 90.40	89.83 – 94.71	93.98 – 99.11	101.10 – 106.57	104.66 – 110.45	109.95 – 116.01	
	Width MC Window	4.10	4.22	4.20	4.17	4.17	4.16	4.22	4.31	4.45	4.64	4.89	5.13	5.47	5.79	6.06	
50,000	LMM MC	74.98	76.07	76.53	77.33	77.62	78.24	79.62	82.66	85.84	89.31	93.52	97.70	103.03	107.69	112.15	1.742
	% Vol Change	−1.36	−1.06	0.36	1.94	0.97	0.89	0.25	1.49	2.05	1.39	1.35	1.19	−0.77	0.12	−0.73	
	MC Window	74.08 – 75.89	75.13 – 77.01	75.59 – 77.47	76.40 – 78.27	76.69 – 78.55	77.30 – 79.17	78.67 – 80.57	81.69 – 83.64	84.83 – 86.84	88.26 – 90.35	92.43 – 94.61	96.56 – 98.84	101.82 – 104.24	106.42 – 108.96	110.81 – 113.48	
	Width MC Window	1.81	1.88	1.88	1.87	1.86	1.87	1.90	1.95	2.01	2.08	2.18	2.28	2.41	2.54	2.67	
100,000	LMM MC	75.32	76.82	77.44	78.22	78.48	79.62	81.56	83.57	86.11	89.15	92.62	97.08	102.08	107.36	111.43	3.591
	% Vol Change	0.45	0.99	1.19	1.15	1.11	1.77	2.44	1.10	0.32	−0.17	−0.96	−0.63	−0.93	−0.31	−0.64	
	MC Window	74.68 – 75.96	76.16 – 77.48	76.77 – 78.10	77.56 – 78.89	77.82 – 79.14	78.95 – 80.28	80.89 – 82.24	82.88 – 84.26	85.40 – 86.82	88.42 – 89.88	91.85 – 93.39	96.28 – 97.89	101.23 – 102.93	106.46 – 108.26	110.49 – 112.38	
	Width MC Window	1.28	1.33	1.33	1.33	1.33	1.33	1.35	1.38	1.42	1.47	1.53	1.61	1.70	1.80	1.89	
500,000	LMM MC	75.19	76.33	76.94	77.47	78.14	79.19	80.80	82.75	85.51	88.80	92.66	97.03	101.84	106.67	110.90	17.309
	% Vol Change	−0.17	−0.64	−0.65	−0.97	−0.43	−0.53	−0.93	−0.99	−0.69	−0.39	0.04	−0.05	−0.23	−0.64	−0.48	
	MC Window	74.91 – 75.48	76.03 – 76.62	76.64 – 77.23	77.17 – 77.76	77.85 – 78.44	78.89 – 79.49	80.50 – 81.10	82.44 – 83.05	85.20 – 85.83	88.47 – 89.13	92.31 – 93.00	96.67 – 97.39	101.46 – 102.22	106.27 – 107.07	110.47 – 111.32	
	Width MC Window	0.57	0.59	0.59	0.59	0.59	0.60	0.60	0.61	0.63	0.66	0.69	0.72	0.76	0.80	0.84	
1,000,000	LMM MC	75.44	76.55	77.09	77.35	78.11	79.21	80.78	82.76	85.40	88.53	92.42	96.92	101.90	106.75	110.99	35.144
	% Vol Change	0.32	0.29	0.20	−0.14	−0.05	0.02	−0.03	0.02	−0.13	−0.31	−0.25	−0.12	0.06	0.07	0.09	
	MC Window	75.24 – 75.64	76.34 – 76.76	76.88 – 77.30	77.15 – 77.56	77.90 – 78.32	79.00 – 79.42	80.57 – 80.99	82.54 – 82.98	85.18 – 85.63	88.29 – 88.76	92.18 – 92.67	96.66 – 97.17	101.63 – 102.17	106.46 – 107.03	110.69 – 111.29	
	Width MC Window	0.41	0.42	0.42	0.42	0.42	0.42	0.43	0.43	0.45	0.46	0.49	0.51	0.54	0.57	0.60	

Table B.2: Results Monte Carlo test, $dt = 0.10$.

H		1Y15Y	2Y14Y	3Y13Y	4Y12Y	5Y11Y	6Y10Y	7Y9Y	8Y8Y	9Y7Y	10Y6Y	11Y5Y	12Y4Y	13Y3Y	14Y2Y	15Y1Y	CPU Time
500	LMM MC	80.67	79.01	80.34	83.09	78.96	76.39	81.72	88.65	89.93	90.75	95.12	105.18	120.31	121.72	125.53	0.164
	% Vol Change	–	–	–	–	–	–	–	–	–	–	–	–	–	–	–	
	MC Window	71.01 – 90.33	69.47 – 88.53	70.96 – 89.71	73.51 – 92.65	69.85 – 88.05	67.21 – 85.56	72.13 – 91.29	78.66 – 98.62	79.75 – 100.10	80.53 – 100.97	84.36 – 105.86	93.45 – 116.90	107.08 – 133.53	107.85 – 135.59	111.15 – 139.91	
	Width MC Window	19.33	19.07	18.75	19.15	18.20	18.35	19.16	19.96	20.36	20.44	21.50	23.44	26.45	27.74	28.75	
1,000	LMM MC	70.65	70.89	72.91	78.58	83.15	84.13	87.32	88.49	89.08	90.47	90.05	92.06	95.94	106.81	112.47	0.319
	% Vol Change	−12.43	−10.27	−9.26	−5.43	5.31	10.13	6.86	−0.17	−0.94	−0.31	−5.33	−12.47	−20.25	−12.26	−10.41	
	MC Window	64.54 – 76.75	64.39 – 77.38	66.35 – 79.45	71.72 – 85.43	76.13 – 90.17	77.13 – 91.11	80.36 – 94.27	81.31 – 95.67	81.75 – 96.41	82.89 – 98.05	82.23 – 97.87	83.94 – 100.17	87.48 – 104.41	97.59 – 116.02	102.77 – 122.16	
	Width MC Window	12.21	12.99	13.11	13.70	14.04	13.98	13.90	14.35	14.66	15.16	15.64	16.23	16.93	18.43	19.39	
5,000	LMM MC	77.99	82.16	81.84	80.44	80.05	80.73	81.27	82.53	84.84	88.33	92.35	97.34	102.27	108.90	113.39	1.373
	% Vol Change	10.39	15.91	12.26	2.37	−3.73	−4.04	−6.92	−6.73	−4.76	−2.37	2.55	5.73	6.59	1.96	0.82	
	MC Window	75.05 – 80.92	79.10 – 85.23	78.77 – 84.91	77.42 – 83.45	77.09 – 83.02	77.73 – 83.72	78.24 – 84.30	79.49 – 85.58	81.68 – 88.00	85.04 – 91.62	88.89 – 95.80	93.74 – 100.94	98.45 – 106.09	104.82 – 112.98	109.10 – 117.68	
	Width MC Window	5.87	6.13	6.14	6.03	5.94	5.99	6.06	6.09	6.32	6.58	6.91	7.20	7.65	8.16	8.58	
10,000	LMM MC	73.28	74.74	77.05	78.41	79.42	80.82	81.65	83.05	86.60	89.96	93.47	97.94	102.11	107.56	111.80	2.872
	% Vol Change	−6.04	−9.04	−5.85	−2.53	−0.79	0.12	0.47	0.63	2.08	1.84	1.22	0.62	−0.16	−1.22	−1.40	
	MC Window	71.30 – 75.26	72.66 – 76.82	74.95 – 79.16	76.30 – 80.51	77.33 – 81.52	78.71 – 82.93	79.50 – 83.80	80.86 – 85.24	84.35 – 88.85	87.62 – 92.29	91.07 – 95.88	95.41 – 100.47	99.45 – 104.77	104.73 – 110.40	108.84 – 114.75	
	Width MC Window	3.96	4.16	4.22	4.21	4.19	4.22	4.30	4.37	4.51	4.68	4.82	5.06	5.32	5.67	5.91	
50,000	LMM MC	75.04	76.86	77.75	77.64	78.53	79.49	81.06	82.93	85.51	88.59	92.25	95.93	100.40	105.09	109.10	14.503
	% Vol Change	2.41	2.84	0.91	−0.98	−1.12	−1.65	−0.73	−0.15	−1.26	−1.52	−1.31	−2.06	−1.67	−2.30	−2.41	
	MC Window	74.14 – 75.95	75.92 – 77.81	76.81 – 78.70	76.70 – 78.58	77.60 – 79.47	78.55 – 80.44	80.10 – 82.02	81.96 – 83.90	84.50 – 86.51	87.55 – 89.63	91.16 – 93.33	94.79 – 97.07	99.21 – 101.59	103.83 – 106.35	107.78 – 110.42	
	Width MC Window	1.81	1.89	1.89	1.88	1.88	1.89	1.91	1.95	2.01	2.08	2.17	2.27	2.38	2.52	2.64	
100,000	LMM MC	74.86	75.77	76.84	77.34	77.89	79.30	80.81	82.71	85.34	88.86	92.96	97.10	101.72	106.18	110.21	30.140
	% Vol Change	−0.25	−1.42	−1.17	−0.38	−0.83	−0.24	−0.30	−0.27	−0.19	0.31	0.77	1.22	1.31	1.03	1.02	
	MC Window	74.22 – 75.50	75.11 – 76.43	76.18 – 77.51	76.68 – 78.01	77.22 – 78.55	78.64 – 79.97	80.14 – 81.49	82.02 – 83.40	84.63 – 86.05	88.13 – 89.60	92.18 – 93.73	96.29 – 97.91	100.87 – 102.57	105.28 – 107.07	109.28 – 111.15	
	Width MC Window	1.28	1.32	1.33	1.33	1.32	1.33	1.35	1.38	1.42	1.47	1.54	1.62	1.70	1.79	1.88	
500,000	LMM MC	75.51	76.71	77.28	77.73	78.44	79.58	81.18	83.25	85.89	89.24	93.08	97.46	102.32	107.28	111.61	148.966
	% Vol Change	0.87	1.24	0.58	0.50	0.71	0.36	0.45	0.65	0.64	0.43	0.14	0.38	0.59	1.04	1.27	
	MC Window	75.22 – 75.80	76.41 – 77.01	76.99 – 77.58	77.43 – 78.03	78.14 – 78.74	79.29 – 79.88	80.88 – 81.48	82.94 – 83.56	85.57 – 86.20	88.91 – 89.57	92.74 – 93.43	97.10 – 97.83	101.94 – 102.70	106.88 – 107.68	111.19 – 112.04	
	Width MC Window	0.57	0.59	0.60	0.59	0.59	0.60	0.61	0.62	0.64	0.66	0.69	0.72	0.76	0.81	0.85	
1,000,000	LMM MC	75.58	76.77	77.37	77.78	78.49	79.62	81.29	83.40	86.06	89.34	93.23	97.62	102.41	107.26	111.36	296.874
	% Vol Change	0.10	0.08	0.11	0.07	0.07	0.05	0.14	0.18	0.20	0.11	0.16	0.16	0.09	−0.02	−0.23	
	MC Window	75.38 – 75.79	76.56 – 76.98	77.16 – 77.58	77.57 – 77.99	78.28 – 78.70	79.41 – 79.83	81.08 – 81.51	83.18 – 83.62	85.84 – 86.28	89.11 – 89.58	92.99 – 93.47	97.37 – 97.88	102.14 – 102.68	106.98 – 107.55	111.06 – 111.66	
	Width MC Window	0.41	0.42	0.42	0.42	0.42	0.42	0.43	0.44	0.45	0.47	0.49	0.51	0.54	0.57	0.60	

Table B.3: Results Monte Carlo test, $dt = 0.010$.

C

Accuracy of Rebonato's Approximation

C.1. SCENARIO 1

Maturity (in years)	Tenor (in years)	Strike	LMM Rebonato vol (in bp)	LMM MC vol (in bp)	Difference (in bp)
1	5	0.01679	269.71	267.60	−2.11
2	4	0.01856	318.54	316.91	−1.64
3	3	0.01972	300.80	299.52	−1.28
4	2	0.02052	235.27	234.94	−0.33
5	1	0.02112	131.81	131.97	0.16

Table C.1: Results for scenario 1, K = ATM.

C.2. SCENARIO 2

Maturity (in years)	Tenor (in years)	Strike	LMM Rebonato price (in bp)	LMM MC price (in bp)	Difference (in bp)
1	15	0.02105	404.83	397.32	−7.51
2	14	0.02195	535.30	527.71	−7.59
3	13	0.02254	605.81	598.97	−6.85
4	12	0.02296	642.33	636.52	−5.81
5	11	0.02326	656.78	650.74	−6.05
6	10	0.02350	655.56	650.54	−5.03
7	9	0.02369	642.28	637.91	−4.37
8	8	0.02382	618.72	615.02	−3.71
9	7	0.02392	585.60	582.75	−2.84
10	6	0.02402	542.82	539.70	−3.12
11	5	0.02409	489.38	486.93	−2.45
12	4	0.02407	423.60	421.89	−1.71
13	3	0.02400	343.18	341.93	−1.25
14	2	0.02395	245.88	244.91	−0.98
15	1	0.02393	130.81	130.51	−0.30

Table C.2: Results for scenario 2, K = ATM.

C.3. SCENARIO 3

Maturity (in years)	Tenor (in years)	Strike	LMM Rebonato price (in bp)	LMM MC price (in bp)	Difference (in bp)
1	10	0.00974	998.35	992.50	−5.84
2	9	0.01092	995.20	986.56	−8.64
3	8	0.01170	962.91	954.89	−8.02
4	7	0.01224	905.95	898.20	−7.76
5	6	0.01265	829.30	823.40	−5.90
6	5	0.01298	735.53	731.89	−3.63
7	4	0.01323	625.20	622.94	−2.26
8	3	0.01342	497.25	496.20	−1.05
9	2	0.01354	350.09	349.82	−0.27
10	1	0.01369	183.40	183.31	−0.09

Table C.3: Results for scenario 3, K = ATM − 1%.

C.4. SCENARIO 4

Maturity (in years)	Tenor (in years)	Strike	LMM Rebonato price (in bp)	LMM MC price (in bp)	Difference (in bp)
1	10	0.02974	74.60	73.80	−0.81
2	9	0.03092	170.77	170.88	0.11
3	8	0.03170	236.68	236.78	0.10
4	7	0.03224	276.48	276.60	0.12
5	6	0.03265	294.99	294.20	−0.79
6	5	0.03298	294.70	294.11	−0.59
7	4	0.03323	276.10	275.39	−0.71
8	3	0.03342	238.12	237.22	−0.90
9	2	0.03354	179.17	178.88	−0.29
10	1	0.03369	98.84	98.85	−0.00

Table C.4: Results for scenario 4, $K = \text{ATM} + 1\%$.

C.5. SCENARIO 5

Maturity (in years)	Tenor (in years)	Strike	LMM Rebonato price (in bp)	LMM MC price (in bp)	Difference (in bp)
1	10	0.03974	7.33	7.65	0.32
2	9	0.04092	44.38	45.53	1.15
3	8	0.04170	87.64	89.02	1.38
4	7	0.04224	124.18	125.05	0.87
5	6	0.04265	150.54	150.97	0.43
6	5	0.04298	165.23	164.81	−0.42
7	4	0.04323	166.63	165.70	−0.93
8	3	0.04342	152.44	151.44	−1.00
9	2	0.04354	120.21	119.35	−0.85
10	1	0.04369	68.72	68.30	−0.42

Table C.5: Results for scenario 5, $K = \text{ATM} + 2\%$.

C.6. SCENARIO 6

Maturity (in years)	Tenor (in years)	Strike	LMM Rebonato price (in bp)	LMM MC price (in bp)	Difference (in bp)
1	10	0.04974	0.31	0.39	0.08
2	9	0.05092	7.97	8.92	0.95
3	8	0.05170	25.87	27.71	1.84
4	7	0.05224	47.61	49.63	2.02
5	6	0.05265	68.29	69.61	1.32
6	5	0.05298	84.61	85.16	0.55
7	4	0.05323	93.63	93.39	−0.24
8	3	0.05342	92.17	91.46	−0.70
9	2	0.05354	76.96	76.45	−0.51
10	1	0.05369	45.92	45.68	−0.24

Table C.6: Results for scenario 6, $K = \text{ATM} + 3\%$.

D

CALIBRATION RESULTS

D.1. STRIP 1 WITH STRIKE $\mathbf{ATM}^{\mathbf{5Y}}_{\mathbf{1Y}} - 1\%$

Maturity (in years)	Tenor (in years)	Market vol.	LMM Rebonato vol.	Difference (in bp)	LMM MC vol.	Difference (in bp)
1	5	0.00729	0.00729	0.0	0.00707	−2.2
2	4	0.00758	0.00758	0.0	0.00741	−1.7
3	3	0.00805	0.00805	0.0	0.00791	−1.4
4	2	0.00810	0.00810	0.0	0.00798	−1.2
5	1	0.00845	0.00845	0.0	0.00837	−0.7

Table D.1: Strip 1 with strike $K = 0.679\%$: calibration results in terms of implied volatilities.

Maturity (in years)	Tenor (in years)	Market price (in bp)	LMM Rebonato price (in bp)	Difference (in bp)	LMM MC price (in bp)	Difference (in bp)
1	5	496.66	496.66	0.00	495.04	1.62
2	4	479.93	479.93	0.00	477.92	2.00
3	3	407.03	407.03	0.00	405.26	1.77
4	2	292.85	292.85	0.00	291.59	1.26
5	1	156.77	156.77	0.00	156.31	0.46

Table D.2: Strip 1 with strike $K = 0.679\%$: calibration results in terms of payer swaption prices.

Maturity (in years)	Tenor (in years)	Market price (in bp)	LMM Rebonato price (in bp)	Difference (in bp)	LMM MC price (in bp)	Difference (in bp)
1	5	13.74	13.74	0.00	12.82	0.92
2	4	28.34	28.34	0.00	26.98	1.36
3	3	38.01	38.01	0.00	36.82	1.19
4	2	33.77	33.77	0.00	33.08	0.69
5	1	22.82	22.82	0.00	22.60	0.23

Table D.3: Strip 1 with strike $K = 0.679\%$: calibration results in terms of receiver swaption prices.

a	b	c	d
0.0030	0.0170	0.7766	0.0029

Table D.4: Strip 1 with strike $K = 0.679\%$: calibrated parameters a, b, c, d.

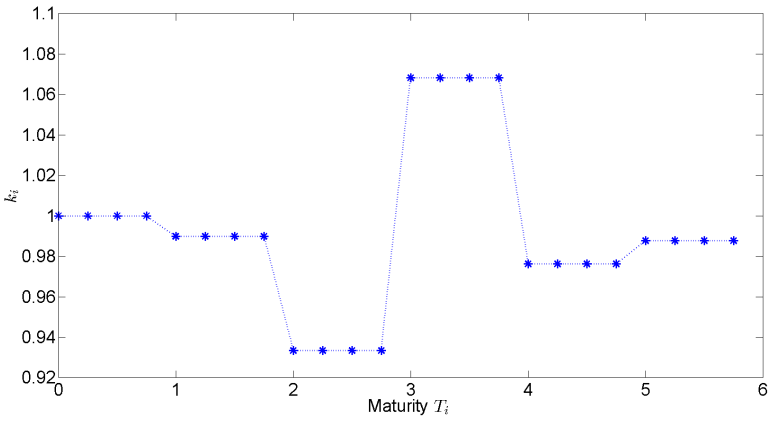

Figure D.1: Strip 1 with strike $K = 0.679\%$: representation of k_i.

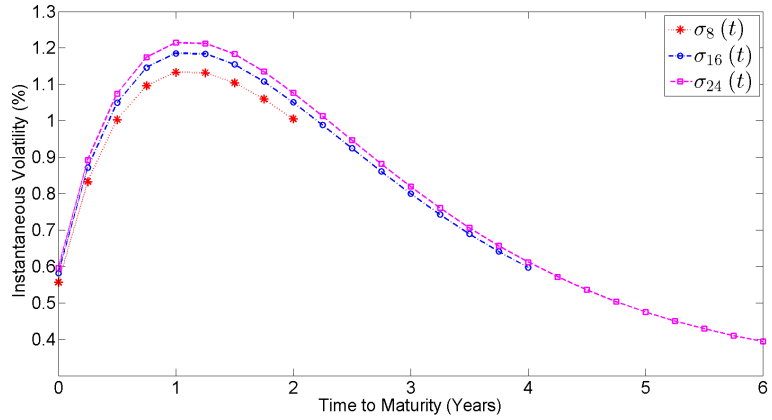

Figure D.2: Strip 1 with strike $K = 0.679\%$:
evolution of the instantaneous volatility.

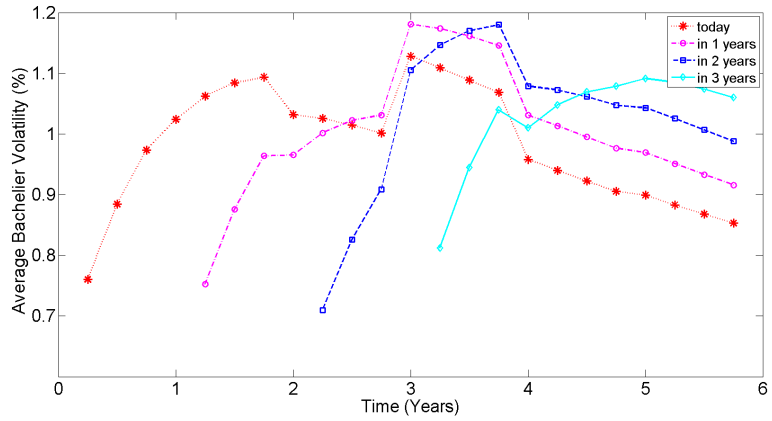

Figure D.3: Strip 1 with strike $K = 0.679\%$:
evolution of the term structure of implied Bachelier volatilities.

D.2. STRIP 1 WITH STRIKE $\mathbf{ATM}_{\mathbf{1Y}}^{\mathbf{5Y}} + 1\%$

Maturity (in years)	Tenor (in years)	Market vol.	LMM Rebonato vol.	Difference (in bp)	LMM MC vol.	Difference (in bp)
1	5	0.00938	0.00938	0.0	0.00933	−0.5
2	4	0.00956	0.00956	0.0	0.00949	−0.7
3	3	0.00974	0.00974	0.0	0.00966	−0.8
4	2	0.00999	0.00999	0.0	0.00992	−0.7
5	1	0.01004	0.01004	0.0	0.00999	−0.5

Table D.5: Strip 1 with strike $K = 2.679\%$: calibration results in terms of implied volatilities.

Maturity (in years)	Tenor (in years)	Market price (in bp)	LMM Rebonato price (in bp)	Difference (in bp)	LMM MC price (in bp)	Difference (in bp)
1	5	33.18	33.18	0.00	32.68	0.50
2	4	86.35	86.35	0.00	85.01	1.34
3	3	107.83	107.83	0.00	106.40	1.42
4	2	98.61	98.61	0.00	97.56	1.05
5	1	59.85	59.85	0.00	59.47	0.38

Table D.6: Strip 1 with strike $K = 2.679\%$: calibration results in terms of payer swaption prices.

Maturity (in years)	Tenor (in years)	Market price (in bp)	LMM Rebonato price (in bp)	Difference (in bp)	LMM MC price (in bp)	Difference (in bp)
1	5	516.10	516.10	0.00	516.33	−0.23
2	4	401.98	401.98	0.00	401.62	0.36
3	3	309.62	309.62	0.00	309.15	0.47
4	2	216.81	216.81	0.00	216.63	0.19
5	1	112.88	112.88	0.00	112.85	0.02

Table D.7: Strip 1 with strike $K = 2.679\%$: calibration results in terms of receiver swaption prices.

a	b	c	d
0.0030	0.0197	0.7425	0.0036

Table D.8: Strip 1 with strike $K = 2.679\%$: calibrated parameters a, b, c, d.

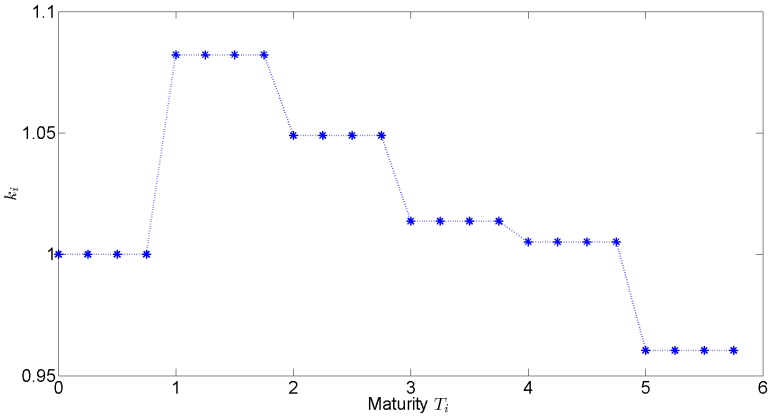

Figure D.4: Strip 1 with strike $K = 2.679\%$: representation of k_i.

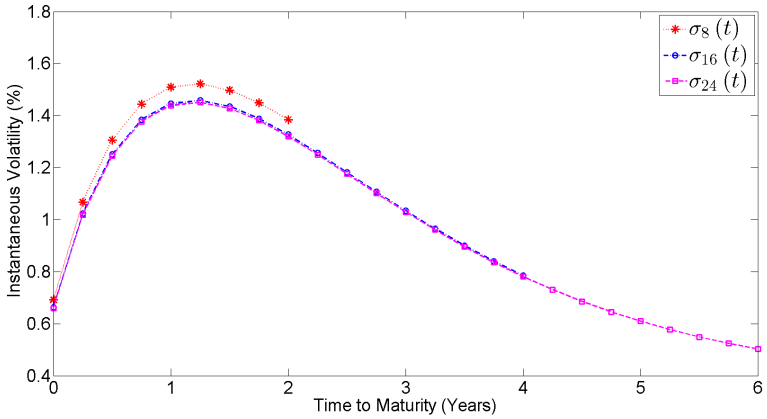

Figure D.5: Strip 1 with strike $K = 2.679\%$:
evolution of the instantaneous volatility.

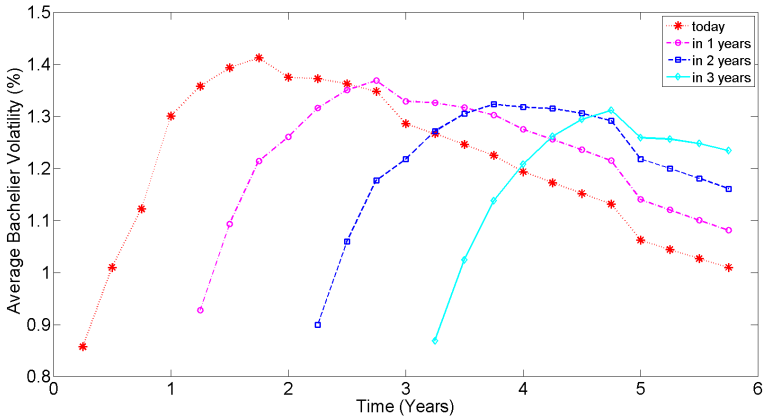

Figure D.6: Strip 1 with strike $K = 2.679\%$:
evolution of the term structure of implied Bachelier volatilities.

D.3. STRIP 1 WITH STRIKE $\mathbf{ATM}_{\mathbf{1Y}}^{\mathbf{5Y}} + 2\%$

Maturity (in years)	Tenor (in years)	Market vol.	LMM Rebonato vol.	Difference (in bp)	LMM MC vol.	Difference (in bp)
1	5	0.01044	0.01044	0.0	0.01042	−0.2
2	4	0.01053	0.01053	0.0	0.01048	−0.5
3	3	0.01047	0.01047	0.0	0.01040	−0.7
4	2	0.01080	0.01080	0.0	0.01073	−0.7
5	1	0.01069	0.01069	0.0	0.01066	−0.3

Table D.9: Strip 1 with strike $K = 3.679\%$: calibration results in terms of implied volatilities.

Maturity (in years)	Tenor (in years)	Market price (in bp)	LMM Rebonato price (in bp)	Difference (in bp)	LMM MC price (in bp)	Difference (in bp)
1	5	5.36	5.36	0.00	5.30	0.07
2	4	30.50	30.50	0.00	30.02	0.48
3	3	48.19	48.19	0.00	47.30	0.89
4	2	53.19	53.19	0.00	52.41	0.78
5	1	34.39	34.39	0.00	34.17	0.22

Table D.10: Strip 1 with strike $K = 3.679\%$: calibration results in terms of payer swaption prices.

Maturity (in years)	Tenor (in years)	Market price (in bp)	LMM Rebonato price (in bp)	Difference (in bp)	LMM MC price (in bp)	Difference (in bp)
1	5	971.19	971.19	0.00	972.34	−1.14
2	4	729.74	729.74	0.00	730.50	−0.76
3	3	535.38	535.38	0.00	535.70	−0.32
4	2	360.04	360.04	0.00	360.35	−0.31
5	1	180.91	180.91	0.00	181.03	−0.12

Table D.11: Strip 1 with strike $K = 3.679\%$: calibration results in terms of receiver swaption prices.

a	b	c	d
0.0029	0.0204	0.7194	0.0039

Table D.12: Strip 1 with strike $K = 3.679\%$: calibrated parameters a, b, c, d.

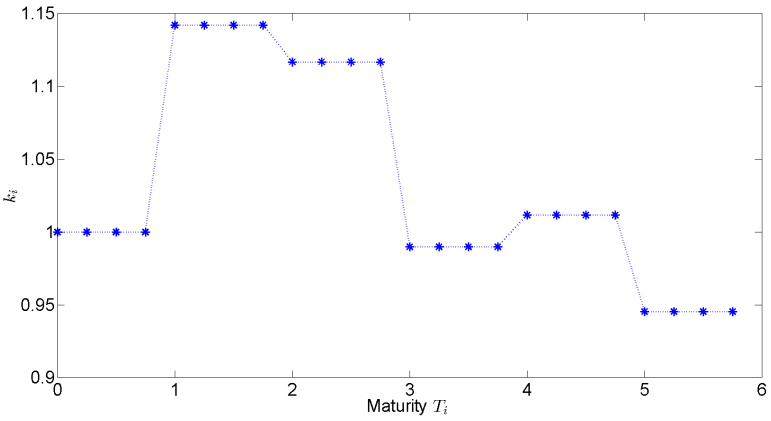

Figure D.7: Strip 1 with strike $K = 3.679\%$: representation of k_i.

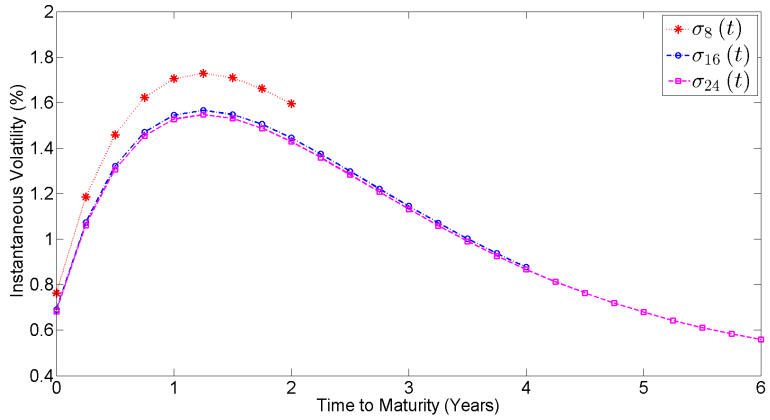

Figure D.8: Strip 1 with strike $K = 3.679\%$:
evolution of the instantaneous volatility.

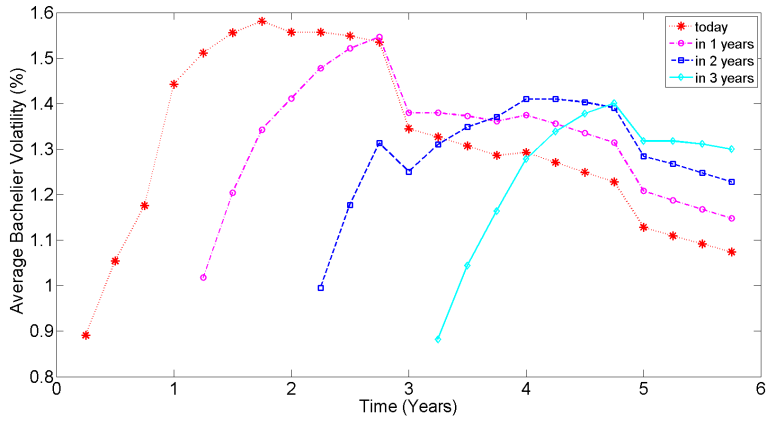

Figure D.9: Strip 1 with strike $K = 3.679\%$:
evolution of the term structure of implied Bachelier volatilities.

D.4. STRIP 1 WITH STRIKE $\mathbf{ATM}_{\mathbf{1Y}}^{\mathbf{5Y}} + 3\%$

Maturity (in years)	Tenor (in years)	Market vol.	LMM Rebonato vol.	Difference (in bp)	LMM MC vol.	Difference (in bp)
1	5	0.01159	0.01159	0.0	0.01166	0.8
2	4	0.01155	0.01155	0.0	0.01158	0.2
3	3	0.01127	0.01127	0.0	0.01123	−0.4
4	2	0.01166	0.01166	0.0	0.01160	−0.5
5	1	0.01138	0.01138	0.0	0.01134	−0.4

Table D.13: Strip 1 with strike $K = 4.679\%$: calibration results in terms of implied volatilities.

Maturity (in years)	Tenor (in years)	Market price (in bp)	LMM Rebonato price (in bp)	Difference (in bp)	LMM MC price (in bp)	Difference (in bp)
1	5	0.85	0.85	0.00	0.90	−0.05
2	4	10.72	10.72	0.00	10.83	−0.11
3	3	21.02	21.02	0.00	20.69	0.33
4	2	28.64	28.64	0.00	28.21	0.43
5	1	19.48	19.48	0.00	19.30	0.18

Table D.14: Strip 1 with strike $K = 4.679\%$: calibration results in terms of payer swaption prices.

Maturity (in years)	Tenor (in years)	Market price (in bp)	LMM Rebonato price (in bp)	Difference (in bp)	LMM MC price (in bp)	Difference (in bp)
1	5	1449.60	1449.60	0.00	1449.38	0.22
2	4	1093.57	1093.57	0.00	1093.36	0.21
3	3	793.62	793.62	0.00	792.81	0.80
4	2	524.12	524.12	0.00	523.83	0.29
5	1	259.48	259.48	0.00	259.46	0.02

Table D.15: Strip 1 with strike $K = 4.679\%$: calibration results in terms of receiver swaption prices.

a	b	c	d
0.0029	0.0210	0.6923	0.0042

Table D.16: Strip 1 with strike $K = 4.679\%$: calibrated parameters a, b, c, d.

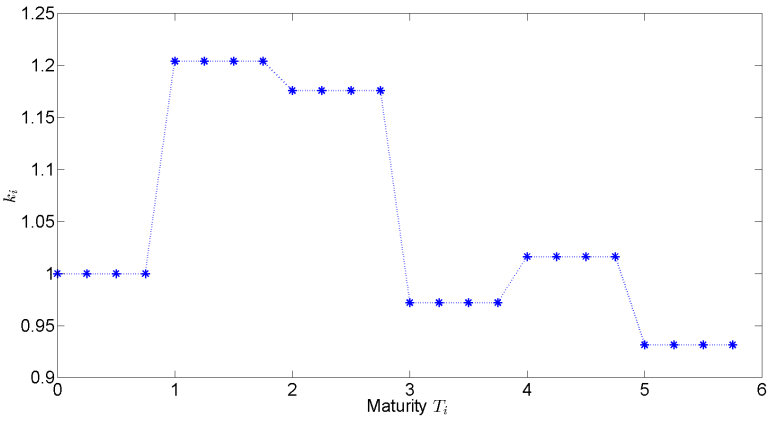

Figure D.10: Strip 1 with strike $K = 4.679\%$: representation of k_i.

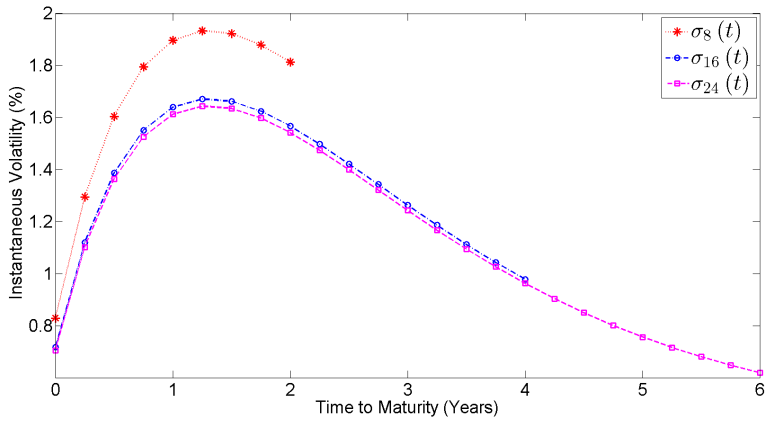

Figure D.11: Strip 1 with strike $K = 4.679\%$:
evolution of the instantaneous volatility.

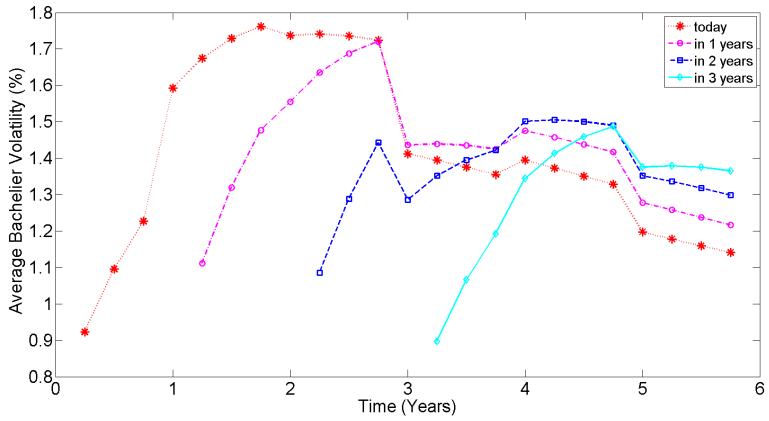

Figure D.12: Strip 1 with strike $K = 4.679\%$:
evolution of the term structure of implied Bachelier volatilities.

D.5. STRIP 2 WITH STRIKE ATM_{1Y}^{10Y}-1%

Maturity (in years)	Tenor (in years)	Market vol.	LMM Rebonato vol.	Difference (in bp)	LMM MC vol.	Difference (in bp)
1	10	0.00763	0.00763	0.0	0.00740	−2.3
2	9	0.00761	0.00761	0.0	0.00740	−2.1
3	8	0.00774	0.00774	0.0	0.00755	−1.9
4	7	0.00779	0.00779	0.0	0.00761	−1.8
5	6	0.00784	0.00784	0.0	0.00768	−1.6
6	5	0.00772	0.00772	0.0	0.00760	−1.2
7	4	0.00768	0.00768	0.0	0.00760	−0.9
8	3	0.00783	0.00783	0.0	0.00775	−0.8
9	2	0.00804	0.00804	0.0	0.00797	−0.7
10	1	0.00840	0.00840	0.0	0.00836	−0.4

Table D.17: Strip 2 with strike $K = 0.974\%$: calibration results in terms of implied volatilities.

Maturity (in years)	Tenor (in years)	Market price (in bp)	LMM Rebonato price (in bp)	Difference (in bp)	LMM MC price (in bp)	Difference (in bp)
1	10	955.07	955.07	0.00	951.62	3.45
2	9	990.48	990.48	0.00	984.78	5.70
3	8	967.43	967.43	0.00	960.96	6.47
4	7	904.22	904.22	0.00	897.79	6.43
5	6	815.47	815.47	0.00	809.82	5.65
6	5	702.52	702.52	0.00	698.38	4.14
7	4	578.75	578.75	0.00	576.07	2.68
8	3	448.47	448.47	0.00	446.55	1.92
9	2	308.57	308.57	0.00	307.37	1.19
10	1	160.60	160.60	0.00	160.23	0.38

Table D.18: Strip 2 with strike $K = 0.974\%$: calibration results in terms of payer swaption prices.

Maturity (in years)	Tenor (in years)	Market price (in bp)	LMM Rebonato price (in bp)	Difference (in bp)	LMM MC price (in bp)	Difference (in bp)
1	10	31.32	31.32	0.00	27.90	3.42
2	9	68.74	68.74	0.00	63.46	5.28
3	8	99.27	99.27	0.00	93.66	5.60
4	7	117.43	117.43	0.00	112.25	5.18
5	6	125.71	125.71	0.00	121.27	4.44
6	5	119.11	119.11	0.00	116.10	3.02
7	4	107.96	107.96	0.00	106.10	1.87
8	3	94.05	94.05	0.00	93.02	1.03
9	2	72.79	72.79	0.00	72.20	0.58
10	1	42.70	42.70	0.00	42.49	0.21

Table D.19: Strip 2 with strike $K = 0.974\%$: calibration results in terms of receiver swaption prices.

a	b	c	d
0.0021	0.0195	0.6874	0.0047

Table D.20: Strip 2 with strike $K = 0.974\%$: calibrated parameters a, b, c, d.

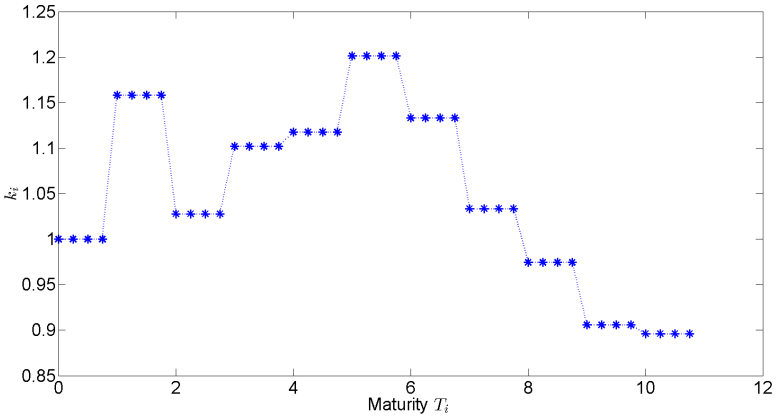

Figure D.13: Strip 2 with strike $K = 0.974\%$: representation of k_i.

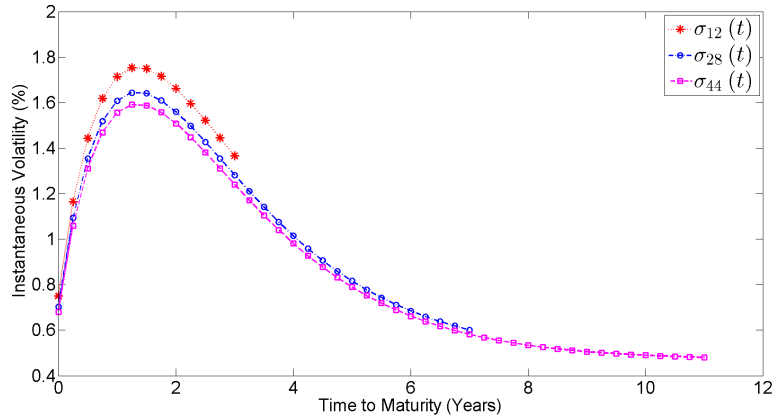

Figure D.14: Strip 2 with strike $K = 0.974\%$:
evolution of the instantaneous volatility.

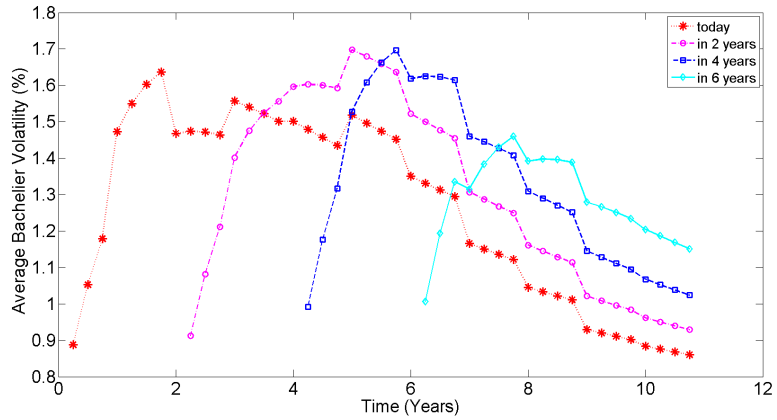

Figure D.15: Strip 2 with strike $K = 0.974\%$:
evolution of the term structure of implied Bachelier volatilities.

D.6. STRIP 2 WITH STRIKE $\mathbf{ATM}_{\mathbf{1Y}}^{\mathbf{10Y}} + 1\%$

Maturity (in years)	Tenor (in years)	Market vol.	LMM Rebonato vol.	Difference (in bp)	LMM MC vol.	Difference (in bp)
1	10	0.00943	0.00943	0.0	0.00950	0.6
2	9	0.00933	0.00933	0.0	0.00939	0.6
3	8	0.00927	0.00927	0.0	0.00933	0.5
4	7	0.00939	0.00939	0.0	0.00944	0.6
5	6	0.00943	0.00943	0.0	0.00947	0.4
6	5	0.00939	0.00939	0.0	0.00942	0.3
7	4	0.00937	0.00937	0.0	0.00938	0.2
8	3	0.00929	0.00929	0.0	0.00930	0.2
9	2	0.00919	0.00919	0.0	0.00922	0.3
10	1	0.00925	0.00925	0.0	0.00930	0.4

Table D.21: Strip 2 with strike $K = 2.974\%$: calibration results in terms of implied volatilities.

Maturity (in years)	Tenor (in years)	Market price (in bp)	LMM Rebonato price (in bp)	Difference (in bp)	LMM MC price (in bp)	Difference (in bp)
1	10	64.69	64.69	0.00	66.05	−1.36
2	9	163.92	163.92	0.00	166.30	−2.38
3	8	230.67	230.67	0.00	233.04	−2.37
4	7	272.50	272.50	0.00	275.06	−2.56
5	6	285.13	285.13	0.00	286.94	−1.81
6	5	272.91	272.91	0.00	273.94	−1.04
7	4	243.31	243.31	0.00	243.91	−0.59
8	3	197.43	197.43	0.00	197.90	−0.46
9	2	139.77	139.77	0.00	140.33	−0.56
10	1	75.22	75.22	0.00	75.66	−0.45

Table D.22: Strip 2 with strike $K = 2.974\%$: calibration results in terms of payer swaption prices.

Maturity (in years)	Tenor (in years)	Market price (in bp)	LMM Rebonato price (in bp)	Difference (in bp)	LMM MC price (in bp)	Difference (in bp)
1	10	988.44	988.44	0.00	988.25	0.18
2	9	891.06	891.06	0.00	890.91	0.15
3	8	814.97	814.97	0.00	813.47	1.51
4	7	744.64	744.64	0.00	742.96	1.68
5	6	664.01	664.01	0.00	663.34	0.67
6	5	571.15	571.15	0.00	569.87	1.28
7	4	470.72	470.72	0.00	469.64	1.09
8	3	361.27	361.27	0.00	360.66	0.61
9	2	245.83	245.83	0.00	245.66	0.17
10	1	126.43	126.43	0.00	126.42	0.02

Table D.23: Strip 2 with strike $K = 2.974\%$: calibration results in terms of receiver swaption prices.

a	b	c	d
0.0018	0.0176	0.5671	0.0050

Table D.24: Strip 2 with strike $K = 2.974\%$: calibrated parameters a, b, c, d.

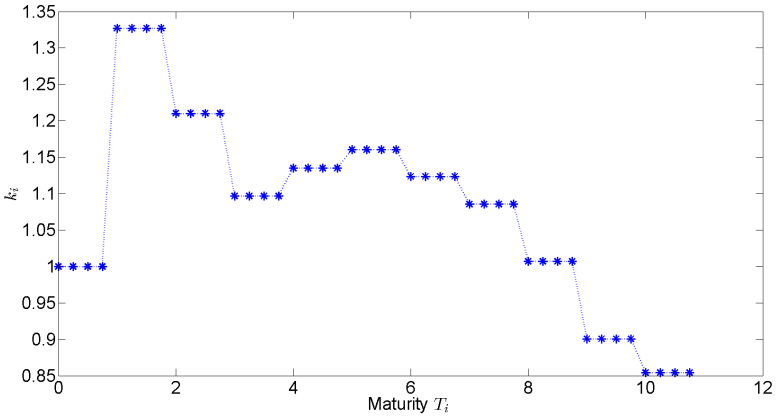

Figure D.16: Strip 2 with strike $K = 2.974\%$: representation of k_i.

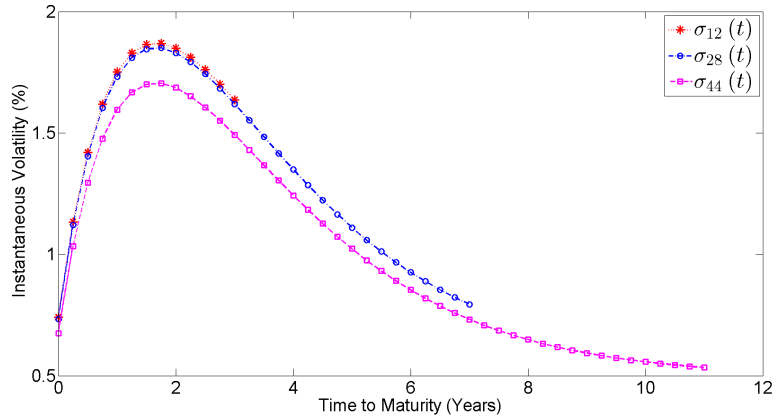

Figure D.17: Strip 2 with strike $K = 2.974\%$:
evolution of the instantaneous volatility.

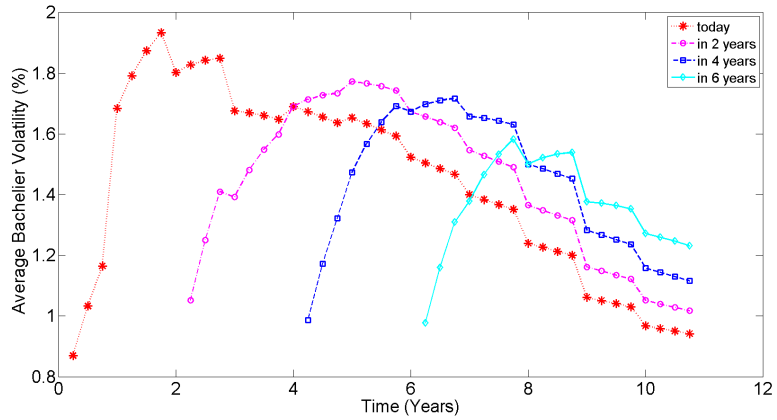

Figure D.18: Strip 2 with strike $K = 2.974\%$:
evolution of the term structure of implied Bachelier volatilities.

D.7. STRIP 2 WITH STRIKE $\mathbf{ATM}_{\mathbf{1Y}}^{\mathbf{10Y}} + 2\%$

Maturity (in years)	Tenor (in years)	Market vol.	LMM Rebonato vol.	Difference (in bp)	LMM MC vol.	Difference (in bp)
1	10	0.01098	0.01098	0.0	0.01118	1.9
2	9	0.01054	0.01054	0.0	0.01067	1.4
3	8	0.01021	0.01021	0.0	0.01031	0.9
4	7	0.01036	0.01036	0.0	0.01044	0.9
5	6	0.01037	0.01037	0.0	0.01042	0.5
6	5	0.01031	0.01031	0.0	0.01034	0.3
7	4	0.01019	0.01019	0.0	0.01020	0.0
8	3	0.01004	0.01004	0.0	0.01003	−0.1
9	2	0.00984	0.00984	0.0	0.00982	−0.2
10	1	0.01004	0.01004	0.0	0.01003	−0.1

Table D.25: Strip 2 with strike $K = 3.974\%$: calibration results in terms of implied volatilities.

Maturity (in years)	Tenor (in years)	Market price (in bp)	LMM Rebonato price (in bp)	Difference (in bp)	LMM MC price (in bp)	Difference (in bp)
1	10	13.74	13.74	0.00	15.13	−1.39
2	9	60.48	60.48	0.00	63.39	−2.90
3	8	103.01	103.01	0.00	105.85	−2.84
4	7	144.72	144.72	0.00	147.76	−3.04
5	6	166.12	166.12	0.00	168.09	−1.98
6	5	169.16	169.16	0.00	170.10	−0.95
7	4	155.57	155.57	0.00	155.70	−0.13
8	3	129.31	129.31	0.00	129.04	0.26
9	2	92.42	92.42	0.00	92.05	0.37
10	1	52.64	52.64	0.00	52.56	0.08

Table D.26: Strip 2 with strike $K = 3.974\%$: calibration results in terms of payer swaption prices.

Maturity (in years)	Tenor (in years)	Market price (in bp)	LMM Rebonato price (in bp)	Difference (in bp)	LMM MC price (in bp)	Difference (in bp)
1	10	1861.23	1861.23	0.00	1861.81	−0.57
2	9	1612.06	1612.06	0.00	1613.69	−1.63
3	8	1413.55	1413.55	0.00	1415.08	−1.53
4	7	1246.34	1246.34	0.00	1248.36	−2.03
5	6	1079.31	1079.31	0.00	1081.89	−2.58
6	5	908.24	908.24	0.00	910.00	−1.76
7	4	732.08	732.08	0.00	732.70	−0.62
8	3	552.27	552.27	0.00	552.43	−0.15
9	2	369.40	369.40	0.00	369.03	0.38
10	1	188.41	188.41	0.00	188.11	0.31

Table D.27: Strip 2 with strike $K = 3.974\%$: calibration results in terms of receiver swaption prices.

a	b	c	d
0.0019	0.0177	0.5303	0.0052

Table D.28: Strip 2 with strike $K = 3.974\%$: calibrated parameters a, b, c, d.

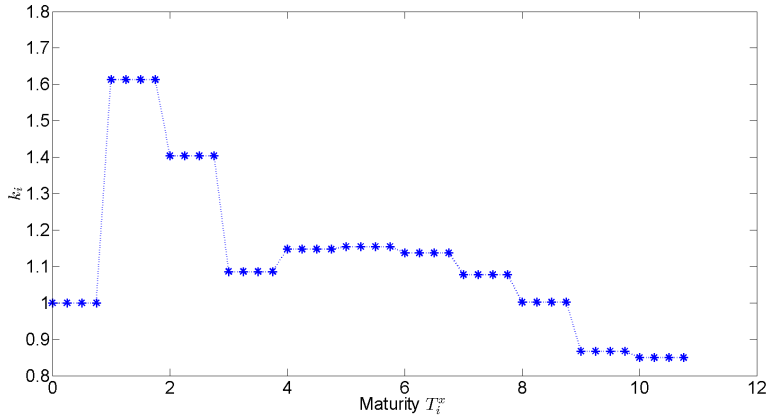

Figure D.19: Strip 2 with strike $K = 3.974\%$: representation of k_i.

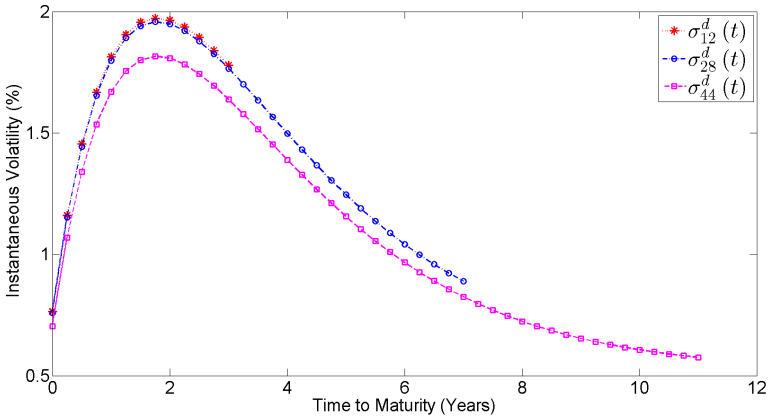

Figure D.20: Strip 2 with strike $K = 3.974\%$:
evolution of the instantaneous volatility.

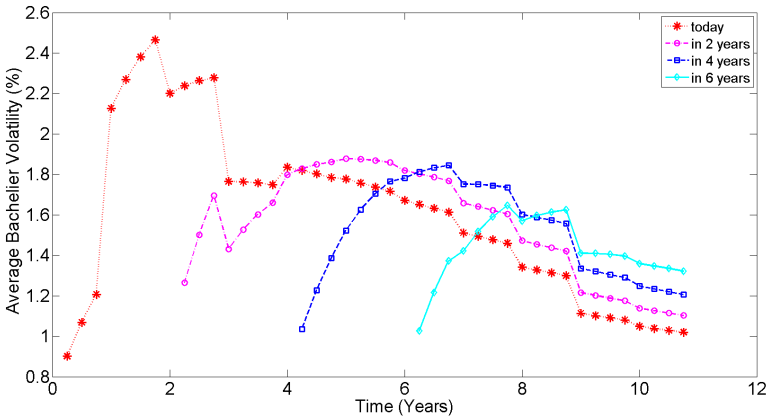

Figure D.21: Strip 2 with strike $K = 3.974\%$:
evolution of the term structure of implied Bachelier volatilities.

D.8. STRIP 2 WITH STRIKE $\mathbf{ATM}_{\mathbf{1Y}}^{\mathbf{10Y}} + 3\%$

Maturity (in years)	Tenor (in years)	Market vol.	LMM Rebonato vol.	Difference (in bp)	LMM MC vol.	Difference (in bp)
1	10	0.01278	0.01278	0.0	0.01325	4.7
2	9	0.01193	0.01193	0.0	0.01226	3.3
3	8	0.01130	0.01130	0.0	0.01148	1.8
4	7	0.01149	0.01149	0.0	0.01164	1.5
5	6	0.01148	0.01148	0.0	0.01160	1.1
6	5	0.01138	0.01138	0.0	0.01144	0.6
7	4	0.01111	0.01111	0.0	0.01112	0.2
8	3	0.01089	0.01089	0.0	0.01088	−0.2
9	2	0.01060	0.01060	0.0	0.01056	−0.4
10	1	0.01103	0.01103	0.0	0.01101	−0.1

Table D.29: Strip 2 with strike $K = 4.974\%$: calibration results in terms of implied volatilities.

Maturity (in years)	Tenor (in years)	Market price (in bp)	LMM Rebonato price (in bp)	Difference (in bp)	LMM MC price (in bp)	Difference (in bp)
1	10	3.76	3.76	0.00	4.97	−1.21
2	9	24.94	24.94	0.00	28.67	−3.73
3	8	48.38	48.38	0.00	51.68	−3.30
4	7	81.75	81.75	0.00	85.42	−3.68
5	6	102.83	102.83	0.00	105.92	−3.10
6	5	110.45	110.45	0.00	111.99	−1.53
7	4	102.66	102.66	0.00	103.03	−0.37
8	3	87.18	87.18	0.00	86.80	0.38
9	2	62.58	62.58	0.00	61.97	0.62
10	1	38.87	38.87	0.00	38.76	0.11

Table D.30: Strip 2 with strike $K = 4.974\%$: calibration results in terms of payer swaption prices.

Maturity (in years)	Tenor (in years)	Market price (in bp)	LMM Rebonato price (in bp)	Difference (in bp)	LMM MC price (in bp)	Difference (in bp)
1	10	2774.99	2774.99	0.00	2775.94	−0.95
2	9	2400.96	2400.96	0.00	2403.37	−2.41
3	8	2085.15	2085.15	0.00	2086.90	−1.75
4	7	1812.83	1812.83	0.00	1814.22	−1.39
5	6	1550.34	1550.34	0.00	1551.51	−1.17
6	5	1290.36	1290.36	0.00	1289.74	0.62
7	4	1028.27	1028.27	0.00	1026.94	1.33
8	3	769.28	769.28	0.00	767.51	1.77
9	2	510.49	510.49	0.00	508.58	1.91
10	1	259.21	259.21	0.00	258.38	0.83

Table D.31: Strip 2 with strike $K = 4.974\%$: calibration results in terms of receiver swaption prices.

a	b	c	d
0.0018	0.0186	0.5066	0.0054

Table D.32: Strip 2 with strike $K = 4.974\%$: calibrated parameters a, b, c, d.

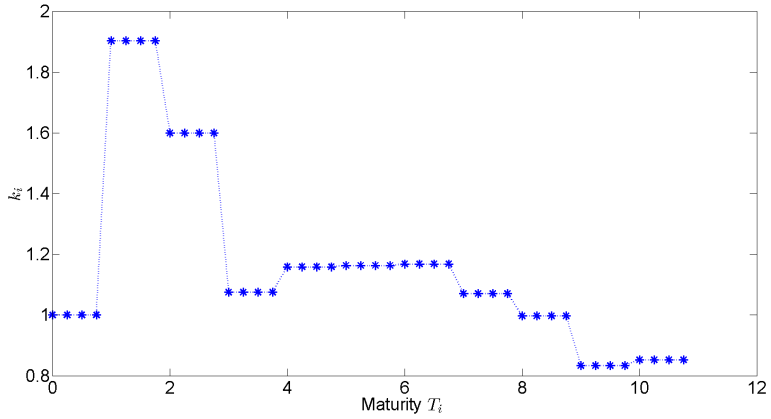

Figure D.22: Strip 2 with strike $K = 4.974\%$: representation of k_i.

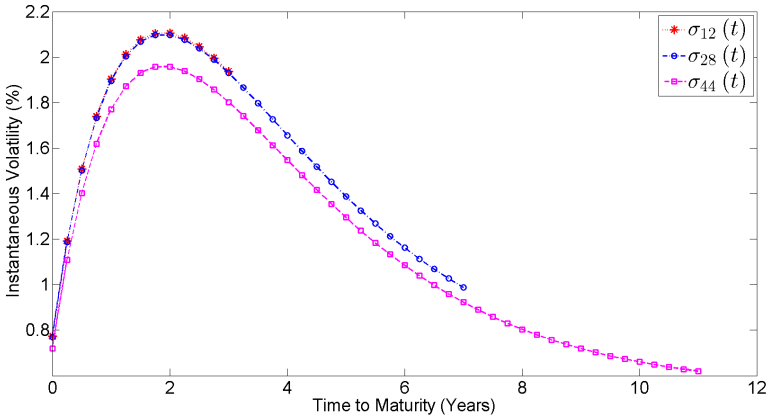

Figure D.23: Strip 2 with strike $K = 4.974\%$:
evolution of the instantaneous volatility.

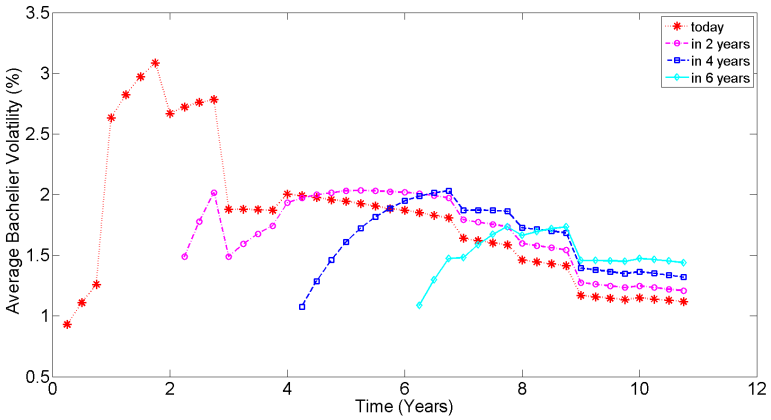

Figure D.24: Strip 2 with strike $K = 4.974\%$:
evolution of the term structure of implied Bachelier volatilities.

D.9. STRIP 3 WITH STRIKE $\mathbf{ATM}_{\mathbf{1Y}}^{\mathbf{15Y}} - 1\%$

Maturity (in years)	Tenor (in years)	Market vol.	LMM Rebonato vol.	Difference (in bp)	LMM MC vol.	Difference (in bp)
1	15	0.00772	0.00772	0.0	0.00739	−3.2
2	14	0.00758	0.00758	0.0	0.00728	−2.9
3	13	0.00748	0.00748	0.0	0.00722	−2.7
4	12	0.00756	0.00756	0.0	0.00732	−2.4
5	11	0.00757	0.00757	0.0	0.00735	−2.3
6	10	0.00750	0.00750	0.0	0.00730	−2.0
7	9	0.00740	0.00740	0.0	0.00722	−1.7
8	8	0.00734	0.00734	0.0	0.00720	−1.4
9	7	0.00731	0.00731	0.0	0.00719	−1.2
10	6	0.00731	0.00731	0.0	0.00721	−1.0
11	5	0.00721	0.00721	0.0	0.00713	−0.9
12	4	0.00716	0.00716	0.0	0.00708	−0.8
13	3	0.00708	0.00708	0.0	0.00702	−0.5
14	2	0.00698	0.00698	0.0	0.00695	−0.3
15	1	0.00716	0.00716	0.0	0.00716	−0.1

Table D.33: Strip 3 with strike $K = 1.105\%$: calibration results in terms of implied volatilities.

Maturity (in years)	Tenor (in years)	Market price (in bp)	LMM Rebonato price (in bp)	Difference (in bp)	LMM MC price (in bp)	Difference (in bp)
1	15	1367.56	1367.56	0.00	1360.43	7.13
2	14	1437.10	1437.10	0.00	1425.31	11.78
3	13	1440.68	1440.68	0.00	1426.99	13.69
4	12	1412.95	1412.95	0.00	1398.57	14.38
5	11	1354.98	1354.98	0.00	1340.48	14.50
6	10	1271.84	1271.84	0.00	1258.84	13.00
7	9	1171.32	1171.32	0.00	1160.29	11.02
8	8	1062.15	1062.15	0.00	1053.47	8.68
9	7	945.50	945.50	0.00	938.53	6.97
10	6	824.70	824.70	0.00	819.36	5.34
11	5	692.62	692.62	0.00	688.69	3.93
12	4	557.23	557.23	0.00	554.23	3.00
13	3	418.24	418.24	0.00	416.64	1.60
14	2	278.45	278.45	0.00	277.94	0.52
15	1	142.09	142.09	0.00	141.99	0.09

Table D.34: Strip 3 with strike $K = 1.105\%$: calibration results in terms of payer swaption prices.

Maturity (in years)	Tenor (in years)	Market price (in bp)	LMM Rebonato price (in bp)	Difference (in bp)	LMM MC price (in bp)	Difference (in bp)
1	15	46.83	46.83	0.00	40.79	6.04
2	14	105.41	105.41	0.00	95.77	9.64
3	13	149.74	149.74	0.00	139.20	10.53
4	12	190.74	190.74	0.00	179.99	10.75
5	11	217.38	217.38	0.00	207.13	10.25
6	10	228.37	228.37	0.00	219.44	8.93
7	9	228.49	228.49	0.00	221.49	7.00
8	8	223.93	223.93	0.00	219.15	4.78
9	7	214.40	214.40	0.00	211.48	2.92
10	6	200.20	200.20	0.00	198.08	2.12
11	5	174.98	174.98	0.00	174.08	0.90
12	4	148.14	148.14	0.00	147.94	0.21
13	3	116.22	116.22	0.00	116.79	−0.56
14	2	80.14	80.14	0.00	80.81	−0.67
15	1	44.14	44.14	0.00	44.50	−0.36

Table D.35: Strip 3 with strike $K = 1.105\%$: calibration results in terms of receiver swaption prices.

a	b	c	d
0.0013	0.0159	0.5665	0.0055

Table D.36: Strip 3 with strike $K = 1.105\%$: calibrated parameters a, b, c, d.

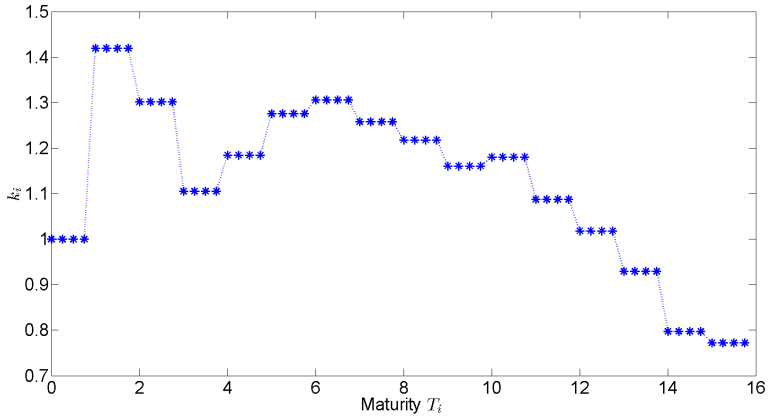

Figure D.25: Strip 3 with strike $K = 1.105\%$: representation of k_i.

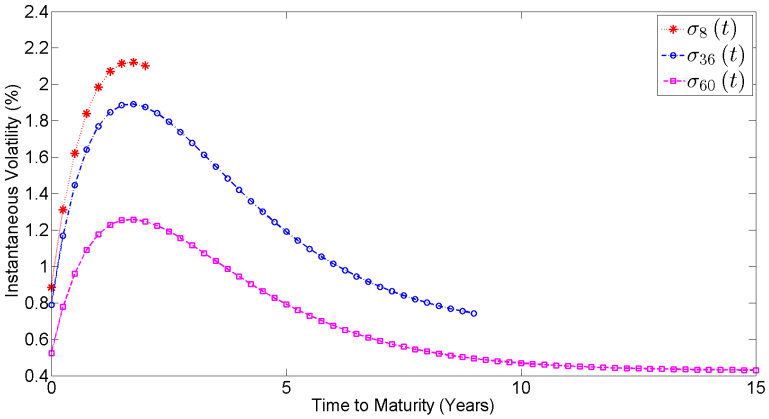

Figure D.26: Strip 3 with strike $K = 1.105\%$:
evolution of the instantaneous volatility.

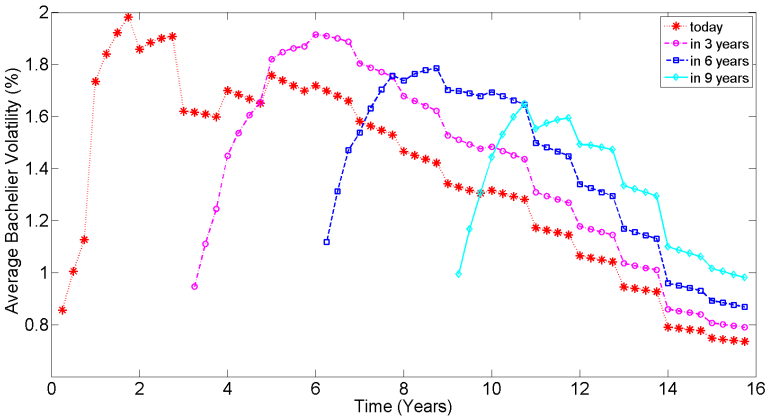

Figure D.27: Strip 3 with strike $K = 1.105\%$:
evolution of the term structure of implied Bachelier volatilities.

D.10. STRIP 3 WITH STRIKE $\mathbf{ATM}_{\mathbf{1Y}}^{\mathbf{15Y}} + 1\%$

Maturity (in years)	Tenor (in years)	Market vol.	LMM Rebonato vol.	Difference (in bp)	LMM MC vol.	Difference (in bp)
1	15	0.00913	0.00913	0.0	0.00919	0.6
2	14	0.00900	0.00900	0.0	0.00906	0.6
3	13	0.00894	0.00894	0.0	0.00899	0.5
4	12	0.00895	0.00895	0.0	0.00899	0.4
5	11	0.00898	0.00898	0.0	0.00901	0.3
6	10	0.00893	0.00893	0.0	0.00895	0.2
7	9	0.00885	0.00885	0.0	0.00887	0.2
8	8	0.00875	0.00875	0.0	0.00876	0.1
9	7	0.00865	0.00865	0.0	0.00865	−0.0
10	6	0.00856	0.00856	0.0	0.00855	−0.1
11	5	0.00841	0.00841	0.0	0.00840	−0.2
12	4	0.00827	0.00827	0.0	0.00825	−0.2
13	3	0.00808	0.00808	0.0	0.00806	−0.2
14	2	0.00784	0.00784	0.0	0.00783	−0.1
15	1	0.00783	0.00783	0.0	0.00784	0.0

Table D.37: Strip 3 with strike $K = 3.105\%$: calibration results in terms of implied volatilities.

Maturity (in years)	Tenor (in years)	Market price (in bp)	LMM Rebonato price (in bp)	Difference (in bp)	LMM MC price (in bp)	Difference (in bp)
1	15	83.63	83.63	0.00	85.33	−1.70
2	14	216.46	216.46	0.00	219.68	−3.23
3	13	318.31	318.31	0.00	321.76	−3.45
4	12	391.54	391.54	0.00	394.52	−2.99
5	11	438.76	438.76	0.00	441.08	−2.32
6	10	457.80	457.80	0.00	459.45	−1.65
7	9	456.54	456.54	0.00	458.07	−1.53
8	8	438.01	438.01	0.00	438.78	−0.77
9	7	407.47	407.47	0.00	407.45	0.02
10	6	368.33	368.33	0.00	367.47	0.86
11	5	317.42	317.42	0.00	316.53	0.89
12	4	260.17	260.17	0.00	259.37	0.80
13	3	196.70	196.70	0.00	196.07	0.63
14	2	130.67	130.67	0.00	130.44	0.22
15	1	67.49	67.49	0.00	67.52	−0.04

Table D.38: Strip 3 with strike $K = 3.105\%$: calibration results in terms of payer swaption prices.

Maturity (in years)	Tenor (in years)	Market price (in bp)	LMM Rebonato price (in bp)	Difference (in bp)	LMM MC price (in bp)	Difference (in bp)
1	15	1404.36	1404.36	0.00	1405.66	−1.30
2	14	1327.61	1327.61	0.00	1329.65	−2.05
3	13	1273.80	1273.80	0.00	1276.41	−2.61
4	12	1222.23	1222.23	0.00	1224.86	−2.63
5	11	1163.75	1163.75	0.00	1163.14	0.61
6	10	1089.95	1089.95	0.00	1088.70	1.25
7	9	1005.87	1005.87	0.00	1004.34	1.53
8	8	912.02	912.02	0.00	909.84	2.18
9	7	812.18	812.18	0.00	809.52	2.66
10	6	706.91	706.91	0.00	703.22	3.69
11	5	593.74	593.74	0.00	590.80	2.94
12	4	479.47	479.47	0.00	477.02	2.45
13	3	360.93	360.93	0.00	359.00	1.93
14	2	239.84	239.84	0.00	238.47	1.36
15	1	121.66	121.66	0.00	121.03	0.63

Table D.39: Strip 3 with strike $K = 3.105\%$: calibration results in terms of receiver swaption prices.

a	b	c	d
0.0016	0.0140	0.4564	0.0055

Table D.40: Strip 3 with strike $K = 3.105\%$: calibrated parameters a, b, c, d.

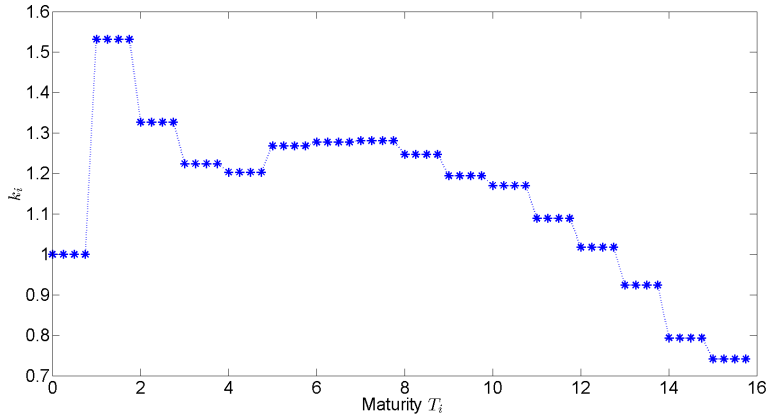

Figure D.28: Strip 3 with strike $K = 3.105\%$: representation of k_i.

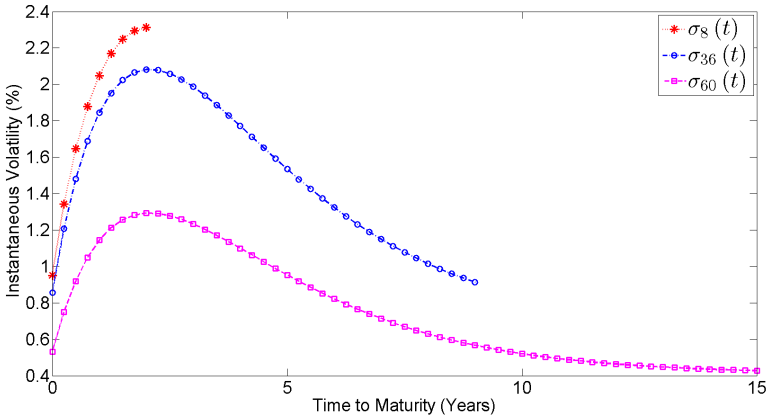

Figure D.29: Strip 3 with strike $K = 3.105\%$:
evolution of the instantaneous volatility.

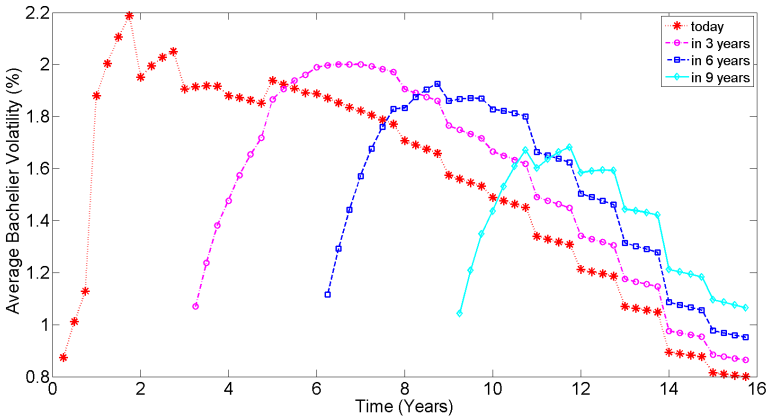

Figure D.30: Strip 3 with strike $K = 3.105\%$:
evolution of the term structure of implied Bachelier volatilities.

D.11. STRIP 3 WITH STRIKE $\mathbf{ATM}_{\mathbf{1Y}}^{\mathbf{15Y}} + 2\%$

Maturity (in years)	Tenor (in years)	Market vol.	LMM Rebonato vol.	Difference (in bp)	LMM MC vol.	Difference (in bp)
1	15	0.01040	0.01040	0.0	0.01076	3.5
2	14	0.01009	0.01009	0.0	0.01040	3.1
3	13	0.00996	0.00996	0.0	0.01022	2.6
4	12	0.00993	0.00993	0.0	0.01016	2.2
5	11	0.00988	0.00988	0.0	0.01007	1.9
6	10	0.00979	0.00979	0.0	0.00994	1.5
7	9	0.00969	0.00969	0.0	0.00981	1.2
8	8	0.00958	0.00958	0.0	0.00967	0.9
9	7	0.00951	0.00951	0.0	0.00958	0.7
10	6	0.00949	0.00949	0.0	0.00954	0.4
11	5	0.00937	0.00937	0.0	0.00941	0.4
12	4	0.00912	0.00912	0.0	0.00913	0.1
13	3	0.00880	0.00880	0.0	0.00879	−0.1
14	2	0.00844	0.00844	0.0	0.00842	−0.1
15	1	0.00859	0.00859	0.0	0.00858	−0.1

Table D.41: Strip 3 with strike $K = 4.105\%$: calibration results in terms of implied volatilities.

Maturity (in years)	Tenor (in years)	Market price (in bp)	LMM Rebonato price (in bp)	Difference (in bp)	LMM MC price (in bp)	Difference (in bp)
1	15	14.32	14.32	0.00	17.44	−3.12
2	14	73.05	73.05	0.00	81.98	−8.93
3	13	140.20	140.20	0.00	151.78	−11.58
4	12	200.71	200.71	0.00	212.96	−12.25
5	11	245.03	245.03	0.00	256.67	−11.64
6	10	272.15	272.15	0.00	281.66	−9.51
7	9	283.83	283.83	0.00	291.43	−7.60
8	8	282.98	282.98	0.00	288.47	−5.49
9	7	273.34	273.34	0.00	277.15	−3.80
10	6	257.07	257.07	0.00	259.49	−2.42
11	5	227.08	227.08	0.00	228.70	−1.62
12	4	184.98	184.98	0.00	185.52	−0.54
13	3	137.97	137.97	0.00	137.76	0.22
14	2	89.88	89.88	0.00	89.63	0.25
15	1	48.95	48.95	0.00	48.83	0.12

Table D.42: Strip 3 with strike $K = 4.105\%$: calibration results in terms of payer swaption prices.

Maturity (in years)	Tenor (in years)	Market price (in bp)	LMM Rebonato price (in bp)	Difference (in bp)	LMM MC price (in bp)	Difference (in bp)
1	15	2655.77	2655.77	0.00	2662.78	−7.02
2	14	2405.61	2405.61	0.00	2418.46	−12.85
3	13	2218.90	2218.90	0.00	2234.62	−15.71
4	12	2057.85	2057.85	0.00	2075.32	−17.47
5	11	1901.32	1901.32	0.00	1918.36	−17.04
6	10	1742.11	1742.11	0.00	1758.81	−16.71
7	9	1579.24	1579.24	0.00	1593.91	−14.66
8	8	1413.09	1413.09	0.00	1424.86	−11.77
9	7	1245.96	1245.96	0.00	1255.99	−10.04
10	6	1077.19	1077.19	0.00	1085.10	−7.91
11	5	900.38	900.38	0.00	905.57	−5.18
12	4	718.47	718.47	0.00	722.12	−3.64
13	3	535.33	535.33	0.00	537.36	−2.03
14	2	352.79	352.79	0.00	353.73	−0.94
15	1	179.19	179.19	0.00	179.56	−0.37

Table D.43: Strip 3 with strike $K = 4.105\%$: calibration results in terms of receiver swaption prices.

a	b	c	d
0.0006	0.0169	0.4624	0.0059

Table D.44: Strip 3 with strike $K = 4.105\%$: calibrated parameters a, b, c, d.

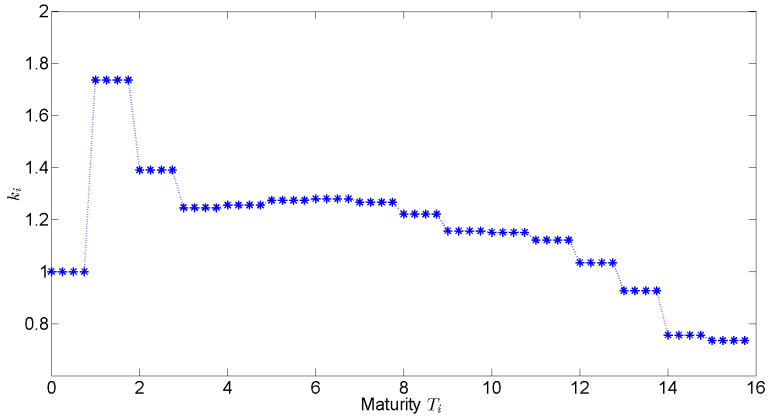

Figure D.31: Strip 3 with strike $K = 4.105\%$: representation of k_i.

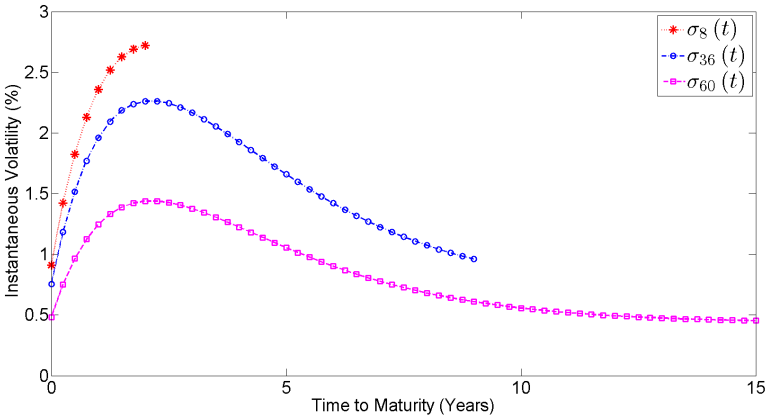

Figure D.32: Strip 3 with strike $K = 4.105\%$:
evolution of the instantaneous volatility.

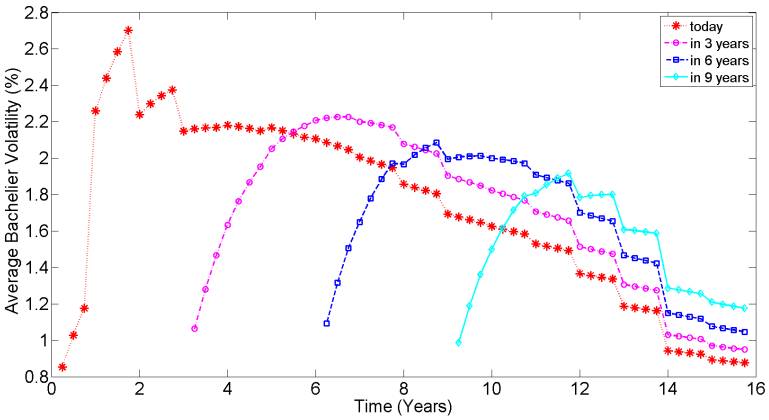

Figure D.33: Strip 3 with strike $K = 4.105\%$:
evolution of the term structure of implied Bachelier volatilities.

D.12. STRIP 3 WITH STRIKE $\mathbf{ATM_{1Y}^{15Y}} + 3\%$

Maturity (in years)	Tenor (in years)	Market vol.	LMM Rebonato vol.	Difference (in bp)	LMM MC vol.	Difference (in bp)
1	15	0.01186	0.01186	0.0	0.01268	8.2
2	14	0.01136	0.01136	0.0	0.01205	6.9
3	13	0.01115	0.01115	0.0	0.01175	5.9
4	12	0.01111	0.01111	0.0	0.01165	5.4
5	11	0.01096	0.01096	0.0	0.01143	4.6
6	10	0.01083	0.01083	0.0	0.01123	4.0
7	9	0.01067	0.01067	0.0	0.01100	3.2
8	8	0.01057	0.01057	0.0	0.01083	2.6
9	7	0.01056	0.01056	0.0	0.01077	2.1
10	6	0.01064	0.01064	0.0	0.01084	2.0
11	5	0.01056	0.01056	0.0	0.01074	1.8
12	4	0.01015	0.01015	0.0	0.01027	1.2
13	3	0.00967	0.00967	0.0	0.00975	0.8
14	2	0.00915	0.00915	0.0	0.00919	0.4
15	1	0.00956	0.00956	0.0	0.00961	0.5

Table D.45: Strip 3 with strike $K = 5.105\%$: calibration results in terms of implied volatilities.

Maturity (in years)	Tenor (in years)	Market price (in bp)	LMM Rebonato price (in bp)	Difference (in bp)	LMM MC price (in bp)	Difference (in bp)
1	15	2.87	2.87	0.00	5.06	−2.19
2	14	27.21	27.21	0.00	37.34	−10.13
3	13	67.24	67.24	0.00	83.59	−16.35
4	12	111.82	111.82	0.00	132.51	−20.69
5	11	146.51	146.51	0.00	167.35	−20.85
6	10	171.99	171.99	0.00	191.47	−19.48
7	9	186.22	186.22	0.00	202.41	−16.19
8	8	193.37	193.37	0.00	205.98	−12.62
9	7	195.48	195.48	0.00	205.55	−10.07
10	6	193.59	193.59	0.00	202.54	−8.96
11	5	176.08	176.08	0.00	183.09	−7.02
12	4	140.59	140.59	0.00	144.56	−3.96
13	3	101.99	101.99	0.00	104.00	−2.00
14	2	64.18	64.18	0.00	64.88	−0.69
15	1	38.03	38.03	0.00	38.48	−0.45

Table D.46: Strip 3 with strike $K = 5.105\%$: calibration results in terms of payer swaption prices.

Maturity (in years)	Tenor (in years)	Market price (in bp)	LMM Rebonato price (in bp)	Difference (in bp)	LMM MC price (in bp)	Difference (in bp)
1	15	3965.05	3965.05	0.00	3967.69	−2.64
2	14	3581.20	3581.20	0.00	3590.45	−9.25
3	13	3269.15	3269.15	0.00	3285.57	−16.42
4	12	2995.41	2995.41	0.00	3015.40	−20.00
5	11	2734.09	2734.09	0.00	2752.82	−18.72
6	10	2479.76	2479.76	0.00	2495.75	−15.99
7	9	2227.71	2227.71	0.00	2242.38	−14.67
8	8	1979.59	1979.59	0.00	1993.07	−13.47
9	7	1736.00	1736.00	0.00	1745.16	−9.16
10	6	1495.25	1495.25	0.00	1502.17	−6.92
11	5	1246.36	1246.36	0.00	1251.89	−5.54
12	4	988.28	988.28	0.00	991.79	−3.51
13	3	732.47	732.47	0.00	733.92	−1.45
14	2	480.84	480.84	0.00	481.53	−0.69
15	1	244.33	244.33	0.00	244.71	−0.38

Table D.47: Strip 3 with strike $K = 5.105\%$: calibration results in terms of receiver swaption prices.

a	b	c	d
0.0029	0.0143	0.3868	0.0056

Table D.48: Strip 3 with strike $K = 5.105\%$: calibrated parameters a, b, c, d.

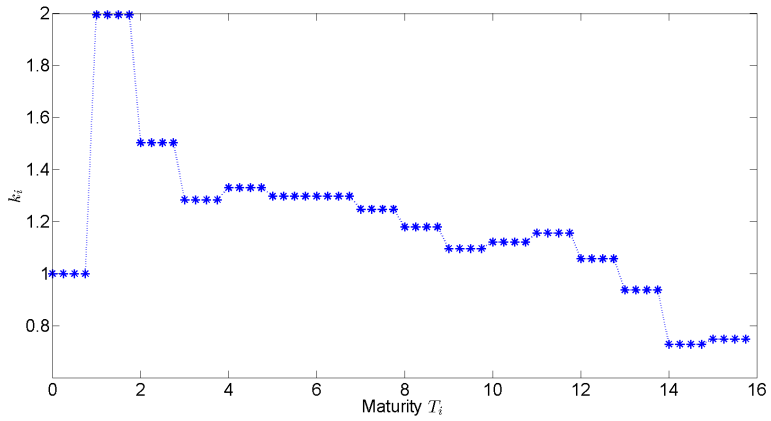

Figure D.34: Strip 3 with strike $K = 5.105\%$: representation of k_i.

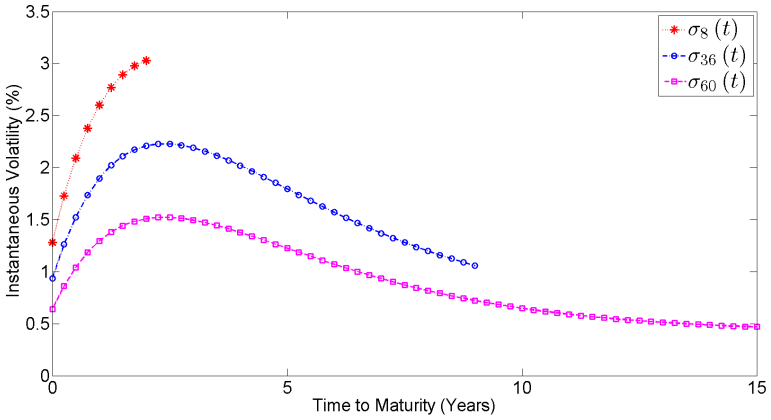

Figure D.35: Strip 3 with strike $K = 5.105\%$:
evolution of the instantaneous volatility.

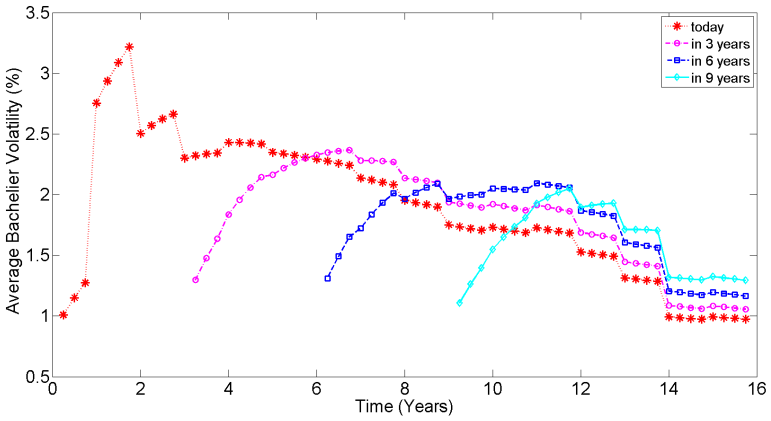

Figure D.36: Strip 3 with strike $K = 5.105\%$:
evolution of the term structure of implied Bachelier volatilities.

E

PAYMENT SCHEDULES

Tenor date	LMM	1FHW	Abs Diff
T_0	0.000	0.000	0.000
T_1	0.250	0.247	0.003
T_2	0.500	0.499	0.001
T_3	0.750	0.751	0.001
T_4	1.000	1.003	0.003
T_5	1.250	1.247	0.003
T_6	1.500	1.499	0.001
T_7	1.750	1.751	0.001
T_8	2.000	2.008	0.008
T_9	2.250	2.247	0.003
T_{10}	2.500	2.499	0.001
T_{11}	2.750	2.756	0.006
T_{12}	3.000	3.005	0.005
T_{13}	3.250	3.247	0.003
T_{14}	3.500	3.504	0.004
T_{15}	3.750	3.753	0.003
T_{16}	4.000	4.003	0.003
T_{17}	4.250	4.252	0.002
T_{18}	4.500	4.501	0.001
T_{19}	4.750	4.753	0.003
T_{20}	5.000	5.005	0.005
T_{21}	5.250	5.249	0.001
T_{22}	5.500	5.501	0.001
T_{23}	5.750	5.753	0.003
T_{24}	6.000	6.005	0.005
T_{25}	6.250	6.249	0.001
T_{26}	6.500	6.501	0.001
T_{27}	6.750	6.753	0.003
T_{28}	7.000	7.005	0.005
T_{29}	7.250	7.249	0.001
T_{30}	7.500	7.501	0.001
T_{31}	7.750	7.753	0.003
T_{32}	8.000	8.011	0.011
T_{33}	8.250	8.252	0.002
T_{34}	8.500	8.510	0.010
T_{35}	8.750	8.759	0.009
T_{36}	9.000	9.008	0.008
T_{37}	9.250	9.258	0.008
T_{38}	9.500	9.507	0.007
T_{39}	9.750	9.756	0.006
T_{40}	10.000	10.008	0.008
T_{41}	10.250	10.255	0.005
T_{42}	10.500	10.504	0.004
T_{43}	10.750	10.756	0.006
T_{44}	11.000	11.008	0.008
T_{45}	11.250	11.252	0.002
T_{46}	11.500	11.504	0.004
T_{47}	11.750	11.756	0.006
T_{48}	12.000	12.008	0.008
T_{49}	12.250	12.255	0.005
T_{50}	12.500	12.507	0.007
T_{51}	12.750	12.759	0.009
T_{52}	13.000	13.016	0.016
T_{53}	13.250	13.255	0.005
T_{54}	13.500	13.507	0.007
T_{55}	13.750	13.764	0.014
T_{56}	14.000	14.014	0.014
T_{57}	14.250	14.255	0.005
T_{58}	14.500	14.512	0.012
T_{59}	14.750	14.762	0.012
T_{60}	15.000	15.011	0.011

Table E.1: Payment schedules of the MC LMM and the 1FHW model.